Università degli Studi di Napoli Federico II

Dipartimento di Ingegneria Elettrica e delle Tecnologie dell'Informazione

Classe delle Lauree Magistrali in Ingegneria Elettronica,
Classe n. LM-29

Corso di Laurea Magistrale in Ingegneria Elettronica

Thesis

An automated measurement system for testing optical modules in particle accelerator detectors

Supervisor:
Prof. Pasquale Arpaia

Candidate:
Lippiello Andrea
Matr. M61/430

Co-Supervisor:
Prof. Ettore Napoli
Ing. Eduardo Brandao De Souza Mendes

Academic Year
2017/2018

Abstract

The TTC-PON system (Timing, Trigger and Control system based on Passive Optical Networks) is proposed to replace the current TTC system, responsible for delivering the bunch clock, trigger and control commands to the LHC experiments. During phase-1 upgrades, it will be installed in the ALICE experiment and PON optical modules will also be deployed in the LHCb experiment. Therefore, a quality assurance campaign was carried out to ensure that the optical components to be installed were within the TTC-PON specifications, an evolution of the XG-PON standard. The transceivers tested were divided in ONU (Optical Network Unit) and OLT (Optical Line Terminal). Their characterization was based on the evaluation of their performances as transmitters and receivers, and on the verification of their behaviour in temperature. In this context, I worked on the software optimization of the custom-made Python library used to execute an automated test routine, I created from scratch the software used for the implementation of the temperature tests, and I analyzed in-depth the outcomes obtained. The results of the quality assurance campaign were significant, since a totally non-working ONU module was detected, and a few OLT and ONU modules out-of-specification were identified. This thesis will cover an overview of the TTC-PON system, focusing on the aforementioned quality assurance process experience and results.

Acknowledgments

I want to start this acknowledgments section expressing my very great appreciation to all the people who made this fantastic experience at Cern possible. I am particularly grateful to my University supervisors Prof. Arpaia and Prof. Napoli, who passed over my mistakes and gave me a valid professional support ensuring my personal and professional growth. Moreover, I would like to offer my special thanks to Ing.Mendes and Ing.Baron, respectively my CERN supervisor and my section leader. I had the chance to benefit from their wide preparation and their teachings, always accompanied by their nice words of encouragement and good mood. My gratitude is extended to all the colleagues of the EP-ESE group, who welcomed me with great kindness and who have always been willing to offer their help in case of need. It would be impossible to mention one by one all the fantastic people I met during this period and who helped me to overcome even the most difficult days. In this sense, I would say thanks to all the players of my futsal team "Dynamo Weasels". Even if our sporting achievements could have been better, I enjoyed our trainings, our matches and our fantastic dinners paid by our beloved captain. I hope that in the future you can achieve all the results that we have not been able to reach together. Finally, a special mention is for the friends who have been close to me every day during these ten months. First of all Antonio, who encouraged me from the beginning to send the application for the Technical Student position. In spite of the short duration of our knowledge, we are actually an inseparable duo as Stanlio and Ollio, or rather, by virtue of the difference in size and height, like Asterix and Obelix. I am sure that a bond of affection, respect and mutual esteem has been established between us and that our relationship will continue also after this experience. Following there are Barbara and Gabriele, with whom I shared many trips to Milan, in addition to the Genevan days. Your company and friendship has been fundamental to me, I wish you could soon reach your goals and, especially for the Milanese lady, to meet us soon in Naples to show you the beauties of my city. Last but not least there is Carmine, who was initially only the technician of my section, but later, knowing each other better outside of CERN, also a friend who can make you laugh simply by talking. I wish you to find the true happiness. At this point, I think it is more appropriate to continue in Italian to thank all the people who have always been by my side and are an indelible part of my life. I primi che voglio ringraziare sono i miei genitori. Questo periodo di lontananza mi ha confermato ancora di più quanto siate una parte fondamentale di me e che, anche se a volte con le parole non sono bravo a dimostrare il mio affetto, vi sono grato per tutto quello che avete fatto, fate e farete per me. Spero di avervi reso orgoglioso e di avervi convinto che, nonostante in passato avrei potuto fare delle scelte che avrebbero reso il mio avvenire più sicuro e roseo, con la mia caparbietà e il mio impegno potrò arrivare ugualmente lontano. Un ringraziamento va anche a mia sorella, la quale ha da poco cominciato una nuova fase della sua vita che mi auguro le consenta di trovare la tranquillità e la stabilità che fino ad ora ha faticato a raggiungere. Inoltre, voglio citare tutta la mia famiglia, gli zii e sopratutto i nonni, che in questo momento attraversano un momento di difficoltà, poiché mi hanno fatto sempre sentire la loro vicinanza a prescindere dai risultati e dalle scelte fatte. Una menzione particolare è dedicata alla mia fidanzata Chiara. Descrivere con parole il nostro legame è davvero difficile, siamo ormai due persone che nelle loro imperfezioni si completano garantendo un tutt'uno indistruttibile. Mi sei stata accanto in tutto il percorso universitario, soprattutto nei momenti di fallimento, e sono certo che senza il tuo supporto e la tua vicinanza non sarei mai riuscito a raggiungere con facilità e successo i traguardi che mi sono posto davanti. Mi auguro che presto entrambi raggiungeremo i nostri successi professionali e che la distanza tra noi, che abbiamo dovuto accettare per inseguire i nostri rispettivi sogni, possa azzerarsi. Voglio inoltre menzionare gli amici "storici" Paolo, Giuseppe (x2), Federico, Massimiliano e Raffaele, conosciuti sui banchi di scuola ma ancora oggi gli uni accanto agli altri e Salvatore, Francesco, Domenico, Lucilla, Rosa e Ilaria, ovvero i fantastici ragazzi incontrati durante il mio percorso di laurea triennale. Per quanto distanti fisicamente, tutti voi siete e sarete sempre parte di me. Concludo ricordando i miei nonni Carolina e Pietro e i miei zii Anna, Antonio e Pietro, che purtroppo non ci sono più e con i quali avrei voluto festeggiare assieme il raggiungimento di questo traguardo. Sono certo che da lassù starete gioendo per me e che continuerete ad affiancarmi nel prosieguo del mio cammino di vita.

Contents

Acknowledgments **I**

List of figures **VI**

List of tables **X**

Introduction **1**

1 Background **5**

1.1 The current TTC system 5

1.2 The TTC-PON project 10

1.2.1 Downstream direction 13

1.2.2 Upstream direction 16

1.3 The PON transceivers 20

2 Proposal **24**

2.1 The reasons behind the quality assurance campaign 24

2.2 Figures of merit used in the test 26

2.2.1 Optical eye diagram 27

2.2.2 Extinction Ratio and Transmitter Power 33

2.2.3 Sensitivity 34

2.3 Technical specifications 35

2.3.1 Technical specifications of OLT modules 36

2.3.2 Technical specifications of ONU modules 39

2.4 Test structure 42

2.4.1 Preliminary phase 43

2.4.2 Measure and analysis of the transmitter and receiver parameters . . . 47
2.4.3 Saving test results . . . 52
2.5 Software contribution . . . 53

3 Experimental results **58**
3.1 General statistics . . . 58
3.2 OLT test . . . 59
3.2.1 Setup and calibration procedure . . . 59
3.2.2 Test results . . . 67
3.3 ONUs test . . . 70
3.3.1 Setup . . . 71
3.3.2 Test results . . . 76
3.4 Temperature test . . . 80
3.4.1 ONUs test . . . 80
3.4.2 OLT test . . . 88

Conclusion **92**

List of Figures

1 CERN Accelerator Complex 2

1.1 Overview of the TTC distribution in LHC experiments[1] 6
1.2 TTC system - Block diagram[2] 7
1.3 Bi-phase mark scheme 8
1.4 Fibre optic distribution network 9
1.5 Examples of various architectures of FTTX 10
1.6 Example of TTC-PON network in LHC experiments[3] 11
1.7 Example of connection through the GBT and the Versatile Link[4] 12
1.8 Frame transmitted by the OLT in the downstream direction[3] . 14
1.9 ONU burst[5] 16
1.10 First part of the oversampling scheme[6] 18
1.11 Second part of the oversampling scheme [6] 18
1.12 Calibration procedure[5] 19
1.13 Block diagram of a PON transceiver[7] 21
1.14 Analog burst-mode APC circuitry[7] 23

2.1 Photo of the system used to test the optical transceivers 26
2.2 Block diagram representation of the system 27
2.3 Working principle used by an oscilloscope to build the eye pattern of a digital stream composed by the sequences 011, 001, 100, and 110 28
2.4 Definition of the one and zero level [8] 29
2.5 Definition of eye height and eye amplitude [8] 30
2.6 Definition of crossing percentage [8] 30

2.7 Definition of deterministic jitter [8] 31
2.8 Definition of rise and fall time [8] 32
2.9 Definition of eye width [8] 33
2.10 Eye mask for OLT transmitter and recommended test set-up . 37
2.11 Extraction of the OLT Rx sensitivity specification at 10^{-4} BER 39
2.12 Eye mask for OLT transmitter and recommended test set-up . . 40
2.13 Sampling window for the burst mode optical eye diagram 41
2.14 Test structure - Block diagram 43
2.15 Eye scan - Block diagram circuit[9] 44
2.16 Eye scan - Working principle and graphical example[9] 44
2.17 Example of results for the system upstream calibration 45
2.18 Correct phase adjustment for the *OLT_RX* signal 46
2.19 Example of results obtained from the SFP IIC monitoring . . . 47
2.20 Eye diagrams for an OLT module non-compliant with the locking range criteria 48
2.21 Eye diagrams for an OLT module compliant with the locking range criteria 49
2.22 Mask margin for a compliant eye diagram 50
2.23 OLT receiver - sensitivity measure with dynamic range 51
2.24 Coding gain influence on ONU receiver sensitivity measure . . . 52
2.25 Example of report produced per each batch tested 53
2.26 Socket definition 54
2.27 Example of optimum offset analysis 56
2.28 Example of middle mask analysis 57

3.1 OLT test setup 60
3.2 OLT Tx - Instruments used for the characterization 61
3.3 OLT Rx - Instruments used for the characterization 62
3.4 Non-compliant OLT - BER vs OMA diagram 68
3.5 Lot diagram - Second batch 69
3.6 FPGA TX_{RESET} signal 70
3.7 ONUs test setup 71

3.8 Eye diagram and mask margin with the initial ONUs test setup 72
3.9 Evolution of the test setup used for the ONU modules 73
3.10 Improvements in the eye diagram and in the mask margin after the setup modification 73
3.11 Batches diagram - Mask margin in continuous mode 74
3.12 Batches diagram - RMS Jitter value in continuous mode 75
3.13 Instruments used in the downstream and in the upstream direction during the ONUs test 76
3.14 ONU n.284 - Sensitivity diagram in case of FEC application . . 77
3.15 ONU n.284 - Sensitivity diagram in case of FEC absence 77
3.16 ONU n.575 - Sensitivity diagram in case of FEC application . . 78
3.17 ONU n.575 - Sensitivity diagram in case of FEC absence 78
3.18 ONU n.265 - Eye diagram in continuous and burst mode 79
3.19 Internal short circuit in the non-working ONU module 80
3.20 Setup used for the first ONU temperature tests 81
3.21 Results of the temperature test on the modified ONU modules . 82
3.22 QA ONUs temperature test - Setup 83
3.23 Results of the temperature test for the ONU modules analysed from the pre-series 84
3.24 Results of the temperature test for the ONU modules analysed from the first batch 84
3.25 Results of the temperature test for the ONU modules analysed from the second batch 85
3.26 Results of the temperature test for the ONU modules analysed from the third batch 85
3.27 QA temperature tests - Power meter measurements for the modules analysed from the pre-series 86
3.28 ONUs QA temperature test - Power meter measurements for the modules analysed from the first batch 87
3.29 ONUs QA temperature test - Power meter measurements for the modules analysed from the second batch 87

3.30 ONUs QA temperature test - Power meter measurements for the modules analysed from the third batch 88
3.31 QA OLT temperature test - Setup 89
3.32 QA OLT temperature test - Tx Power measured by the power-meter 90

List of Tables

2.1 Nominal rates for the ONU and OLT transceivers - TTC-PON vs XG-PON 35
2.2 TTC-PON OLT operating line rates 35
2.3 TTC-PON ONU operating line rates 35
2.4 Numeric values for OLT eye mask coordinates 37
2.5 OLT Tx locking range 38
2.6 OLT - Criteria 3 specification values 38
2.7 Numeric values for ONU eye mask coordinates 41
2.8 ONU Tx locking range 41
2.9 ONU - Criteria 3 specification values 42
2.10 Accuracy of the parameters obtained with SFP IIC monitoring interface 47

3.1 Modules quantities to be delivered per batch 58
3.2 Instruments used for the OLT test setup 60
3.3 First phase measurements 64
3.4 Second phase measurements 64
3.5 Transceivers used for the network uniformity evaluation 65
3.6 Measurements of the ONUs received power 66
3.7 Total loss measurements 66
3.8 Devices used for the first temperature test 81
3.9 Data registered by the I2C monitoring interface during the first ONU temperature test 82

Introduction

Nowadays particle accelerators are used in many fields of research, and, because of this, they are one of the most powerful instruments we can find around us. Contrary to what people generally believe, accelerators are not only used to study particle physics. As an example, they are deployed in materials science to examine and develop new materials, in biological science to analyze the protein structure, and finally in the medical field to kill cancer cells thanks to radiation. This is only a small subset of their applications, but it is enough to understand their importance and their diffusion in the research.

The world's largest and most powerful particle accelerator is the Large Hadron Collider (LHC). It is only the last element in the accelerator complex used at CERN, which is shown in Fig.1. CERN, the European Organization for Nuclear Research, is a prestigious research center whose seat is in Geneva, but the previous mentioned accelerator complex is extended both in France and Switzerland. CERN's mission is to answer the questions about the Universe origin and, to this end, it designs, builds and operates particle accelerators and the associated experimental areas. The accelerator complex at CERN is a sequence of machines that progressively increase the energy of a beam of particles, and then inject it in the following one. Starting from a bottle of hydrogen gas and using the electric field, the electrons are removed from the hydrogen atoms to obtain protons. The latter are first accelerated in the Linac 2, reaching an energy of 50 MeV, then are injected into the Proton Synchroton Booster, where their energy arrives to 1.4 GeV, and following in the Proton Synchrotron (PS), which pushes the beam to 25 GeV. The next to the last

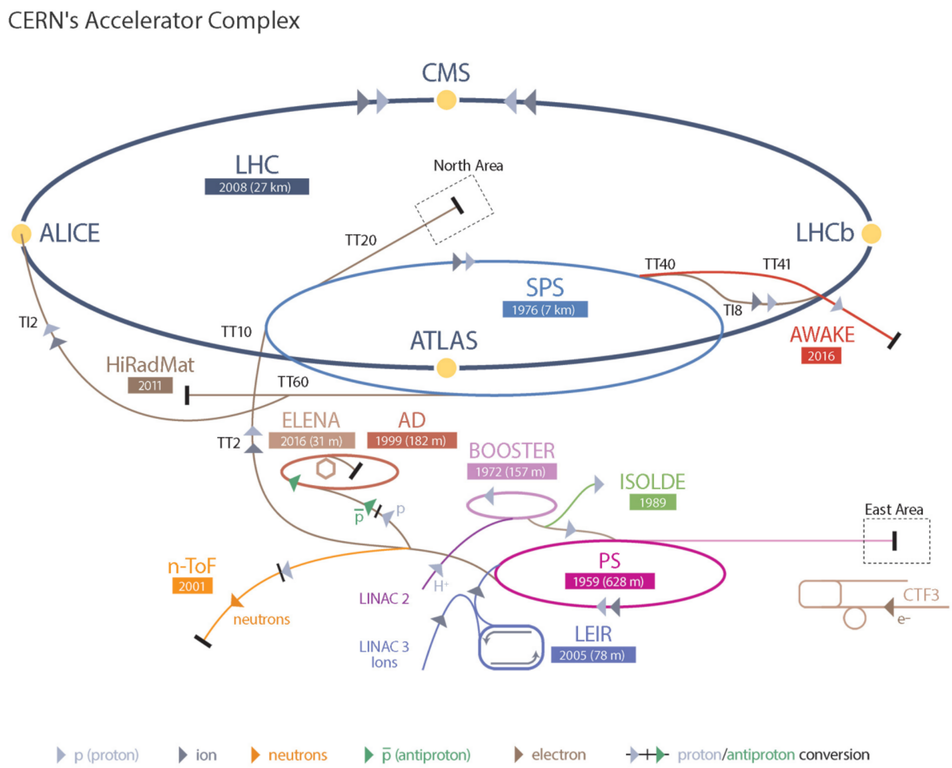

Source: *https://cds.cern.ch*

Figure 1: CERN Accelerator Complex

stage is the Super Proton Synchrotron (SPS) where protons are accelerated to 450 GeV. Finally, they are transferred to the two beam pipes of the LHC that are brought into collision inside four detectors, i.e. ALICE, ATLAS, CMS and LHCb. Distribution systems are required for the transmission of timing, trigger and control signals to the numerous electronic systems located in the detector caverns and in the underground electronics hall.[10] The system that provides this functionality is called Timing, Trigger and Control (TTC) system. Its first version was developed during the early 2000s, and it was based on an optical communication system that implemented a point-to-multipoint architecture where all the previously mentioned signals could travel only in one direction, i.e. from a global trigger unit to a front-end controller, but not vice versa. The design of the current TTC system was a remarkable work, but nowadays its performance and its concept are not keep up with the times.

Because of this, starting from 2010, a new project of TTC system based on Passive Optical Network (PON) started being conceived. The first version of the TTC-PON system was based on the FPGAs available at that time and on 1-Gigabit Ethernet PON transceivers. Its big innovation was the possibility to have a bidirectional link, but the data rate from the central trigger processor to local trigger units was limited to the value of 1.6 *Gb/s*, while it was 800 *Mb/s* in the opposite direction. In 2014 an upgrade of the project, called 10G-TTC-PON, was proposed. It included all the features of its predecessor, but with enhanced performance. More specifically, the data rates were increased in both directions and some new features were introduced, like the possibility to serve up to 128 nodes per network tree instead of 64, and various improvements in the downstream payload and in the trigger latency. Thanks to the progress of the PON technology, in 2017 a new version of the system, based on the XG-PON technology, was officially released. It ensured a data transmission rate of 9.6 *Gb/s* and 2.4 *Gb/s* in the downstream and in the upstream direction respectively, introduced the application of an error correcting scheme in the downstream direction, and used a new protocol in the upstream direction with a relative reduction of the latency achieved.

This thesis is related to the last version of the TTC-PON system, which will be entirely used by ALICE during phase-1 upgrade, while only the PON optical modules deployed in the system will be used by LHCb. They have to be compliant with the TTC-PON specifications, which are the sum of the specifications provided by the International Telecommunication Standard (ITU) for the XG-PON technology, and some other custom-made conditions based on CERN needs. In order to verify these components, which are provided by the Asian company **Go!Foton**, a quality assurance campaign was carried out. Its final aim was to characterize the PON modules measuring both the transmitter related parameters like the average power, the extinction ratio and the optical eye diagram, but also to evaluate the modules performance as receivers through the measure of the sensitivity. Furthermore, also some temperature tests were executed to verify that the modules were able to adapt to temperature variations within the operating range without showing performances degradation. The setups used for the testing were based on Kintex FPGA evaluation boards as data-generator or data-checker and various high-end laboratory instrumentation like high-speed oscilloscope, optical attenuator, clock generator, climatic chamber, et cetera, which were controlled over Ethernet or GPIB. The test routines were automated thanks to a custom-made Python library. Part of my work consisted of implementing test optimizations in view of saving time. Then, after becoming confident with this new coding language, I wrote autonomously the test routine for the temperature test and some other scripts useful for the next generation TTC-PON system targeting the phase-2 upgrades of the LHC experiments. After the execution of the test routines for all the components, I carried out a deep-analysis of the data gathered from the various components in order to detect and analyse any module out-of-specification or any quality discrepancy over the production process.

The thesis is intended to describe the quality assurance campaign I was responsible for. To this purpose it has been subdivided into three chapters, which can be summarized as follows:

- in **Chapter 1** the background information will be provided. I will present a general overview of the current TTC system and of the TTC-PON concept and features;
- in **Chapter 2** the proposal is defined. The reasons why the QA campaign was carried out, the kind of tests performed, the test structure, and the main figures of merit used to characterize the modules will be specified;
- in **Chapter 3** I will describe the setups used for testing the OLT and the ONU modules and I will present the experimental results focusing on the non-compliant modules detected.

Chapter 1

Background

This chapter defines the main features of the TTC system currently used in the LHC experiments. More specifically, the main limitations of this system will be underlined in order to figure out the need of an upgrade. In this regard, the TTC-PON system will be presented firstly describing the concept behind it, and then focusing on its main features. In the last part of the chapter, a brief description of the PON modules will be provided. These information are fundamental to fully understand the quality assurance process carried out on the optical modules deployed in the system.

1.1 The current TTC system

All the LHC experiments require an element that ensures the distribution of the trigger, timing and control information to the various sub-detector front-end and read-out systems. These consist of the 40 Mb/s bunch-crossing clock, the orbit signal, the level-1 trigger decision, bunch and events numbers, and various reset commands or calibration parameters. Directly from the LHC machine interface it is possible to acquire the bunch-crossing clock, which ensures the correct bunch crossing identification, and the orbit signal that is a square wave long 5 ns at the revolution frequency for the two rings of the LHC. These signals are recovered from the interface thanks to an apposite circuitry, and then they are distributed from the Prevessin Control Room to the Trigger Control System (TCS) through single-mode optical fibres, like is shown in the following figure.

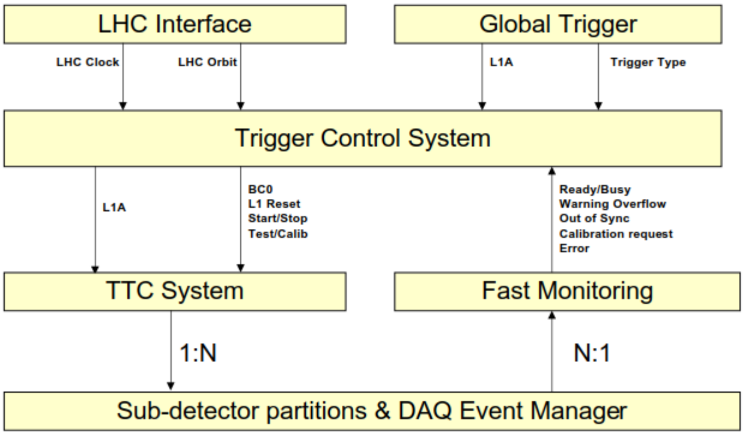

Figure 1.1: Overview of the TTC distribution in LHC experiments[1]

Meanwhile, the Global Trigger Unit performs the final steps of the trigger algorithm and provides to the TCS also the L1 trigger decision (L1 accept or L1A) and the trigger type. To explain the functionality of the trigger signal is important to specify that, in each detector, physicists want to select only a certain type of events and they need to identify the bunch crossing from which the latter come from. In order to detect properly the event of interest, there are different levels of selection in which complex algorithms define the value of the trigger decision. Therefore, the TCS receives the trigger decision of the highest level (the level 1) and the type of event that is reported by the trigger signal. Following the TCS performs various functions, like the generation of the commands distributed by the TTC system, the generation of calibration and test sequences for the trigger signal, the processing of the feedback from the sub-detector partitions, and finally the regulation of the transfer rate of the L1A. [1] Once the context in which the TTC system operates is clarified, is now possible to examine and describe this network more in-depth.

The TTC system is an optical communication system that implements a point-to-multipoint architecture thanks to the use of optical splitters and uni-directional fibres. Furthermore, to complete the main elements that define the structure of the system, it is worth mentioning that also some VME modules are used to perform various functions. In the figure 1.2, few of them are reported, i.e the TTCvi, the TTCex, and the TTCrx. The TTCvi module has the important task of selecting the trigger source from the different input trigger signals. Following the chosen trigger source is made available on the communication channel indicated as channel A. All the remaining control commands are sent on the other channel, labelled as channel B. The TTCex module receives the information sent from the TTCvi on the two channels, and multiplex and encode the data to transmit them to the TTCrx modules through the optical fibre network. The channels are sampled alternately each half period of the clock signal, that is LHC bunch clock, and then encoded on the base of a Bi-Phase Mark (BPM) scheme driven by an internal PLL with very low jitter.[2]

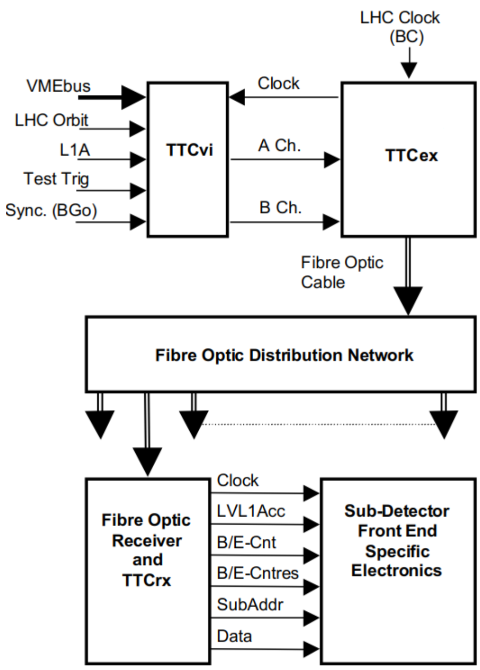

Figure 1.2: TTC system - Block diagram[2]

In this scheme the logical one is represented as a pair of two different bits (10 or 01), while the logical zero by a pair of equal bits (00 or 11). Each logical

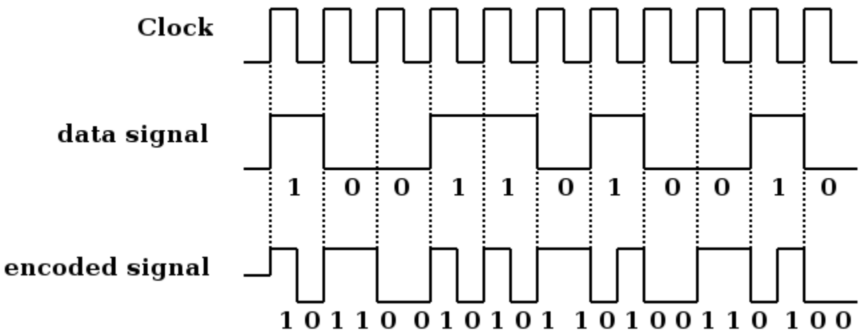

Source: *https://it.wikipedia.org*

Figure 1.3: Bi-phase mark scheme

level at the beginning of a cell is inverted with respect to the level at the end of the previous cell. This scheme allows better synchronization since there is a polarity reversal at least every two bits. In this way it is possible to avoid long sequences of zeros or ones that would cause synchronization problems. The only disadvantage is the doubling of the clock frequency. This problem is handled by a PLL frequency synthesizer circuit inside the TTCex module. Moreover, inside the module there is also the laser transmitter that ensures the transmission of the encoded data over the optical fibre network toward the TTCrx module. The latter works as interface between the optical network and the front-end buffers. It is a radiation hardened Application Specific Integrated Circuit (ASIC) that performs two main functions, i.e. to recover and distribute the LHC bunch clock with a low jitter, and to decode and provide the data sent by the TTCex module.[11]

Two limitations of this system are related to the high latency between the input of the TTCvi module and the output of the TTCrx module, and to the low bandwidth for both channel A and channel B, which is 40 *Mb/s*. To understand properly the other shortcomings of the current TTC system, it is necessary to observe in detail the fibre optic distribution network.

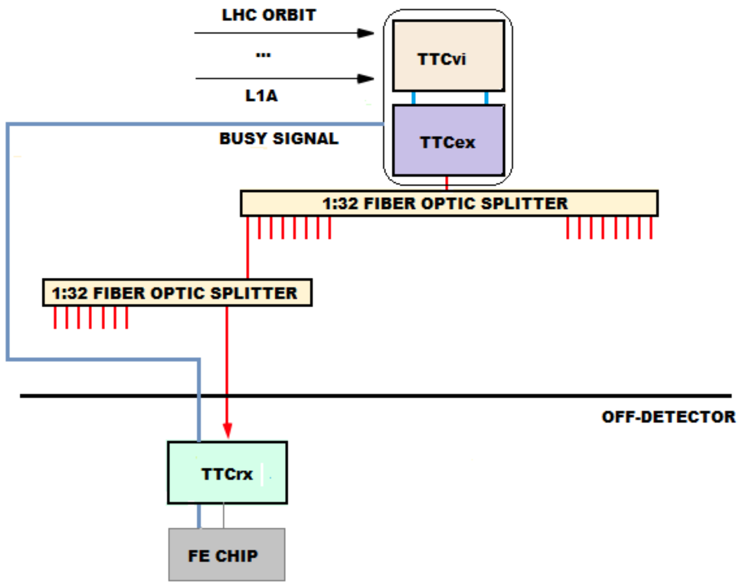

Figure 1.4: Fibre optic distribution network

In figure 1.4 is shown how the useful signals are distributed thanks to a hierarchy of various fibre optical splitters. The main problem is that the maximum split ratio the current system is able to achieve is 1:32, which can be considered a quite limited value with respect to the number of front-end buffers that need to receive the timing, trigger and control information. Moreover, such a system requires a control of the front-end buffers. For this purpose is adopted the busy signal, which is a separate electrical link used to communicate the status of the buffers. This signal is generated when the buffer is nearly full and is not able to receive other data. It is not part of the optical network since the system, how it has already been said several time, is unidirectional and, therefore, the information can move through the fibres towards the front-end buffers but not vice versa.
To conclude this overview about the current TTC system, is useful to summarise its main limitations that have been underlined so far:

- Low bandwidth in the two channels used to send the trigger, timing and control information (40 Mb/s);

- High latency in the transmission between the TTCvi modules and the

TTCrx modules;

- Limited maximum split ratio in the optical network (1:32);
- Need of a separate electrical link to communicate the state of the front-end buffers due to the unidirectional optical fibre based transmission scheme.

1.2 The TTC-PON project

The TTC-PON project was first proposed in 2010 as a possible solution to overcome the limitations of the TTC system mentioned in the previous section. The project is based on two commercial applications widely adopted in the telecommunications field, i.e "fibre to the x" (FTTx) and passive optical networks. The FTTx is a broadband network architecture that uses optical fibres to provide all or part of the local loop in the last mile telecommunications. On the other hand, passive optical networks are a telecommunication technology that implement a point-to-multipoint architecture where optical splitters are used to enable a single optical fibre to serve multiple ending points. With regard to the distance between the optical fiber and the end user, it is possible to distinguish different architecture of FFTx. In the figure 1.5 some of them are represented.

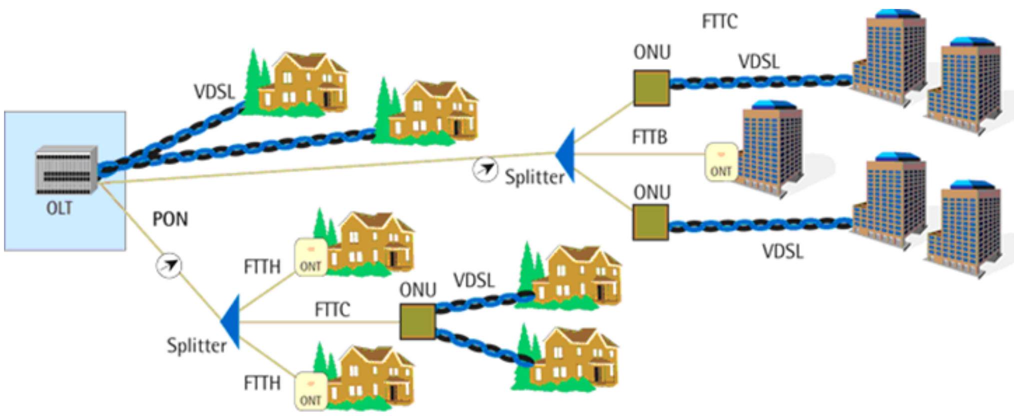

Source: *https://www.3-edge.de*

Figure 1.5: Examples of various architectures of FTTX

As an example, the FTTH, which stays for “Fibre to the Home”, is a kind of network where the fibre moving from the Optical Line terminal (OLT) reaches the boundary of the living space of the final user arriving to an Optical Network Terminal (ONT). Instead, the FTTC, which means ”Fibre to the Cabinet”, is an architecture based on the use of fibre optic cables right up to the Optical Network Unit (ONU) and, then, on the classical VDSL connection to arrive to homes and buildings. In these networks the information can be exchanged in two different directions. From the master node, which is the OLT, to the slave nodes, which are the ONUs or the ONTs, is referred to as downstream direction, whereas, vice versa, as upstream direction. In the downstream direction the OLT broadcasts packets to all the slave nodes, while in the upstream direction a channel arbitration mechanism is used to prevent overlapping between multiple transmissions by the various slaves. [12] The scheme in use in the TTC-PON system is the time division multiple access. In figure 1.6 is shown an example of TTC-PON network used in the LHC experiments.

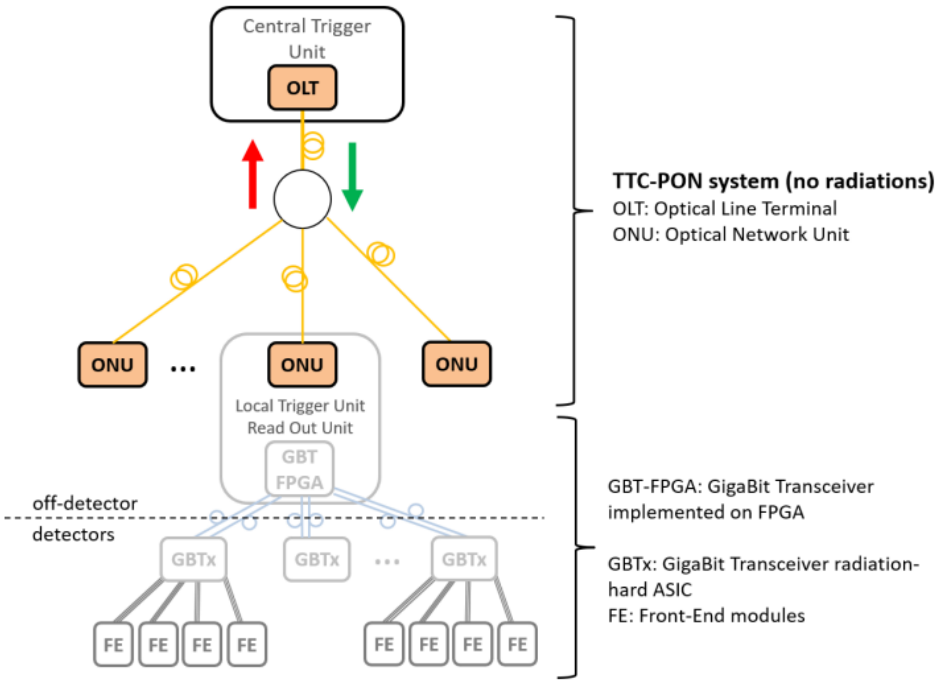

Figure 1.6: Example of TTC-PON network in LHC experiments[3]

In the central trigger unit there is an OLT module, which works as master node, sending the timing and control information to various ONU modules, which behave as slave nodes, located in local trigger units or in read-out units. The connection between OLT and ONUs is realized with optical fibers and optical splitters. The most important difference with respect to the current TTC system is that between the OLT and the ONUs there is a bidirectional link. In fact, there is no more need of the separated electrical link to communicate the status of the front end buffer, since this information can arrive directly to the OLT through the optical fiber. Moreover, another difference is that the VME modules described in the first part of this chapter are no longer used. The functionalities that were previously provided by the TTCex and the TTCrx are now implemented in some Field Programmable Gate Arrays (FPGAs) used at the top and at the end nodes of the optical tree. The TTC-PON system is a back-end system, therefore to communicate with the detectors another link is needed. The figure 1.6 shows a link example based on two complementary parts, i.e. the Versatile Link opto components and the GBT link chips. The ensuing image represents in detail this kind of link.

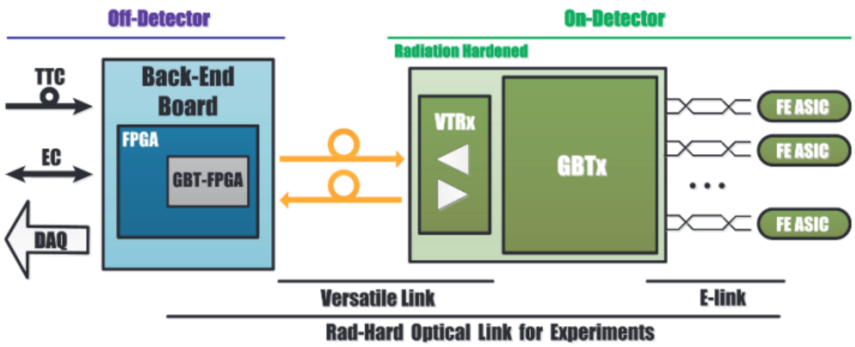

Figure 1.7: Example of connection through the GBT and the Versatile Link[4]

The Versatile link is a bi-directional digital optical data link characterized by many features, like the radiation hardness and the tolerance to high magnetic field. The architecture of the link is based on a simple scheme. In the back-end there is a transceiver or an array of transceivers, in this case the ONU modules, while in the front-end there is typically a Versatile Transceiver (VTRx), which is a bidirectional radiation-hardened custom-developed module

in compliance with the SFP+ form-factor. On the base of different requirements in terms of bandwidth in the upstream and in the downstream direction, it is also possible to use as front-end component a Versatile Twin Transmitter (VTTx), which is a unidirectional module with the same features of the VTRx. The link between the front-end components and the back-end components is provided thanks to optical fibres.[13] In the detector side, in addition to the VTRx there is also the GBTX. It is a radiation-hardened ASIC that sends the TTC and the experiment control (EC) information to the front-end buffers, and reads their status thanks to an electrical link called E-link. On the other hand, in the back-end side the board with the ONU modules also includes a FPGA programmed with the GBT-FPGA VHDL based firmware that sends the TTC and the EC information toward the detector, and also transmits data to the Data AcQuisition (DAQ).[4] However, the TTC-PON protocol does not fix the link between the off-detector zone and the on-detector zone, therefore also different link implementations are possible.
So far the last mentioned improvement introduced by the TTC-PON system is the possibility to have a bidirectional link. To present the other advantages, it is important to examine in-depth the protocol and the main features of the system both in the downstream and in the upstream direction. This is the aim of the following paragraphs.

1.2.1 Downstream direction

In the downstream direction, i.e. from the OLT module to the ONU modules, there is a broadcast at 9.6 *Gb/s* with a wavelength of 1577 *nm*. The frames transmitted by the OLT are based on a bunch clock period basis. More specifically, the frame is composed by 240 bits per bunch clock and it is divided in four fields, like it is represented in figure 1.8.

The first eight bits in the header field (HDR) are used for the frame alignment, the following 4 bits are for the system monitoring and for the internal initialization (Slow Control field), and then the final user has 200 bits of payload each 25 *ns*. The whole frame is protected with a forward error cor-

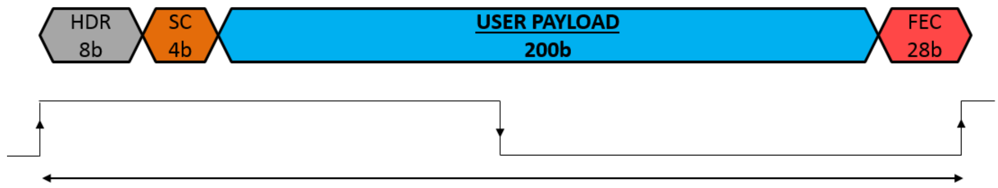

Figure 1.8: Frame transmitted by the OLT in the downstream direction[3]

rection (FEC) scheme that is based on Bose–Chaudhuri–Hocquenghem (BCH) codes that allow double random errors correction. This feature ensures to have around 3 *dB* of coding gain with 88.5 % efficiency in the downstream path. Moreover, on the top of the FEC there is also a Cyclic redundancy check (CRC) protection for the slow control field, since it carries some sensitive information for the system to work properly. In this approach a fixed number of check bits are appended to the data stream to be transmitted, and the receiver checks them by calculating the remainder of the polynomial division of the contents transmitted. The FEC scheme was proposed to ensure a higher optical margin for a 1:64 network (in reality the system is able to support a maximum split ratio of 1:128 giving up on a larger optical margin) and to improve the system power performance in the downstream direction.[5] It is a technique used in data transmission by the receiver to detect and correct errors without asking for the re-transmission of the data packet. In fact, adding redundancy bits in the information sequence, the latter can be reconstructed by the receiver even in presence of noise and interference, at the expense of a lower and fixed bandwidth. FEC codes are mainly divided in two categories, i.e. block codes and convolutional codes. The first family of codes is based on a partition of the information stream into messages of k elements. Then each message is mapped to a bigger block of n elements, defined as codeword, with n-k redundant bits added, called parity bits, to the k element word. In this way, when the transmitter wants to send a long stream, the latter is divided in multiple messages that are then encoded in blocks where the information bits are followed by parity bits. These blocks are sent to the receiver that, using decoding mechanism, tries to recover the original message starting from eventually corrupted blocks. This family of code is memory less and uses longer codewords in comparison to convolution codes, even if achieving the same quality. These last have a completely different working principle since they do not need to segment the data stream into blocks of fixed size and, as a consequence, they encode the entire data stream into a single codeword. Moreover, there is also a difference in the encoding strategy. In fact, the encoder in the convolutional codes has a memory and therefore is implemented with sequential logic circuits. Thanks to this memory, the information bits are not followed by parity bits like in block codes, but they are spread along the sequence. In the downstream path the TTC-PON project is based on a FEC scheme through block codes due to the previously described frame-nature of the protocol. Among the various codes available in literature, like Hamming codes and cyclic codes, the BCH codes, how it has already been said, were the selected ones. The reason why they were chosen is their low complexity and their good quality in the detection and the correction of random errors.[14] The last feature to underline in the downstream direction is that, differently from what is usually required in the telecommunication applications, the system has to show a fixed and deterministic latency following a reset or a switch on. This result is obtained circumventing the internal FIFO of the transceivers and performing a phase and frame alignment procedure.[5]

Concluding this subsection about the features in the downstream path, it is interesting to summarise the main improvement achieved by the TTC-PON system in this direction with respect to the current TTC system:

- Low and deterministic latency;
- Increase of maximum split ratio in the optical network, currently equal to 1:64 with 3 dB of optical margin, but with the possibility to reach 1:128 with a reduced security margin;
- Higher user bandwidth (200 bits per bunch clock, which means 8 Gb/s).

1.2.2 Upstream direction

In the upstream direction the ONU modules transmit information to the OLT module. How it has already been said, a TDMA scheme is adopted to avoid overlapping between various ONU modules bursts. In this scheme each ONU has a fixed window of 125 *ns* for the transmission, which has a different data rate compared to that in the downstream direction. In fact, in the upstream path it is 2.4 *Gb/s* with a wavelength of 1270 *nm*. It is relevant to have very short bursts because an important parameter for the whole system is the so called waiting time, which is the time between two consecutive transmissions by the same ONU. This parameter is crucial since it will be translated in the busy latency for the feedback system. Therefore, shorter are the bursts, lower is the waiting time and, as a consequence, lower is also the latency in the upstream direction. To shorten the burst duration, designers tried to minimize as much as possible the first two fields of the burst structure, which is represented in figure 1.9.

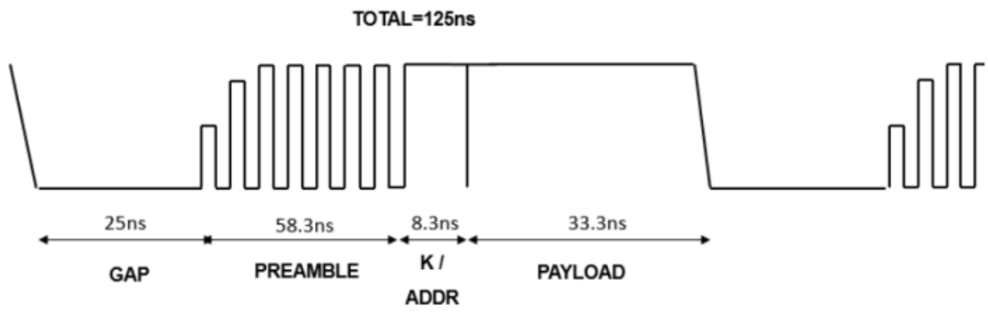

Figure 1.9: ONU burst[5]

It is divided in four main fields, i.e the gap, the preamble, the K/Address and the user payload. To understand the meaning of the overhead (gap and preamble), it is necessary to define the main difference between continuous and burst mode receivers. In the first case, the average power of the signal transmitted to the receiver is not rapidly variable, while in burst-mode transmission it can change significantly in very short time intervals. Therefore, the receiver must be able to adapt to these rapid changes in the power level of the incoming signal. For this purpose, the preamble is a long sequence of zeros and ones that is used by the burst-mode receiver to adapt to the threshold of the incoming burst. On the other hand, in the gap field there is an external reset that is used, how the XG-PON standard suggests, to delete the power setting related to the previous burst, and to get ready for the incoming one.[5] To conclude the explanation about the meaning of the four fields, it is worth mentioning that the field K/Address is used to have the frame alignment and to communicate the address of the ONU that is transmitting to the OLT, while the user payload contains eight bits for the system monitoring and for the internal initialization and 56 bits of data destined to the master node. These last are encoded with the 8b/10b scheme. This is an encoding algorithm where eight bits of data are transmitted as a word, called symbol, 10 bits long. In particular, the low five bits of the original data are encoded into a 6-bit group, while the remaining three bits are encoded into a 4-bit group. From the combination of these two groups of bits it is possible to obtain the final symbol. Starting from the checksum and the encoding tables of the 3b/4b portion and of the 5b/6b portion is achievable the reconstruction of the original data. The main advantage of this encoding scheme is to reduce the number of re-transmissions and to detect single-bit errors.

An important feature in the upstream direction is that the ONU transmission has to be synchronous to the OLT clock. This can be ensured thanks to an external phase locked loop (PLL) that cleans the clock signal recovered from the downstream direction, and then drives the PLL of the FPGA boards where the ONUs are connected. A further characteristic in the upstream direction is the fast phase alignment of the short bursts received by the OLT. This alignment is necessary since the various bursts have random phases between them. Using the classical clock and data recovery schemes, the time needed to recover the acquisition phase would be too high. Therefore an oversampling method is adopted to solve this problem. More specifically, in the upstream direction the ONUs are transmitting at 2.4 Gb/s, which means 20 bits transmitted at 120 *MHz*. The OLT, instead, can work at 9.6 Gb/s since it has not to recover the clock thanks to the synchronous transmission of the ONUs. As a result, it receives 80 bits at 120 *MHz*. Therefore for each bit transmitted by the ONU, the OLT can receive four bits. In this way a $\times 4$ oversampling scheme is possible. The 80 bits received by the OLT are divided in 20 groups of 4 bits. Three other copies of the sequence transmitted by the ONU are stored, but each one is shifted by an additional bit, like it is shown in figure 1.10.

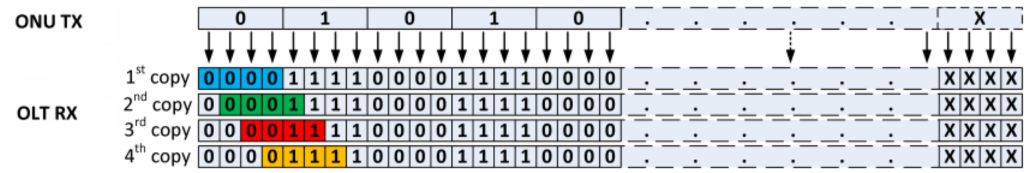

Figure 1.10: First part of the oversampling scheme[6]

For each group of four bits of the four copies, it is possible to find out if the ONU sent a "0" or a "1" and if the sample contains an edge thanks to a look-up table and an algorithm. The final results are four words of 20 bits characterized by different phases, like in figure 1.11. Following, four parallel word aligners try to align the data searching for a comma. Typically only one or two of them are able to detect it and, therefore, to provide useful output data.[6] Thanks to this scheme the phase is updated continuously for each ONU burst with a very high speed.

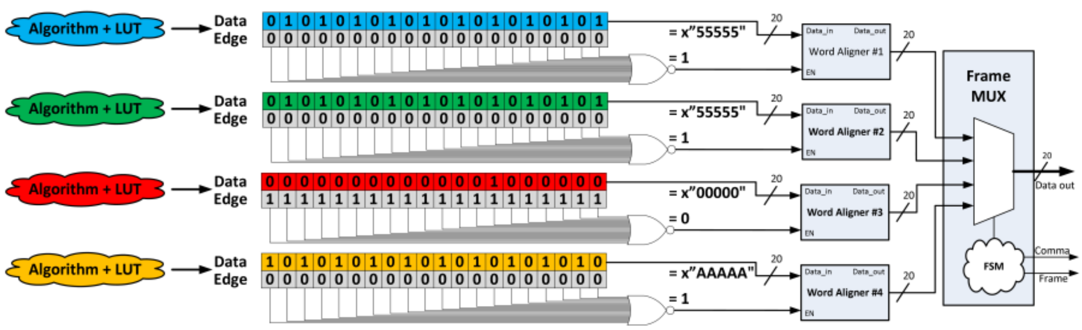

Figure 1.11: Second part of the oversampling scheme [6]

The last fundamental procedure used in the upstream direction is the calibration process. From a theoretical point of view, since the number of the ONUs used in the system and the upstream bandwidth allocated to each ONU are fixed, every ONU can have the same internal counter used to know when they can transmit to the OLT. Just an offset value added to this counter could be enough to avoid the collision. In the system this counter is reset each time the slave receives a specific signal, named heartbeat, that is broadcasted to each ONU with a period $T_{HB} = N_{ONU} \times 125\ ns$. Therefore, looking to the ONU burst in figure 1.12, is clear that in addition to the classical header that is sent each 25 ns, there is now also a heartbeat header with a period equal to T_{HB}. If the heartbeat signal arrives contemporary to all the ONUs, the offset is enough to avoid collisions. At the contrary, if the heartbeat signal is not simultaneous to all the slaves, there could be a collision. In a real system, a classical situation where this could happen is when the optical fibre lengths are not equal.

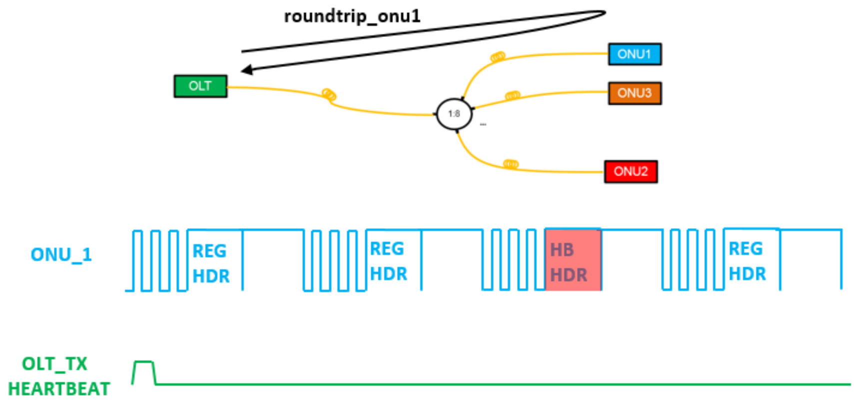

Figure 1.12: Calibration procedure[5]

To remedy this eventuality a calibration procedure is executed. It is arbitrated by the OLT module, which measures the roundtrip time for each ONU of the system through the following operations:

1. The OLT module sends a heartbeat header;

2. The ONU under test enters in calibration mode, which consists of an

operation mode where it sends back the received header in a continuous way behaving as a comma-mirror. During this phase all the other ONU modules disable transmission;

3. The OLT module can measure the roundtrip time by measuring the time distance between the transmitted heartbeat header and the received one.

Once the roundtrip latency measurement for each ONU is over, a compensating offset value is added on the base of the latency measured to avoid the overlapping between bursts.[5]

1.3 The PON transceivers

The components that were tested in the quality assurance campaign are the OLT and the ONU transceivers that ensure the connection between the central trigger processor and the local trigger unit and/or the read-out buffers in the detectors. A transceiver is a device that is composed both from a transmitter and a receiver, which share the same circuitry to guarantee the correct functionality. More specifically, a PON transceiver is a particular type of transceiver that shares different wavelengths to receive and send information. Typically the OLT transceiver is more complex than the ONU transceiver since, while it has to communicate with a high number of slaves, the ONU has to interact with only one master. This higher complexity has a direct outcome in terms of cost. In fact an OLT module has a price that is usually five times higher than that of an ONU module. The PON transceivers are mainly based on two different protocols, i.e. Ethernet Passive Optical Networking (EPON) and Gigabit Passive Optical Networking (GPON). Without going into details since this is not a fundamental point in this thesis work, the main differences are related to a different architectural approach and different efficiency, bandwidth, costs and management. In the TTC-PON system, the transceivers are based on the XG-PON technology, which is the latest version of GPON, even if some parameters like the data-rates in the downstream and in the upstream direction are modified on the base of CERN's needs.

To understand which are the main electronic components that are used inside a PON transceiver, it is useful to observe the block diagram in figure 1.13. The transmitter structure is synthesized by the sequence of a laser diode (LD), which generates the optical signal when is correctly stimulated, and a driver that either modulates the current conducted by the laser diode, in this case we talk about laser driver, or modulates the voltage across a modulator when external modulation is used. In the latter situation the driver is called modulator driver.

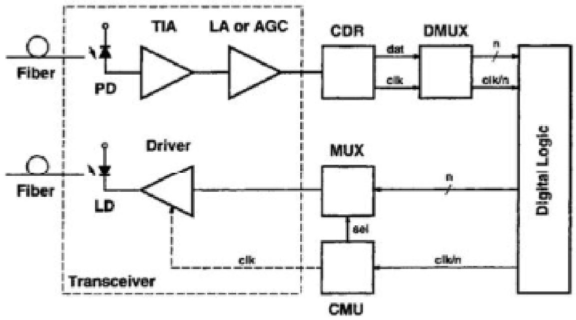

Figure 1.13: Block diagram of a PON transceiver[7]

Considering a laser driver, its main functions are:

1. To regulate the laser current when a logical zero is transmitted or, considering an ONU transceiver, between two consecutive bursts. In these situations the current should be turned off;

2. To reduce as much as possible the turn on and the turn off time, especially for the ONU when it is working in burst mode. This feature could be ensured with a bias current always above the threshold value.

Since these two requirements are in contrast, what is usually done is to keep the bias current equal to zero only between two bursts, while it is set to a value higher than the threshold for the duration of the burst. Other design strategies are based on the idea of switching off the laser current also when a logical zero is transmitted and not only between two bursts. Moreover, to shorten the turn off time, the use of shunt transistors to drain the carriers from the laser diode is frequently adopted.

The receiver structure is based on three main components, i.e. a photodiode (PD), a transimpedence amplifier (TIA) and a main amplifier that is realized in the *Go!Foton* modules as a limiting amplifier (LA). In general, another possibility is to use an automatic gain amplifier (AUG) instead of the aforementioned LA. The PD receives the optical signal and transforms it in a current that is amplified by the LA and then converted in a voltage. Following, the main amplifier amplifies additionally this voltage. From the design point of view there are many possibilities both in the choice of the photodiode and in the various amplifiers used. For example, the photodiode could be implemented both with a PIN diode and with an avalanche diode. The latter, thanks to its working principle, is characterized by a higher sensitivity but, at the same time, has a higher price, a higher added noise, and the need of a compensation circuitry to take in account the dependence between temperature and gain. About the amplifiers, choosing the LA it is possible to obtain higher performances in terms of power dissipation, bandwidth or noise, but using an AGC there is the advantage of having a linear transfer function and, as a consequence, a simple analog post-processing on the output signal. [7]

Another important element that is used in the *Go!Foton* transceivers and that is not shown in the block diagram in figure 1.13 is the microcontroller. It is used to implement a diagnostic monitoring interface. In fact, all the diagnostic and monitoring information are handled by the latter, which is accessible via I2C protocol. These diagnostic data are digitalized starting from internal analog signal, while the monitoring, which is performed with a a system of alarm and warning flags, is possible thanks to the generation of some status bits that are compared with factory preset limits. To have further information about the system and monitoring interface, it is possible to refer to the *SFF-8472* standard.

The last fundamental circuit that is used in PON transceivers and that will be recalled in the following chapters of the thesis is the Automatic Power Control (APC). Its main task is to avoid the degradation of the light output power despite ambiental and temperature variations. The APC circuit can be implemented both with analog and digital circuitry. In figure 1.14 there is a burst-mode APC in an analog version. The control on the power is implemented through the comparison between the voltage proceduced by the transimpedence amplifier and a reference voltage fixed by the manufacturer. The same circuit can be used also to detect when the transceiver is entering in the end-of-life phase. In this case the reference voltage, that is always chosen by the manufacturer, is a lower value compared with that used in the APC circuit.

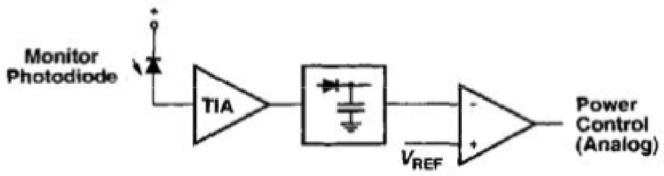

Figure 1.14: Analog burst-mode APC circuitry[7]

Chapter 2

Proposal

This chapter presents the main information related to the reasons that led to the quality assurance campaign and the test structure. Furthermore, the technical specifications used and the figures of merit adopted for the transceivers characterization will be described and motivated. Some details concerning the Python code used will be omitted by virtue of confidentiality requirements.

2.1 The reasons behind the quality assurance campaign

Before describing the proposed solution for testing the optical transceivers, it is appropriate to clarify the reasons why the quality assurance campaign has been conducted. In this respect, it could be objected that since all the received components had already passed the manufacturer quality assurance, our QA campaign is redundant and meaningless. In reality, there are three main reasons that justify its need. The first one is that the manufacturer tests the optical transceivers against the specifications of the PON protocol we use, which is the XG-PON, provided by the International Telecommunication Union (ITU). But how it has already been said, we have a set of specifications that is only partially based on the ITU specification, since in addition there are some further conditions that came from our specific needs. Therefore, we need to test the modules against our tailor-made specifications rather than against the ones fixed by the ITU, which are universally adopted in the transceiver market. The second reason is that we perform a kind of test that is different from the one executed by the manufacturer. In fact, we carry out a system level test, while the manufacturer execute a component test. There are many explanations to justify this choice. Firstly, doing a component test we would not have had the time to test all the modules. In fact, in our system level test we can test more than one module at the same time and thanks to this all the components were tested in time. Furthermore, doing a system level test we have the possibility to detect some failures that a component test would not be able to show. Moreover, we also have the chance to observe how the modules behave in a configuration that is closer to that our users can adopt. Finally, the last reason that account for our QA campaign can be explained with a popular idiom, i.e. *"trust is good, but control is even better"*. In fact, even if the manufacturer does a careful quality assurance process, no one ensures that all the modules will work properly. This is exactly what we fully realized with our QA campaign and that will be clearer in the last chapter when I will describe the test results.

Since the concept of system level test has been introduced, it is appropriate to specify how our system is composed. In this sense is useful to observe the figure 2.1, where the system itself is shown. It is composed by an OLT and eight ONUs. On the bottom-left hand side, the OLT is plugged through the SFP+ module connector available on the TTC-PON FMC module, which in turn is connected to the FMC HPC connector of the Xilinx KCU105 board. The TTC-PON FMC is a tailor-made module designed by CERN engineers specifically for this project. Its specifications and features are reserved. Following an optical splitter ensures the connection to the eight ONU slaves. In the foreground of the figure there are four Xilinx KC705, each one connected with two ONU modules. One of them is directly plugged inside the SFP+ module connector located on the board, while the other is connected to the TTC-PON FMC module in the same way as the OLT module. Furthermore, each Xilinx KCU705 board is connected to an external PLL to recover and

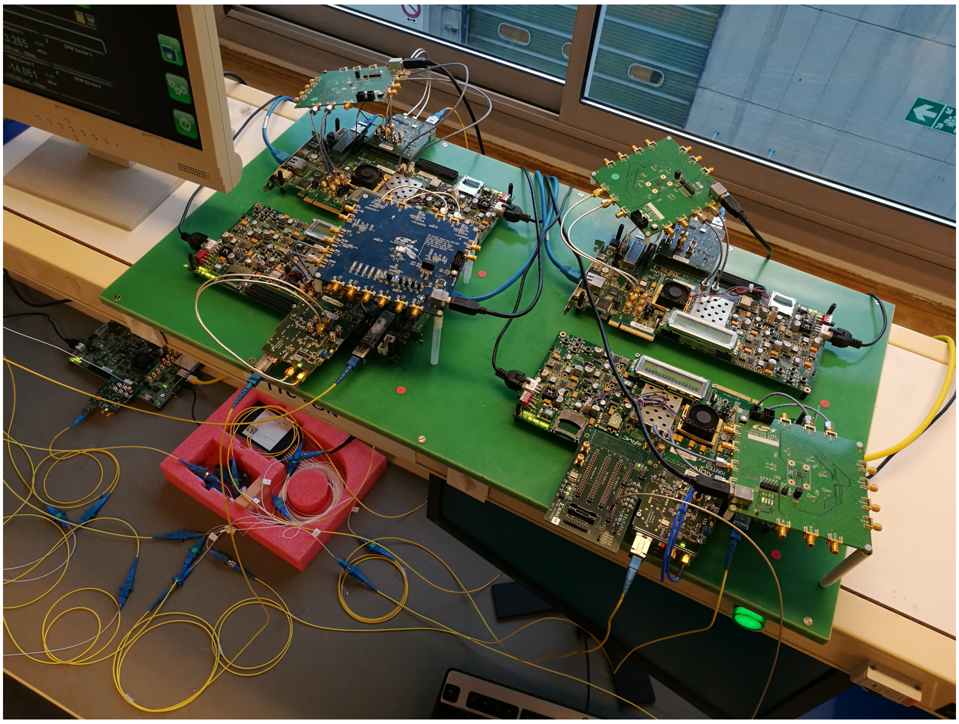

Figure 2.1: Photo of the system used to test the optical transceivers

clean the clock signal from the downstream direction, and, in addition, the bottom right board is connected to the Xilinx FMC XM105 Debug Card that is used to carry the trigger signal to the scope.
From this point forward, especially when in the last chapter the experimental setups will be presented, the system will be represented as a block diagram like is shown in figure 2.2.

2.2 Figures of merit used in the test

In order to evaluate the performances of the ONU and the OLT transceivers as transmitters and receivers, in our test we measure and monitor some fundamental parameters. From the transmitter point of view we adopt as figures of merit the optical eye diagram, the extinction ratio, and the average value of the transmitted power. From the receiver perspective, we measure the sensitivity. In the following subsections the definition and the meaning of these parameters are provided.

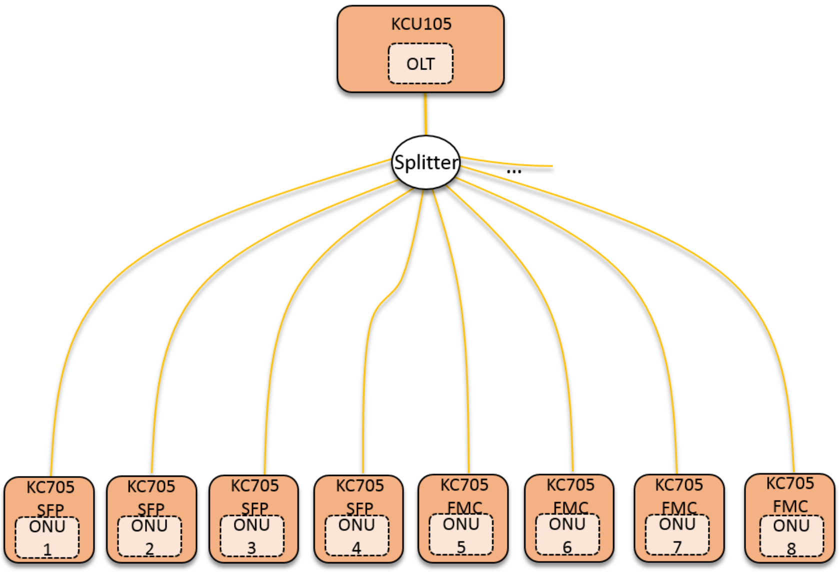

Figure 2.2: Block diagram representation of the system

2.2.1 Optical eye diagram

The eye pattern is a tool used to verify the quality of a digital stream in optical transmission. In fact, eye diagrams ensure a complete analysis of serial data giving useful information about the signal integrity and the problems that could afflict the transmission path. The measurement instrument used to build these diagrams is the oscilloscope. It receives the digital stream under test and samples it in little chunks that are accumulated and then superimposed on the screen. Higher the number of samples accumulated, more statistically relevant the eye pattern is. The name of the diagram derives from the fact that the final result observable on the oscilloscope screen remember in its shape a human eye. The principle according to which the eye diagram is built by the oscilloscope can be better understood by observing the graphic example shown in figure 2.3.

Many parameters can be extracted to describe amplitude and time characteristics of an eye diagram. It is relevant to specify that they are automatically evaluated by the oscilloscope. Starting from the amplitude related ones, they include:

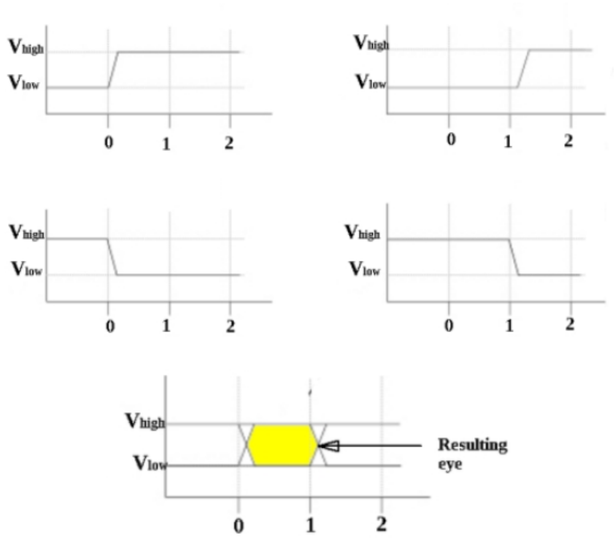

Source: *https://www.testandmeasurementtips.com*

Figure 2.3: Working principle used by an oscilloscope to build the eye pattern of a digital stream composed by the sequences 011, 001, 100, and 110

- One and Zero Level

  To define these levels is useful to observe the figure 2.4. The diagram on the right shows the starting time/voltage digital stream. It is initially characterized by a regular sequence of ones and zeros, while thereafter it starts becoming more irregular with clusters of consecutive zeros and ones. The arrows are used to highlight the ones and the zeros. The diagram on the left, instead, is the resulting optical eye where the one and the zero levels are clearly indicated. They are respectively defined as the mean value of the top and the bottom peak of the vertical histogram built from the samples captured inside the middle 20% (40 to 60% points) of the eye period.

- Eye Amplitude and height

  The eye amplitude is simply the difference between the one level and the zero level of the eye diagram calculated as described previously. The data receiver logic circuits will determine whether a received data bit is a zero or a one basing on the eye amplitude. On the other hand, the

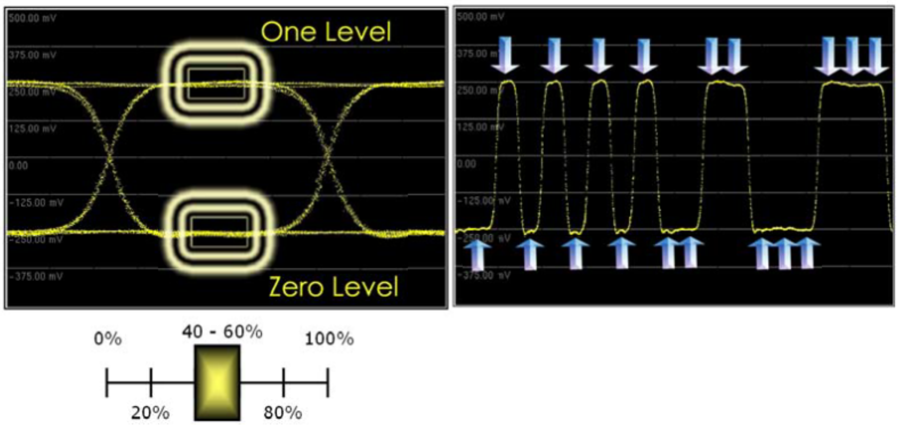

Figure 2.4: Definition of the one and zero level [8]

eye height is a measure of the vertical opening of an eye diagram. This parameter can be evaluated when the color grade persistance is on in the oscilloscope. It ensures to show the optical eye in different colors corresponding to frequency and voltage level on a per pixel basis. The eye height is calculated on the base of the following equation:

$$Eye\,height = (V_{top} - 3\sigma_{top}) - (V_{base} + 3\sigma_{base}) \tag{2.1}$$

where V_{top} and V_{base} are the one and the zero level respectively, σ_{top} is the standard deviation of the top peak in the vertical histogram, and σ_{base} is the standard deviation of the bottom peak in the vertical histogram. The eye height is a very important parameter since it ensures to understand how the noise overlapped on the signal is influencing his integrity. In fact, higher is the noise more closed is the eye and, therefore, lower is the eye height.

- Eye crossing percentage

  Defining the crossing level as the mean value of the vertical histogram centered on the crossing point of the eye, the eye crossing percentage can be evaluated with the following formula:

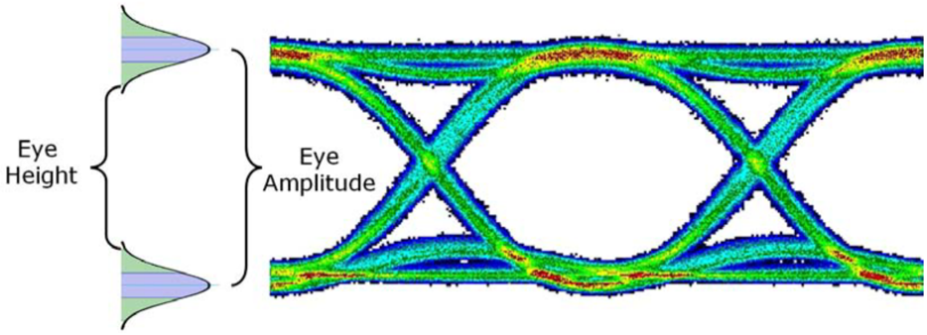

Figure 2.5: Definition of eye height and eye amplitude [8]

$$Eye\,crossing\,percentage = 100 * \frac{crossing\,level - V_{base}}{V_{top} - V_{base}} \tag{2.2}$$

The graphical interpretation of this parameter is shown in the figure 2.6. The eye crossing percentage is useful to have an indication about the duty cycle distortion of the signal stream or the asymmetry of the signal transmitted. The perfect value for this parameter is 50%, since it means that the stream is exactly symmetric. If the value is higher than 50%, the time duration of logic ones is higher than that of logic zeros and, as a consequence, the crossing point is pushed up. Vice versa, a value lower than 50% can be explained with zeros longer in duration than ones and with the crossing point moved down in the eye pattern.

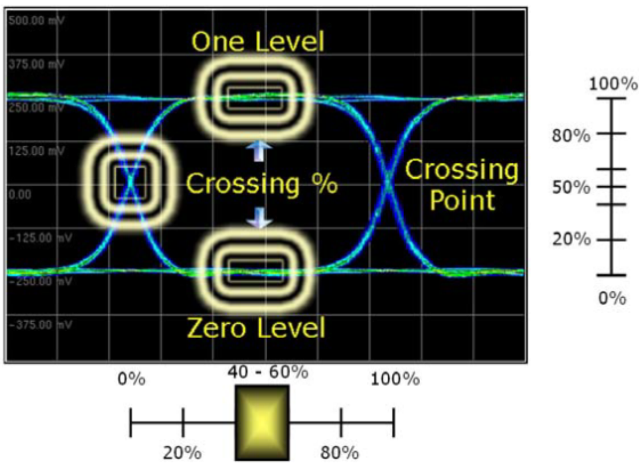

Figure 2.6: Definition of crossing percentage [8]

About the time related parameters, they can be defined as follows:

- Deterministic jitter

  The deterministic jitter is defined as the time deviation of a data-bit event from its ideal timing. This is one of the most important parameters to monitor in an eye diagram. The timing variations of the rising edge and the falling edge are evaluated over the crossing points of the eye to extrapolate this parameter. It is possible to express the jitter in terms of peak-to-peak value, mean value and root mean square (RMS) value. In our test we monitor the RMS jitter value. It is defined as the standard deviation of the time histogram across the crossing point, as shown in figure 2.7.

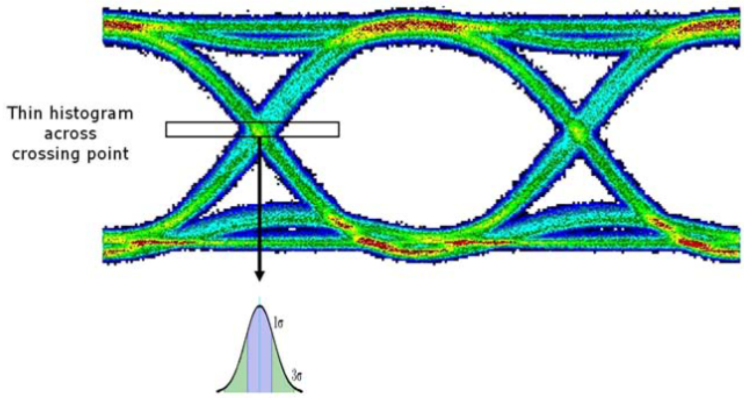

Figure 2.7: Definition of deterministic jitter [8]

- Fall and rise time

  The rise time is defined as the transition time to move from the 10% (or 20%) level to the 90 % (or 80%) level on the upward slope of an eye diagram. Vice versa, the fall time is the transition time of the data from the 90 % (or 80 %) level to the 10 % (or 20 %) level on the downward slope of an optical eye. In this definition the percentage levels are referred to the one and the zero level. The oscilloscope evaluates these parameters subtracting the mean value of two thin histograms placed at the appropriate percentage level, like is shown in figure 2.8.

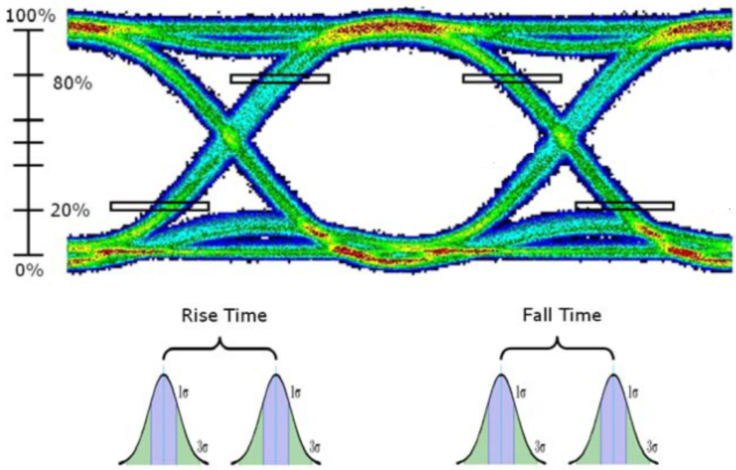

Figure 2.8: Definition of rise and fall time [8]

- Eye width

  The eye width is a measure of the horizontal opening of an eye diagram. In principle, it should be measured between the crossing points of the eye. However, noise and jitter cause a large variance in their location and this result in the closure of the eye. In our case, the oscilloscope adopts the following equation to calculate this parameter:

$$Eye\,width = (t_{cross,left} - 3\sigma_{cross,left}) - (t_{cross,right} + 3\sigma_{cross,right}) \quad (2.3)$$

  The graphical meaning of this parameter is depicted in figure 2.9.

In conclusion, eye diagrams are a fundamental tool to analyze the quality of an optical digital data stream. In fact, thanks to the various parameters that can be extracted from them, a complete investigation about amplitude and timing distortions can be carried out.

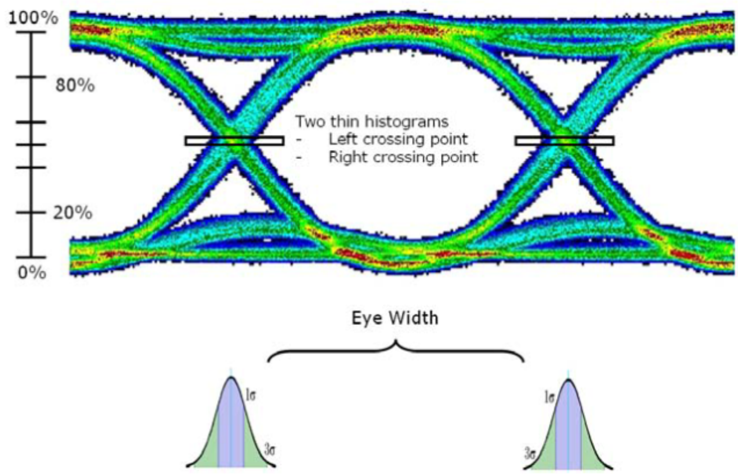

Figure 2.9: Definition of eye width [8]

2.2.2 Extinction Ratio and Transmitter Power

The extinction ratio (ER) is another important parameter used to analyze the quality of an optical signal. It is the ratio between the optical power used in transmitting a binary one divided by that used in transmitting a binary zero. This quantity may be expressed as a power measurement in dB, or as a percentage according to the following formulas:

$$ER_{dB} = 10 \cdot \log_{10} \frac{P_1}{P_0} \qquad ER_{\%} = 100 \cdot \frac{P_1}{P_0} \tag{2.4}$$

In an ideal transmitter, P_0 would be zero and thus the ER would be infinite. However, in the optical transceivers the laser diode is biased so that P_0 is close to the laser threshold. Therefore, a certain amount of optical power is emitted even at the zero level, thus $P_0 > 0$ and the ER is a finite number. The measure of this parameter is suddenly critical since it requires a very accurate measurement of the zero level as it is in the denominator of the equation. For low power levels it is very difficult to discern a binary zero and a binary one and, as a consequence, the estimation of the extinction ratio is affected by large errors. This parameter has an important impact on the system performance and has a close relationship with the bit-error ratio (BER). It is recalled that the latter indicates the number of errors per unit time in a data stream and is calculated as the number of bit errors divided by the total number of transferred bits during a fixed time interval. As the ER increases, the BER improves meaning that there is a reduction of the error bits. Vice versa, a decrease of the ER value will be translated in a worst BER and, therefore, in a power penalty (PP) for the system. This last is defined as the increase of signal power needed to achieve the same BER performance to compensate the system degradation.

About the transmitter power, it is simply the power associated to the the signal transmitted by the optical transceiver. This quantity can be measured both in milliwatt and dBm (DeciBels at one Milliwatt), which is a unit of level used to indicate a power level in decibel (dB) referenced to one milliwatt. The decibel-milliwatt is widely used in fibre-optical communication networks since it ensures to express both very large and small values in a compact form. Because of this in our test we adopt this unit of measure to express both the transmitted power and the received power by the optical transceivers.

2.2.3 Sensitivity

The receiver sensitivity is defined as the the minimum optical modulation amplitude (OMA) of the input signal required to obtain an output that achieves a certain condition. In our test this condition is about the value of the BER on the output signal. Moreover, about the sensitivity definition, it is useful to point out that the OMA is the difference between the power associated to the logical one and that associated to the logical zero. Therefore, the sensitivity defines how faint an input signal should be in order to be successfully received, where the grade of satisfaction is specified by the BER value at which we evaluate the sensitivity. Obviously the lower the sensitivity, the better is. According to the definition previously provided, the sensitivity is a negative number and, in our test, it is expressed in dBm. In this case the larger the absolute value of the sensitivity is, the better is.

2.3 Technical specifications

All the specifications and features that the ONU and the OLT transceivers have to respect are provided in the price enquiry, which is the document produced by the engineers responsible for the TTC-PON project to find a manufacturer able to supply optical modules with that characteristics. As it has already been said several times, the modules have to be compliant with the specifications provided by the ITU for the XG-PON technology, defined in the ITU-G.987 standard, and some additional requirements on the base of CERN needs. More specifically, the main discords between the ITU standard and the XG-PON specifications are the protocol and the line-rate. About the nominal rates, the differences can be understood from the following table:

Transmission Direction	XG-PON Nominal Rate [Gbit/s]	TTC-PON Nominal Rate [Gbit/s]
Downstream	9.95328	9.61896
Upstream	2.48832	2.40474

Table 2.1: Nominal rates for the ONU and OLT transceivers - TTC-PON vs XG-PON

	Tx Rate [Gbit/s]	Rx Rate [Gbit/s]
OLT	9.61896	2.40474

Table 2.2: TTC-PON OLT operating line rates

	Tx Rate [Gbit/s]	Rx Rate [Gbit/s]
ONU	2.40474	9.61896

Table 2.3: TTC-PON ONU operating line rates

Therefore, the line-rates for the TTC-PON project are slightly different from the ones indicated in the XG-PON standard, more precisely by 3% . The reason is that they have to be a multiple of the LHC radio frequency clock, thus the values provided from the standard are not suitable. In terms of protocol, which has been fully described in the first chapter, the main difference with

the standard is the short length of the ONU bursts. In fact, in the XG-PON standard it is in the microsecond order, while in the CERN protocol it is 125 *ns*. Due to the short length of these upstream frames, another difference is that the upstream data recovery at the level of the OLT is not ensured by a Clock and Data Recovery scheme, as usually happens in the XG-PON protocol, but rather by a $\times 4$ oversampling scheme.
In general, all the specifications are based on the aforementioned standard, and some of them are also ported to the CERN line-rates. One CERN specific request is about the locking range, which is not fixed in the ITU recommendation, to ensure a reasonable margin around the LHC operating frequency. Since the technical specifications the OLT and the ONU transceivers have to be compliant with are different, they will be described separately in the next two paragraphs.

2.3.1 Technical specifications of OLT modules

The first two basic requirements that the OLT modules have to respect are the implementation of all the PON signals as specified in the SFF-8431 and the ITU-T Gseries Recommendations, and the implementation of the diagnostic monitoring interface for optical modules as defined in the SFF-8472 specification. Furthermore, in the quality assurance campaign we verify that the OLT modules are compliant with respect of the following criteria that shall be fulfilled at an ambient temperature between 10 and 70°C.

- Criterion 1: Optical Eye Diagram

  The OLT transmitters shall present eye diagrams compliant with the mask defined in the ITU-T G.987.2 Recommendation when transmitting continuous frames at standard line rate, but also at CERN specific downstream line rate. In the figure 2.10 and in the table 2.4 the mask, the recommended setup and the relative coefficients are shown.

  In our QA campaign the optical transmitter is tested using the board Xilinx KCU105 as data sender, the board Xilinx KC705 as data checker,

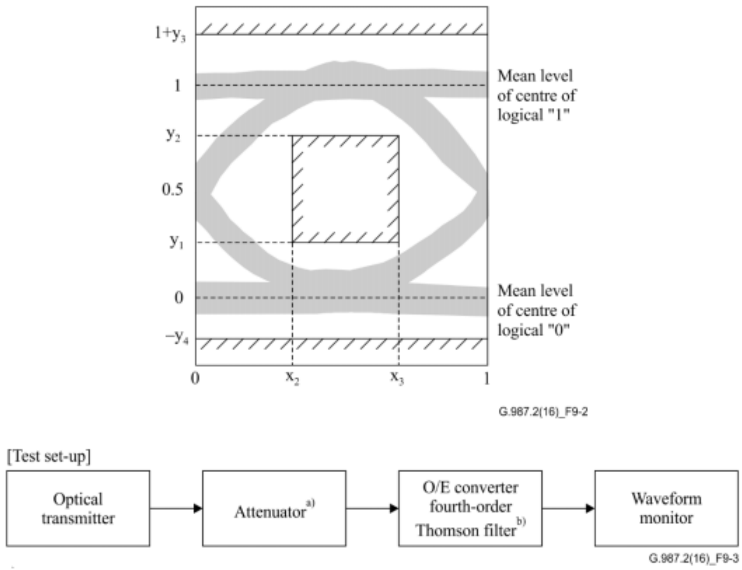

Figure 2.10: Eye mask for OLT transmitter and recommended test set-up

Coordinate	Value
$x_3 - x_2$	0.20
y_1	0.25
y_2	0.25
y_3	0.25
y_4	0.25

Table 2.4: Numeric values for OLT eye mask coordinates

and implementing the fourth-order filter with a cut-off frequency of 7.2 *GHz* thanks to the low-pass filter function of the oscilloscope used to display the optical eye diagram. In this kind of test, usually referred as eye mask compliance test, we compare the eye diagram with the mask defined by the ITU and if there are no samples in the keep-out area, the optical eye is compliant, otherwise it is non-compliant. The eye mask and the comparison with the eye diagram evaluated through the oscilloscope are implemented via software thanks to a Python script and are completely automated.

- Criterion 2: Locking Range

  This is a specific CERN request not included in the ITU specifications according to which the OLT transceiver shall be able to lock in the minimum range of line-rates indicated in the table 2.5.

	Minimum Line Rate [Gbit/s]	Maximum Line Rate [Gbit/s]
OLT Tx locking frequency	9.3	10.2

Table 2.5: OLT Tx locking range

- Criterion 3: Transmitter power and extinction ratio

  As suggested in the ITU standard, the mean value of the transmitted power by the OLT modules at the CERN downstream line rate shall be in a fixed range, and the corresponding extinction ratio shall be higher than a fixed minimum measure. The reference values are provided in the table 2.6.

Parameter	Unit	Value
Mean transmitted power MIN	dBm	4.0
Mean transmitted power MAX	dBm	8.0
Minimum extinction ratio	dB	8.2

Table 2.6: OLT - Criteria 3 specification values

- Criterion 4: OLT Receiver sensitivity (upstream)

  According to the ITU-T G.987.2 recommendation, the end-of-life sensitivity (EOL) of OLT receivers evaluated at 10^{-4} BER shall be equal or less than –29.5 dBm using a pseudorandom binary sequence (PRBS) 2^{23}-1 pattern sequence. A PRBS is a binary random sequence that, even if generated by a deterministic algorithm, shows a behaviour similar to that of a real random sequence. Converting this value in OMA using a standard extinction ratio of 8.2 *dBm*, the equivalent value is -27.8 *dBm* at EOL. Adopting a standard penalty of 0.5 *dBm* for the ageing of the receiver, the CERN sensitivity specification at the beginning-of-life (BOL) for the OLT receiver at CERN upstream line rate of 2.40474 *Gbit/s* is defined as below:

$$BOL\,OLT\;Rx\;Sensitivity\,(OMA)\;at\,10^{-4}\;BER < -28.3\;dBm \quad (2.5)$$

In addition to the ITU specification, CERN requires a receiver sensitivity (OMA) of -24 dBm or below at 10^{-11} BER reference level. This requirement has to be verified using again a PRBS 2^{23}-1 pattern sequence at the CERN upstream line rate. This value is extrapolated from the ITU recommendation at 10^{-4} BER as shown in figure 2.11. It uses the 0.5 *dB* ageing factor, and ensures that no error floor is observed at higher attenuation.

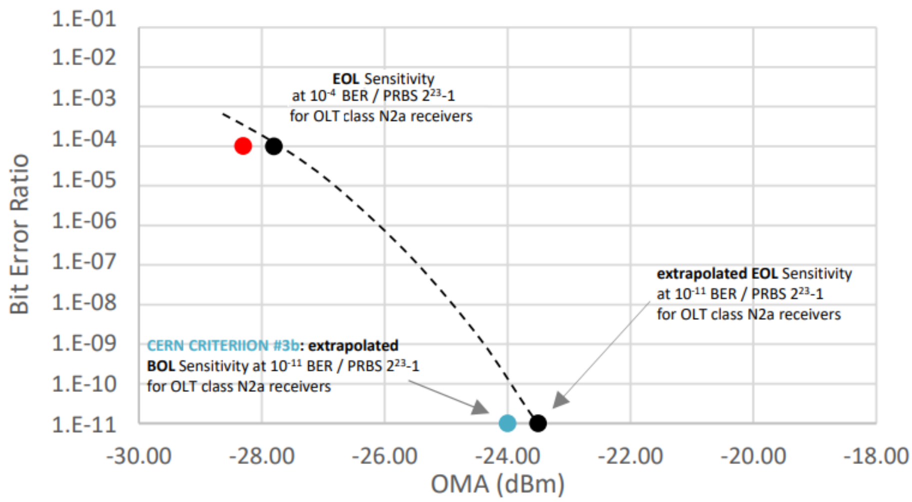

Figure 2.11: Extraction of the OLT Rx sensitivity specification at 10^{-4} BER

2.3.2 Technical specifications of ONU modules

Also for the ONU modules the first two basic requirements are the implementation of all the PON signals as specified in the SFF-8431 and the ITU-T Gseries Recommendations, and the realisation of the diagnostic monitoring interface for optical modules as described in the SFF-8472 specification. In the quality assurance campaign we verify that the modules are compliant with the following four criteria that should be respected in the temperature range between 10 and 70°C.

- Criterion 1: Optical Eye Diagram

  The ONU transmitters shall present eye diagrams compliant with the masks defined in the ITU-T G.987.2 Recommendation when transmitting burst frames at standard line rate, but also at CERN specific upstream line rate of 2.40474 *Gbit/s*. The eye diagram according to this criteria shall be evaluated in burst mode. It means that the optical eye is obtained sampling the original signal through a fixed acquisition window from the beginning of the preamble to the end of the payload of the 100 *ns* burst. This principle is shown in figure 2.13. In terms of setup, in this case we use the board Xilinx KC705 as data sender, the board Xilinx KCU105 as data checker, and we implement the fourth-order filter with a cut-off frequency of 1.8 *GHz* thanks to the low-pass filter function of the oscilloscope used to display the optical eye diagram.

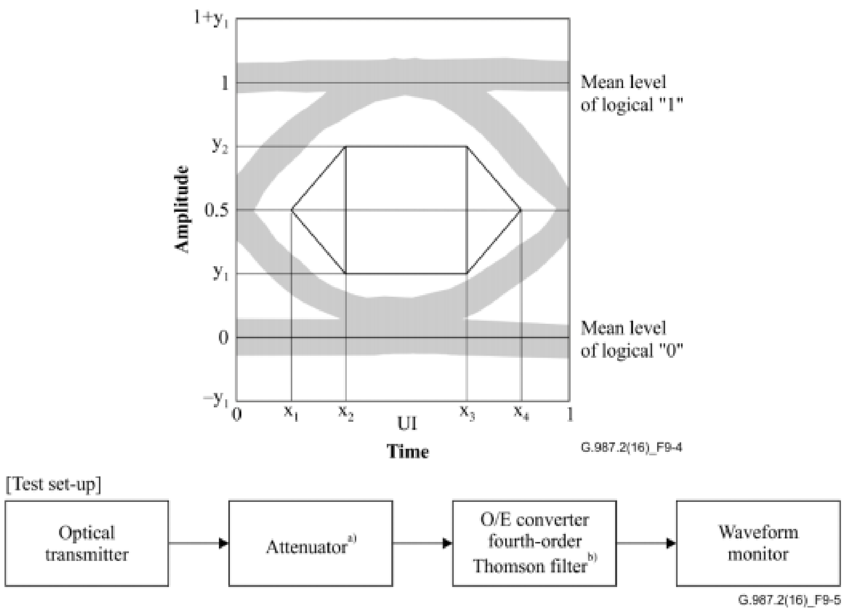

Figure 2.12: Eye mask for OLT transmitter and recommended test set-up

Coordinate	Value
$x_3 - x_2$	0.20
y_1	0.25
y_2	0.25

Table 2.7: Numeric values for ONU eye mask coordinates

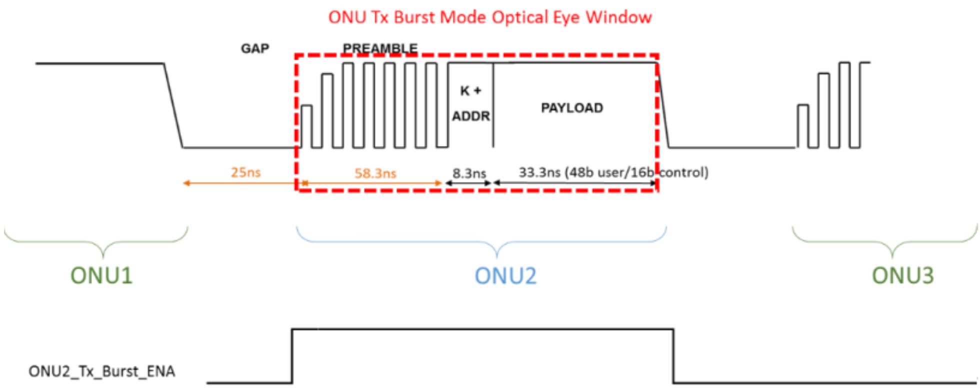

Figure 2.13: Sampling window for the burst mode optical eye diagram

In reality, as it will be explained in the next paragraph, we evaluate the eye diagram also in continuous mode even if there is not a defined specification. In this case no sampling mask is used. All the ONU modules are disabled with the last exception of the ONU module analysed and the resulting signal is used for the optical eye diagram.

- Criterion 2: Locking Range

  The ONU transceiver shall be able to lock in the minimum range of line-rates indicated in the following table.

	Minimum Line Rate [Gbit/s]	Maximum Line Rate [Gbit/s]
ONU Tx locking frequency	2.2	2.6

Table 2.8: ONU Tx locking range

- Criterion 3: Transmitter power and extinction ratio

  As defined in the ITU recommendation, the mean value of the power transmitted by the ONU modules at the CERN upstream line rate shall be in a fixed range and the corresponding extinction ratio shall be higher than a fixed minimum amount. The reference values are provided in the following table.

Parameter	Unit	Value
Mean transmitted power MIN	dBm	2.0
Mean transmitted power MAX	dBm	7.0
Minimum extinction ratio	dB	8.2

Table 2.9: ONU - Criteria 3 specification values

- Criterion 4: ONU Receiver sensitivity (downstream)

  According to the ITU-T G.987.2 recommendation, the end-of-life sensitivity (EOL) of ONU receivers evaluated at BER equal to 10^{-3} shall be equal or less than –28 dBm using a PRBS 2^{23}-1 pattern sequence. Converting this value in OMA using a standard extinction ratio of 8.2 *dBm*, the equivalent value is -26.3 *dBm* at EOL. Adopting a penalty of 0.5 *dBm* for the ageing of the receiver, the CERN sensitivity specification at the beginning-of-life (BOL) for the ONU receiver at CERN downstream line rate is defined as:

  $$BOL\,ONU\;Rx\,Sensitivity\,(OMA)\,at\,10^{-3}\,BER < -26.8\,dBm \quad (2.6)$$

  In addition to this criteria, CERN requires a receiver sensitivity (OMA) of -22 dBm or below at 10^{-11} BER reference level using again a PRBS 2^{23}-1 pattern sequence. This value is extrapolated from the ITU recommendation at 10^{-3} BER with a procedure identical to that already presented for the OLT receivers, and using the 0.5 *dB* ageing factor ensuring that no error floor is observed at higher attenuation.

2.4 Test structure

The general structure of the QA test we execute for the OLT and the ONU modules can be summarised with the scheme in figure 2.14. Before starting measuring all the figures of merit previously described, there is a preliminary phase related to the system diagnostic. It is based on three different tools, i.e the electrical eye scan, which is referred to the ONU modules of our system, the internal calibration and the SFP IIC monitoring. Then the real test starts, we measure the OLT or the ONU transmitter and receiver related parameters, systematically we save the results obtained, and finally doing a comparison between the measured parameters and the TTC-PON specification we conclude whether the module is compliant or not. In the preliminary operations there is no difference between the ONU and the OLT test, while there are some dissimilarities in the type of analysis that are executed in the two tests. The various steps in which the test is divided are separately described in the following subsections.

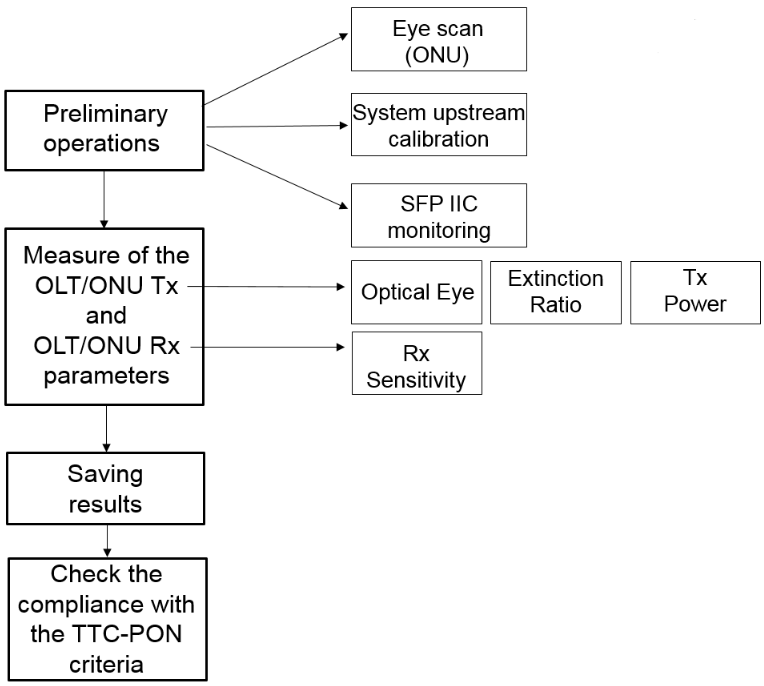

Figure 2.14: Test structure - Block diagram

2.4.1 Preliminary phase

Proceeding with the same order adopted in the scheme in figure 2.14, the first tool used in this phase is the eye scan. It is a functionality offered by the 7-series Xilinx FPGA to visualize the post-equalization signal quality in a receiver, which is an ONU module in our system. The eye scan is based on the comparison between the sample acquired by the CDR data sampler and the one obtained by a second sampler that can be programmed providing horizontal and vertical offsets, which correspond to time and amplitude offsets respectively. This architecture is shown in figure 2.15.

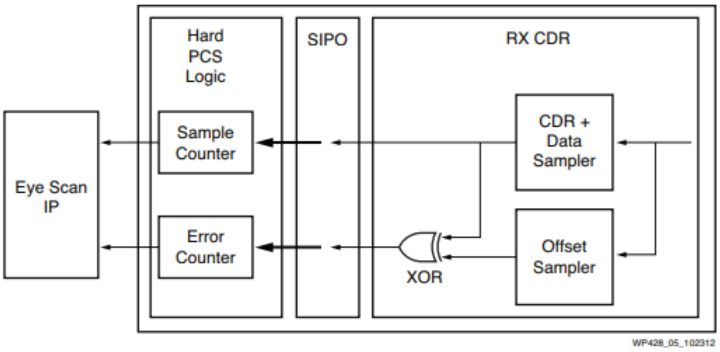

Figure 2.15: Eye scan - Block diagram circuit[9]

A fixed number of bits are transmitted per each offset setting. If the samples are not equal, the error counter is incremented. The eye scan IP calculates the BER dividing the number of errors by the fixed number of bits transmitted. Finally, it correlates the various bit error rates calculated with the offsets analyzed to build statistically the electrical eye diagram.[9] An example of eye scan is reported in figure 2.16.

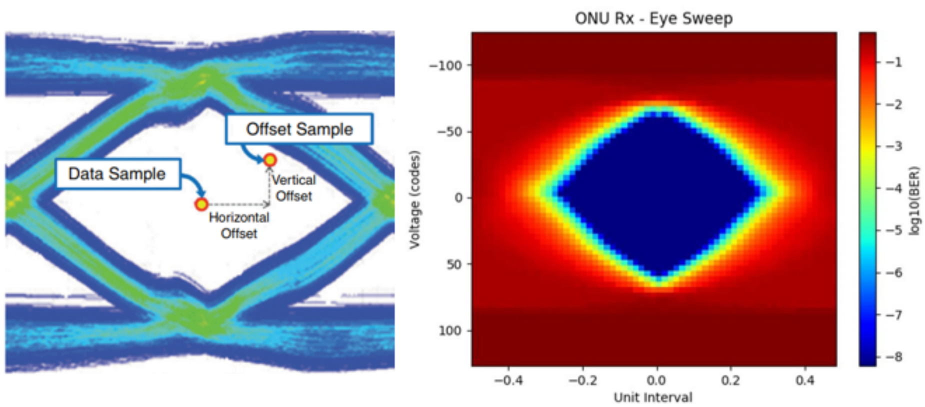

Figure 2.16: Eye scan - Working principle and graphical example[9]

The second tool is the system upstream calibration. This procedure is implemented via software through a Python script and allows to adjust the timing of some OLT signals modifying the phase of the ONU modules. It is in this step that the calibration procedure described in the first chapter is executed. As an example, the result of the script can be observed for a subsystem of 4 ONU modules in figure 2.17 . In a first moment the OLT tries to detect the various slave transceivers measuring for each one the roundtrip time. When an ONU is detected, thanks to the IIC monitoring interface also its received power is displayed. In this example, one of the four ONU modules was not detected due to a bad connection with the SFP+ connector of the Xilinx KC705 board. This shows how this procedure is useful also in this sense, since it ensures to detect any improper connection before going on with the test. Following, the offset of the ONU modules is adjusted so that the *OLT_RX* signal has a value equal to a binary one when an ONU is transmitting, and is equal to a binary zero between two bursts. For example, assuming seven time units burst length plus one time unit for the gap, the behaviour of the signal shall be that illustrated in figure 2.18.

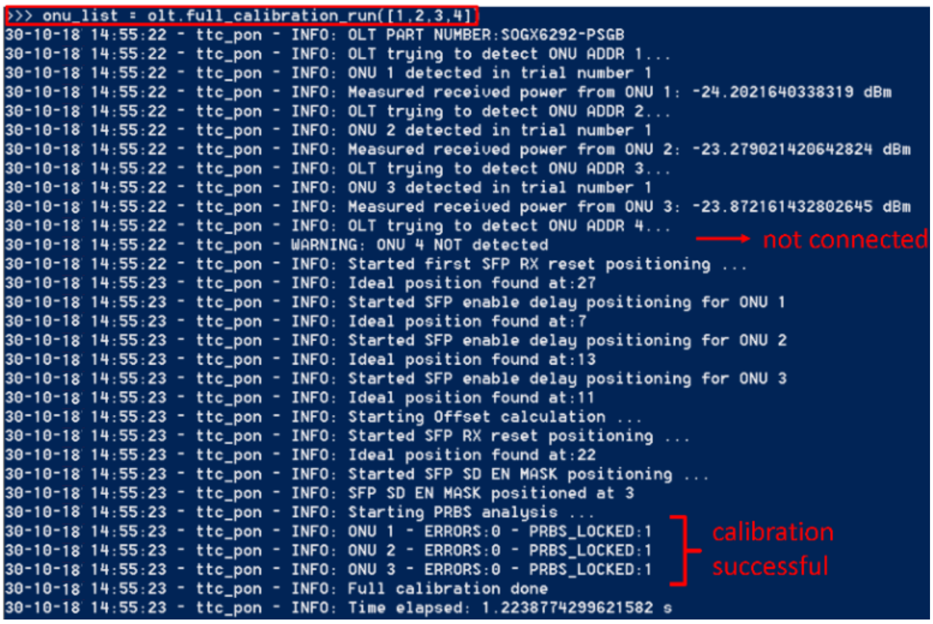

Figure 2.17: Example of results for the system upstream calibration

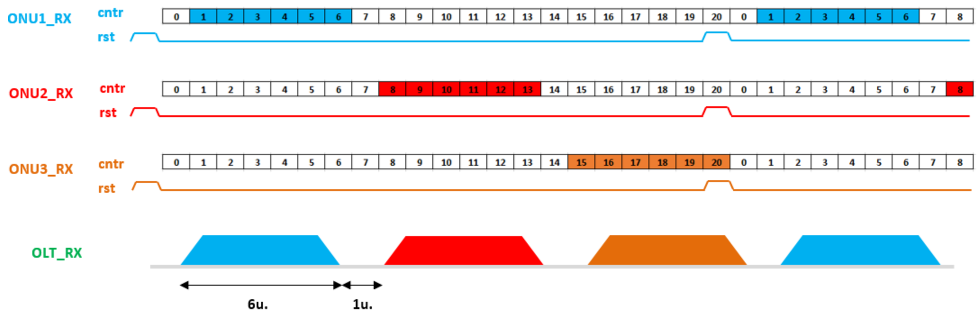

Figure 2.18: Correct phase adjustment for the *OLT_RX* signal

Without going into the details, the calibration continues to run in order to adjust the timing of other signals, and, at the end, a fast BERT is executed to verify that the system is error free.

The last tool of the preliminary phase is the SFP IIC monitoring. This diagnostic interface has been already introduced in the first chapter. The most important information to recall is that all the operating and diagnostic information are monitored and accessible thanks to the microcontroller inside the transceiver and the IIC protocol. In our test we use the diagnostic and monitoring interface to acquire information related to the vendor and the serial number of the transceiver, and to monitor some fundamental parameters like the temperature, the supply voltage, the bias current and the transmitted and received power. An example of the results obtained from a reading is shown in figure 2.19. First the TTC-PON FMC is programmed, then is possible to read the information about the vendor name, vendor part and vendor serial number, and finally the data related to the other parameters are displayed. It is relevant to clarify that the diagnostic readings have the accuracy indicated in the table 2.10 as reported in the SFF-8472 standard. Therefore, these data can be used as a reference to check the condition of the transceiver, but they are not suitable for its characterization.

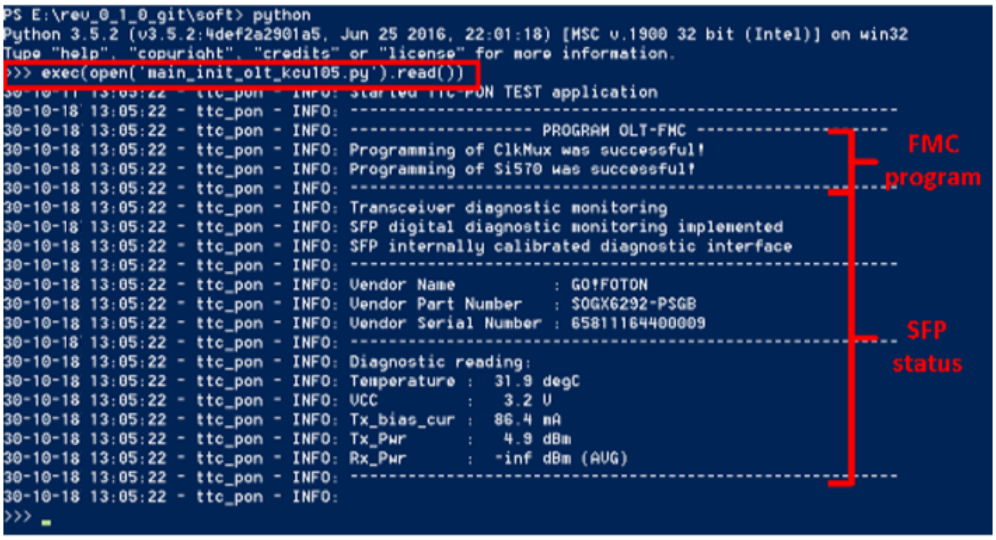

Figure 2.19: Example of results obtained from the SFP IIC monitoring

Parameter	Accuracy
Temperature	$\pm 3°C$
Supply voltage	$\pm 3\,\%$
TX bias current	$\pm 10\,\%$
TX output power	$\pm 3\,dBm$
RX average power	$\pm 3\,dBm$

Table 2.10: Accuracy of the parameters obtained with SFP IIC monitoring interface

2.4.2 Measure and analysis of the transmitter and receiver parameters

There are some important differences between the OLT and ONU modules in the measurement and analysis procedures of the Tx and Rx related parameters. The main dissimilarities are following summarised.

- Optical eye diagram

  In the OLT test we build the optical eye diagram and execute the eye mask compliance test at three different data rates, i.e 9.3 Gb/s, 9.6 Gb/s and 10.2 Gb/s. As it will be clearer when the setup will be presented, we can change the data rate through frequency modifications by a clock generator connected to the Xilinx KCU105 board where the OLT is plugged.

The data rate we consider relevant is 9.6 Gb/s, in fact only at this value we check the eye related parameters mentioned in the previous section. At the contrary, the eye mask compliance is evaluated at each data rate as a control of the locking range criteria, which requires that all the OLT transmitters shall either not be equipped with a CDR, or have a CDR able to lock in the range $[9.3, 10.2]$ Gb/s. An OLT module non-compliant with this requirement typically shows a failure in the eye mask test at the line rate of 9.3 Gb/s, while is compliant in the other cases. An example is provided in figure 2.20. Vice versa, an OLT module in accordance with the locking range criteria is compliant to the three data rates analysed, like in figure 2.21.

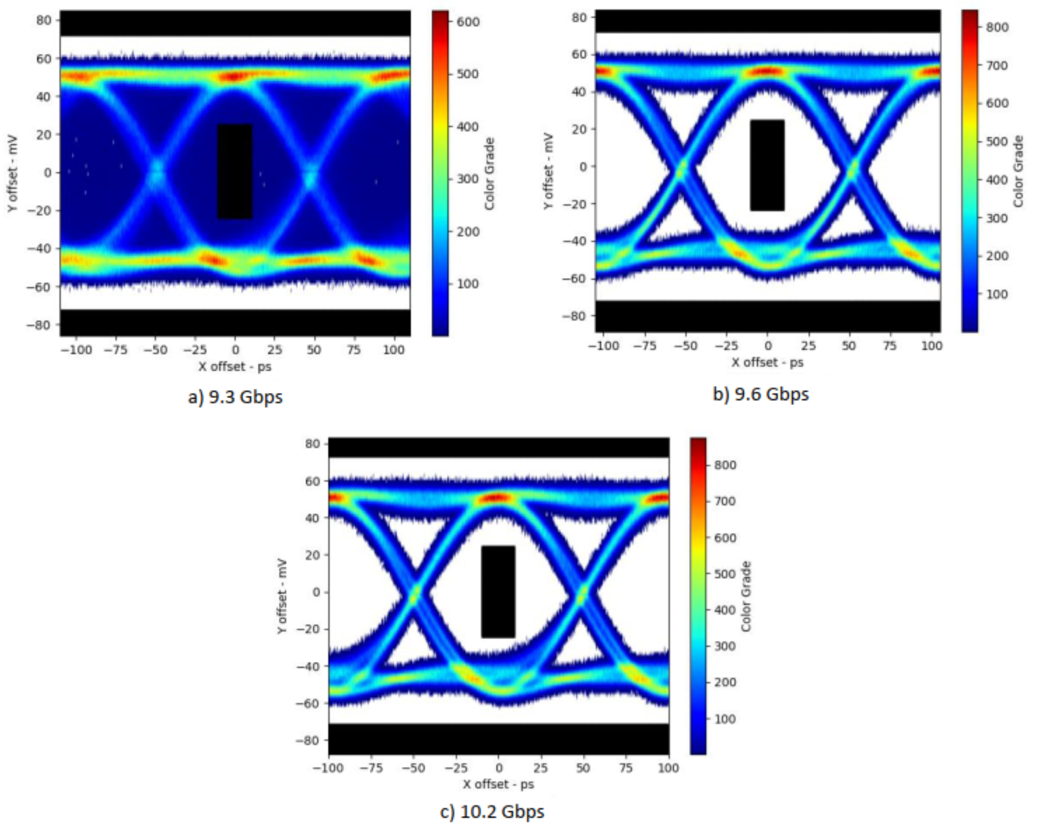

Figure 2.20: Eye diagrams for an OLT module non-compliant with the locking range criteria

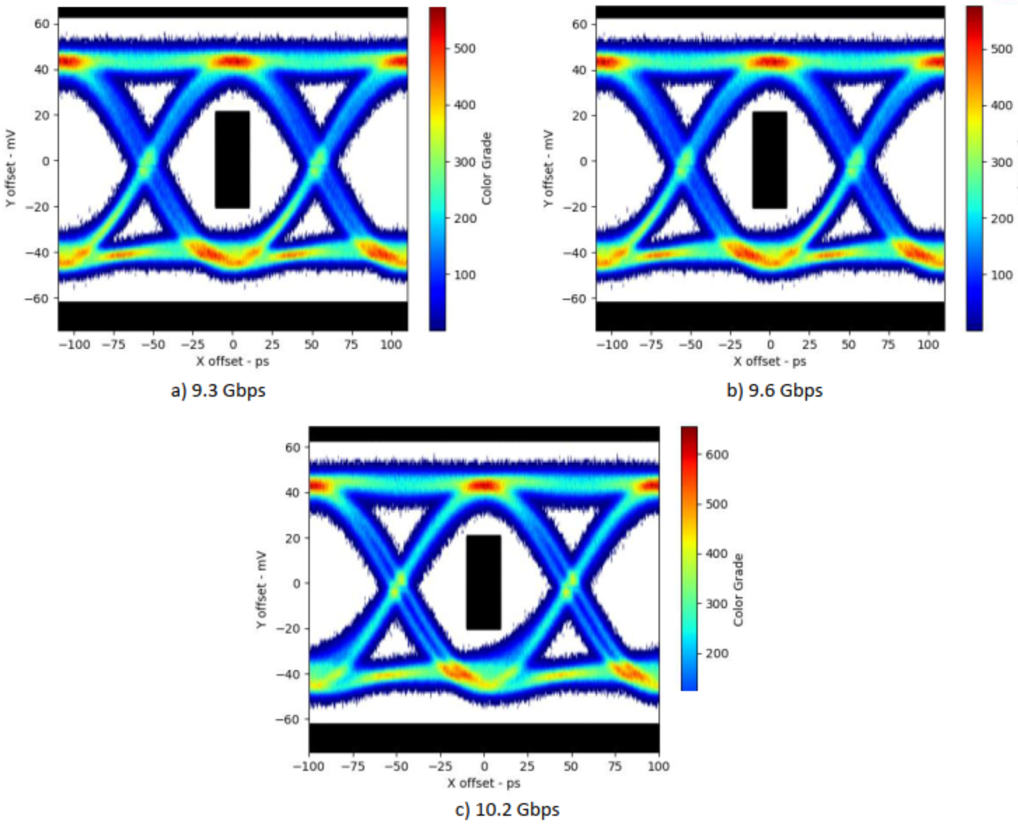

Figure 2.21: Eye diagrams for an OLT module compliant with the locking range criteria

In the ONU test the first difference is that the eye diagram is built both in continuous and in burst mode, while obviously in the OLT test the eye diagram is executed only in continuous mode. It is useful to recall that in the first case all the ONUs are disabled with the last exception of the ONU module analysed, while in burst mode we build the eye using a fixed acquisition window from the beginning of the preamble to the end of the payload of the 100 ns burst. The second dissimilarity is that in this case we conduct also a mask margin analysis to optimize the pass/fail eye mask compliance test. As it can be seen from the image 2.22, since the original eye diagram is compliant with respect to the starting mask (displayed in red), the area of the mask is increased until the non-compliance is detected. Vice versa, if the starting eye diagram is non-compliant, the mask area is decreased until the compliance is obtained. In this way we can have a measure of how much the eye is compliant or non-compliant. The last difference is that both the eye diagram and the eye mask compliance test are carried out only at the data rate of 2.4 Gb/s and not also for the upper and lower limit of the locking range interval like in the OLT test. The reason why we adopt this strategy is that, since the duration of the test is already increased by the two different eye modes and by the mask margin test, considering also three different data rates the test duration would increase excessively.

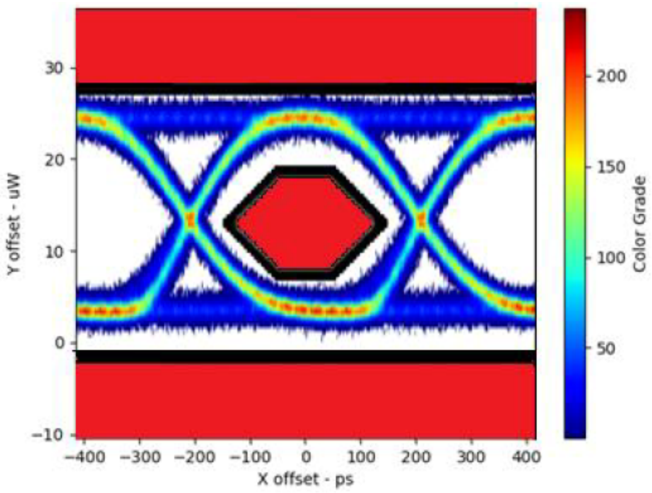

Figure 2.22: Mask margin for a compliant eye diagram

- Receiver sensitivity

  There are two main differences to underline about the evaluation of the receiver sensitivity in the OLT and ONU test. The first one is that in the OLT test we execute a normal sensitivity test and a sensitivity test with dynamic range. The latter is not executed in the ONU test since it does not have a particular meaning for these transceivers. To clarify what is intended as measure of the receiver sensitivity with dynamic range, is useful to observe the figure 2.23. As an example, considering only two ONU modules, to apply a dynamic range of 2 dB on an ONU means that we are attenuating by 2 dB the burst amplitude of the module.

In this operating condition we measure the sensitivity of the receiver. The reason why we conduct this type of test is that in this way we can have a measure of the system robustness. It is worth mentioning that initially the OLT *Go!Foton* modules were characterized by around 3 *dB* of penalty with 6 *dB* of dynamic range, as shown by the diagram in figure 2.23. After some modifications performed by the manufacturer, the tested pre-series modules have displayed no penalty up to 9 *dB* of dynamic range. This is only one example of the various modifications fulfilled by the manufacturer to adjust the performance of their modules on the base of our requests.

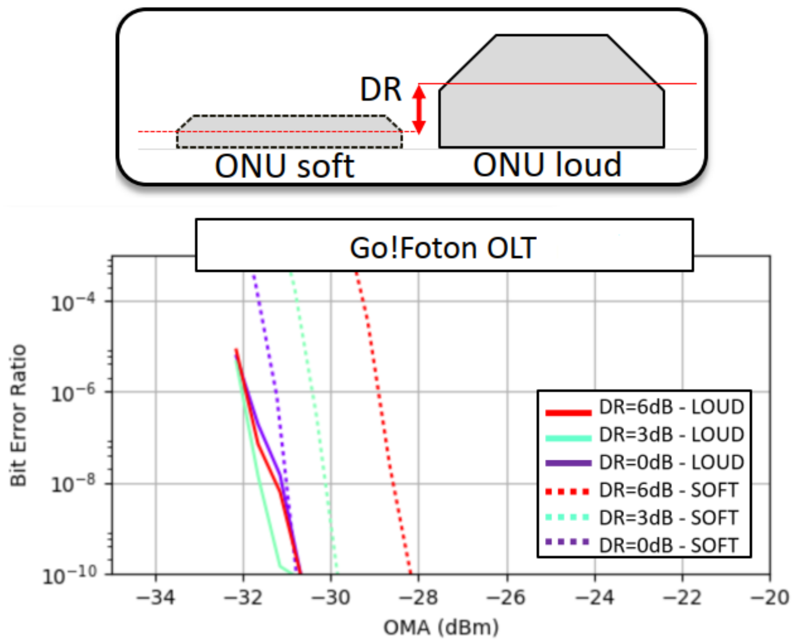

Figure 2.23: OLT receiver - sensitivity measure with dynamic range

The second difference is that in the ONU test we have two options to evaluate the receiver sensitivity, i.e. before or after the application of the FEC scheme. The latter, how is depicted in figure 2.24, ensures 3 *dB* of coding gain and this shall be considered when the sensitivity value is compared with that provided by the ITU standard. In fact, it is referred to the case of no FEC scheme applied. Since our interest is also to verify if the FEC has been correctly implemented in the system, we check the receiver sensitivity after the FEC application and we assume as specification the one indicated by the ITU standard, but adding the 3 dB of coding gain. Then, in the event that an ONU is non-compliant with this approach, our methodology is to verify if the module is non-compliant even without FEC and, in case, conclude the test with a failure.

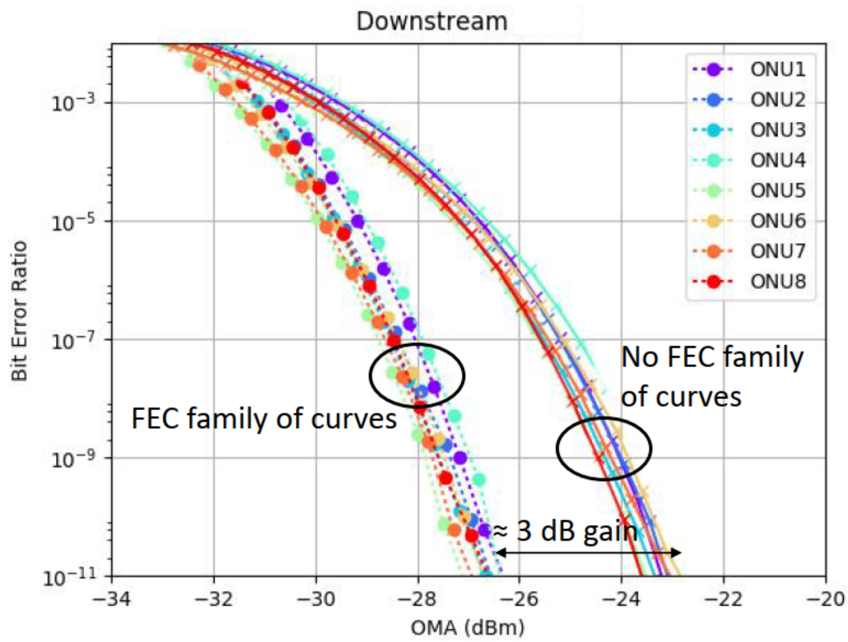

Figure 2.24: Coding gain influence on ONU receiver sensitivity measure

2.4.3 Saving test results

At the end of each measure we stock all the relevant data in various *.csv* files. Therefore, each result of the test is later available. These files are also the basis for the Python scripts that generate the plots and that verify the compliance with respect of the specifications previously described. Moreover, there is an apposite Python script that produces automatically a report like the one shown in figure 2.25.

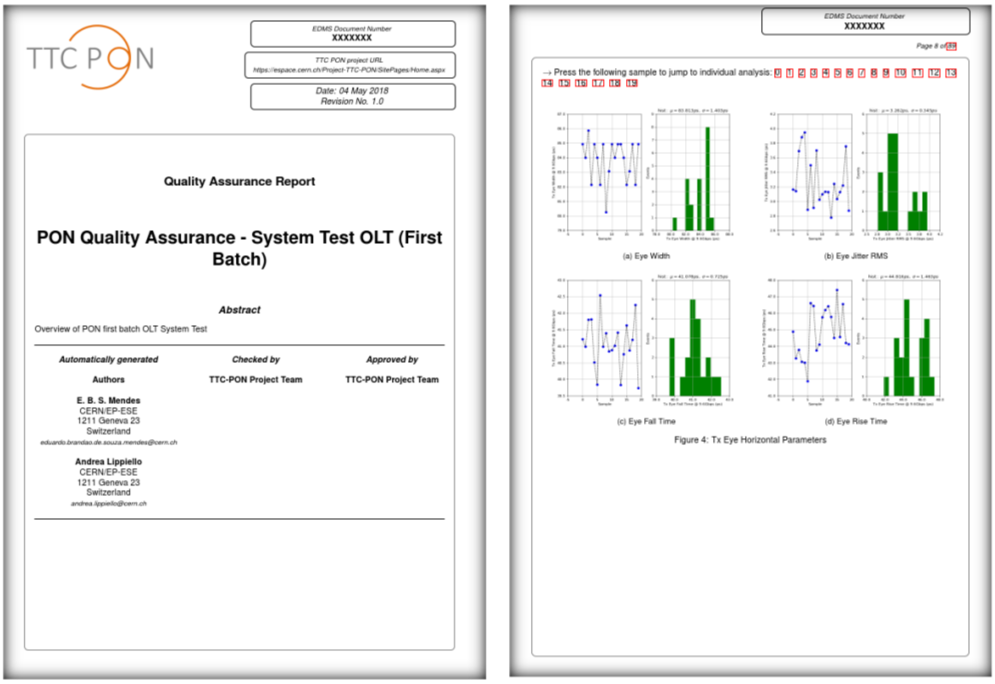

Figure 2.25: Example of report produced per each batch tested

This report, which is divided in two major sections, is produced for each batch of ONU or OLT modules received. In the first part, we do a lot analysis that ensures to observe the trend of the whole batch for each parameter measured. There are some examples of this analysis on the right in the aforementioned figure. The second part of the report contains an accurate description of each individual module tested. To be more precise, this is not really a report, but rather a resume of the main information we acquire from the tests. In fact, beyond this document, during my working period I produced various technical reports that are focused on the data analysis and on the interpretation of the results that I will describe in the third chapter.

2.5 Software contribution

During my first month at CERN, all my efforts were centred around the optimization of the test routine, which was partially already elaborated. More specifically, my aim was to reduce the duration of the test as much as possible. Initially, the ONUs test was 50 minutes long, while the OLT test was 55 minutes long. My first modification to the test routine was about the electrical eye scan function. At the beginning, the eye scans of the eight ONU modules were performed sequentially, while, thanks to my changes, they started to be executed simultaneously. Considering that each eye scan requires forty seconds, to complete them for all the ONU modules with the original script five minutes and thirty seconds were necessary. Thanks to my contribution, only three minutes and thirty seconds were required, ensuring to save around two minutes.

The second change was about the oscilloscope control. To explain properly this point, it is useful to recall some basic concepts regarding the Transmission Control Protocol/Internet Protocol (TCP/IP) devices. The TCP/IP is a suite of protocols used to interconnect networked devices. In particular, the TCP establishes how data have to be transmitted over the Internet and how they have to be reconstructed once they reach their destination, while the IP specifies how to address and route data ensuring they arrive to the right device. The internal ending points for receiving and sending data between the devices, in our case the PC and the oscilloscope, are called sockets.

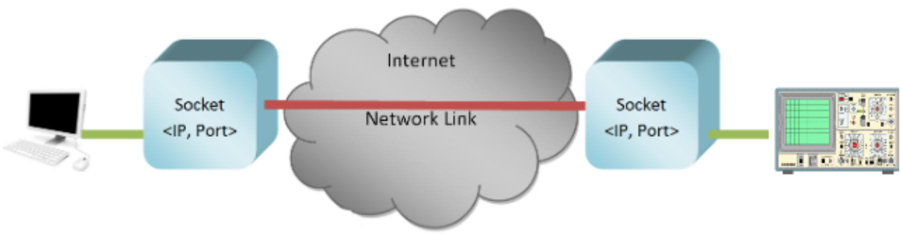

Figure 2.26: Socket definition

Each socket is uniquely identified with an address that is composed by an IP address and a port number for the local node. In Python there are different ways to manage a socket. Before my modification, the oscilloscope socket was handled with the Python socket module, which provides access to the Berkeley Software Distribution (BSD) socket application programming interface (API). I observed that when the scope was controlled in this way, it was slow in the implementation of its operations and, therefore, the time needed to complete an optical eye diagram was very high. Because of this, I tried to handle the oscilloscope socket with the VISA sockets API. The improvement I obtained with this modification was significant since fifty seconds were saved for each optical eye in burst mode and in continuous mode. Considering that in the ONUs test we execute eight optical eyes in continuous mode and eight optical eyes in burst mode, I saved approximately 14 minutes per test. In the OLT test the time gain is only two minutes and a half since, in this case, we perform only three eye diagrams.

Other two modifications were related to the calculation of the BER used for the evaluation of the sensitivity. As it will be fully explained in the next chapter, in origin we studied the BER in an attenuation range between 0 dB and 21 dB. Since we have never observed errors for attenuation values lower than 10 dB, it was useless to include in our test the range $[0, 10]$ dB. Therefore, I modified the script to reduce the number of attenuation steps to examine for evaluating the receiver sensitivity. Considering that 25 seconds were needed to calculate the BER for each point, in this way I saved eight minutes. This modification was adopted only for the ONU module since, being the number of the ONU modules much higher than that of the OLT, to reduce the range of attenuation analyzed has not a relevant cost benefit for the OLT modules. About the second change, in the initial script we were always waiting 10^{11} bits down before moving from one attenuation point to the next one. This strategy was not optimized since, if the errors number is very high, it is unuseful to wait that all the bits are transmitted, but rather it is possible to move immediately to another attenuation step. Consequently, I changed the script ensuring that if a threshold value of 1000 errors is exceeded, it is possible to move directly to the next attenuation point. Proceeding in this way, I saved two minutes and a half. Finally, removing some redundant operations, like reprogramming the OLT in each run of the ONUs test or, vice versa, reprogramming the ONU modules for each OLT test, other two minutes were saved.

To sum up, thanks to my modifications each run of an ONUs test is 26 minutes long, while an OLT test is 48 minutes long. Therefore the duration of the ONU test was reduced by 48%, while that of the OLT test by 13%.

Beyond the test routine software optimization, I also created the Python function that executes the eye mask margin test, which was originally not included in the test routine, and I produced some scripts that perform two auxiliary analysis to use in case of non-compliant eye detected. These examinations, which I called optimum offset analysis and the middle mask analysis, ensure to have a better comprehension of the failure. The first one helps to center the mask exactely in corrispondence of the crossing points of the eye. In fact, since the original algorithm centres the mask vertically by evaluating the average value between the zero and the one level, in case of eye diagrams with a low SNR this approach can lead to a wrong mask positioning. The idea behind my script is to find the best offset starting from the position found by the original script, and then moving the mask above and below until a non-compliance is detected. The final offset is provided by the mean value between the last two offsets which were able to ensure the compliance of the eye when the mask was moved in the two opposite directions. In figure 2.27 is possible to observe an example of result provided by my function.

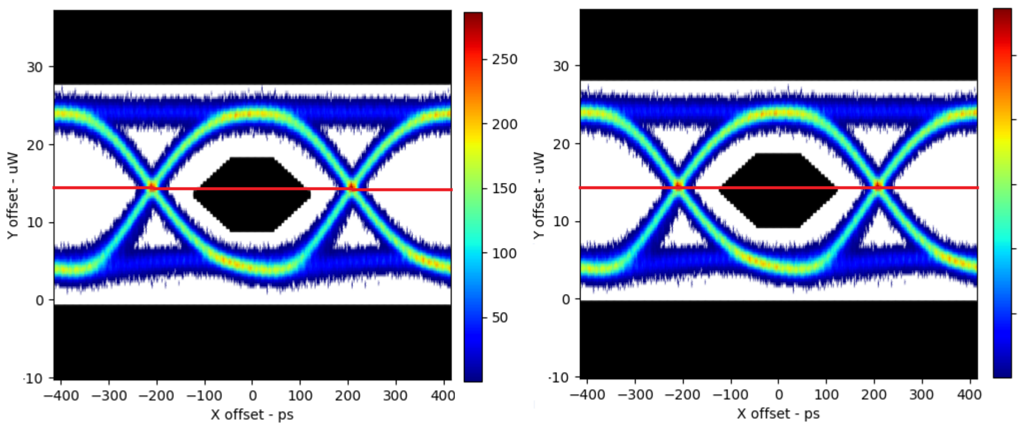

Figure 2.27: Example of optimum offset analysis

On the other hand, the middle mask analysis ensures to verify the compliance of the eye considering only the central part of the mask. This kind of study is once more useful in case of eye with a low SNR, since we can evaluate if the points under the mask are in the boundary or in the centre of the mask, which is the most sensitive part.

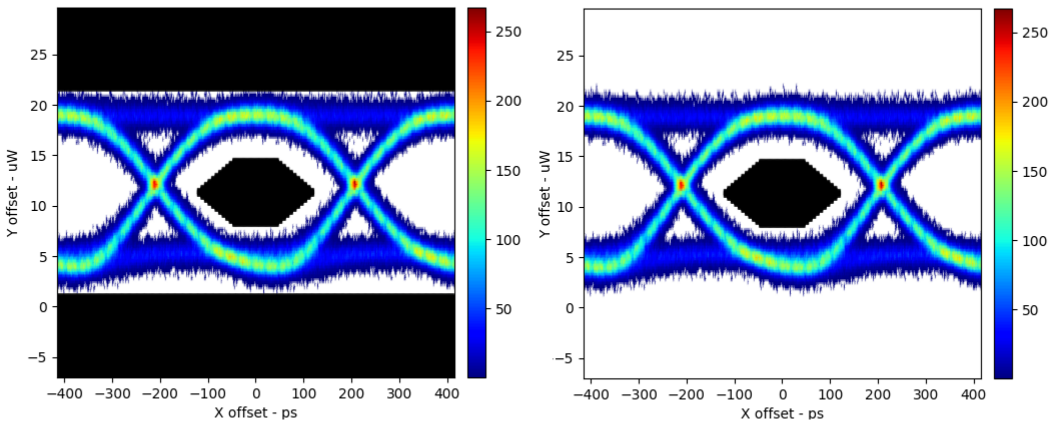

Figure 2.28: Example of middle mask analysis

To conclude this section I want to mention that I also created from scratch the software used for the temperature tests of the OLT and the ONU modules, and I contributed to the software development for testing the TTC-PON modules under radiation from the perspective of the next-generation TTC-PON system targeting the phase-2 upgrades of the LHC experiments.

Chapter 3

Experimental results

This chapter includes all the information related to the experimental setups used for testing the OLT and the ONU transceivers, and the results obtained. I will provide a complete description of the main types of failures detected, giving some examples of non-compliant modules. Moreover, a specific section will be reserved for the temperature tests that, differently from the QA tests, were performed only on a small subset of modules to verify that some requested modifications had been correctly implemented by the manufacturer.

3.1 General statistics

Before to start describing the results of the quality assurance campaign, it is useful to give an indication about the amount of modules tested. In this regard, a total number of 1145 ONU and 100 OLT modules has been evaluated. These transceivers were delivered by the manufacturer according to the following schedule:

Batch	Arrival date	ONUs number	OLTs number
Pre-series	12/2017	25	20
Batch n.1	04/2018	200	20
Batch n.2	05/2018	200	80
Batch n.3	06/2018	200	//
Batch n.4	07/2018	200	//
Batch n.5	08/2018	340	//

Table 3.1: Modules quantities to be delivered per batch

Among these modules, 60 OLTs and 570 ONUs will be used in the ALICE experiment, while 32 OLTs and 555 ONUs will be used in the LHCb experiment. The remaining ones are used as a stock by the section. This opportunity is taken to point out that while ALICE will use the system in its entire form, LHCb will employ only the optical module because they are just interested to the high split ratio they can achieve through these devices.
In the following sections the OLT and the ONUs tests will be described separately due to different setups used and for reasons of clarity.

3.2 OLT test

To present the OLT test I will start explaining the setup adopted, doing a division between the instruments used to characterize the OLT transceivers as transmitters and as receivers. As it will be clearer soon, our setup also needs to be calibrated for different reasons. The precise grounds and the various steps of this procedure will be clarified before outlining the test results and some examples of non-compliant modules.

3.2.1 Setup and calibration procedure

The experimental setup has to meet the requirement of allowing to measure all the figures of merit presented in the second chapter when the OLT is not used as a single component, but rather is part of the system previously described. The configuration we adopted is shown in figure 3.1. Each OLT module is tested with eight ONU transceivers that are fixed for all the OLTs we test. This choice derives from the need of keeping the system as much unchanged as possible in order to test all the OLTs in the same conditions. A clock generator is connected to the TTC-PON FMC mounted on the Xilinx KCU105 board and, initially, it provides a 240 MHz clock. Following there is a 1:2 optical splitter used to connect the power meter 1, which measures the power given by the ONU modules in the upstream direction, namely the received power by the OLT. Continuing in the downstream direction, there is a variable optical attenuator and a 1:16 splitter connected to the eight ONUs, the power meter

2, which is used to measure the power transmitted by the OLT, and finally the optical head and the scope that ensures to visualize the eye diagram. About the optical head, it is an instrument that measures the power emitted from a connected optical fiber. The analog output is a voltage directly proportional to the strength of the optical signal at the input and, in our case, it is used to monitor the optical power on the oscilloscope. The optical head used in our setup is AC-coupled, therefore it generates an analog output starting from the optical input, but the information about the received power is lost.

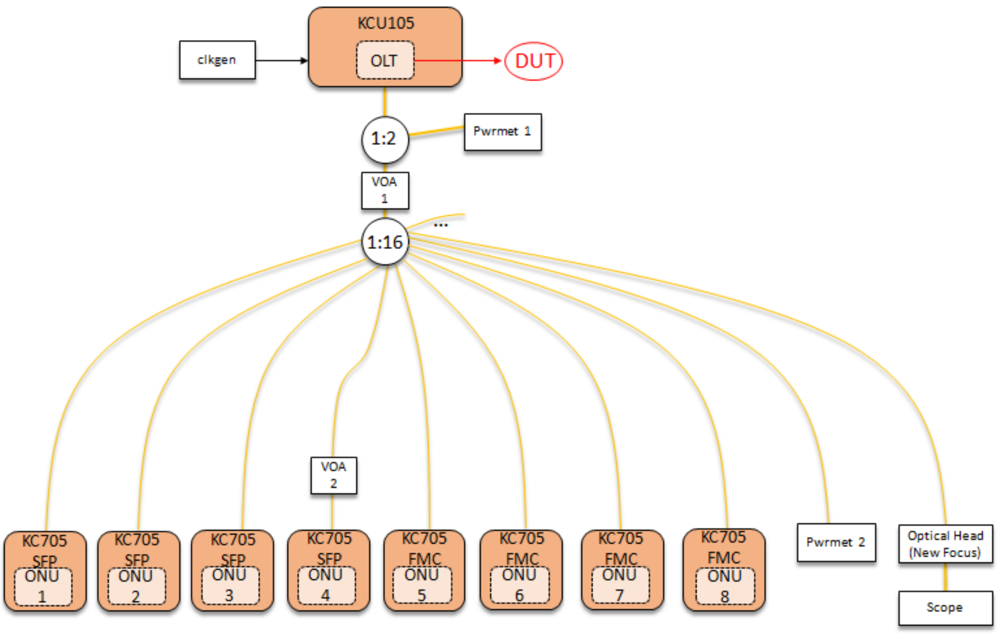

Figure 3.1: OLT test setup

Device	Manufacturer	Part number	Serial number
VOA1	JDSU	VOA	00003728
VOA2	JDSU	VOA	00003728
Pwrmet1	JDSU	OPM-B	00000909
Pwrmet2	JDSU	OPM-B	00000909
Scope	Agilent	DSA91204A	MY48240177
Clkgen	Stanford	CG635	002954
Optical head	New Focus	1544-A	5468

Table 3.2: Instruments used for the OLT test setup

During the characterization of the OLT as a transmitter, the instruments involved are those marked in figure 3.2. The clock generator is used to change the data rate according to the following formula:

$$clock\,frequency = \frac{data\,rate}{9.6\;Gb/s} \cdot 240\;MHz \tag{3.1}$$

In this way, we can evaluate the eye diagram at the data rates of interest, i.e 9.6, 9.3 and 10.2 Gb/s. About the power meter 2, how explained before, it is employed to measure the power transmitted by the OLT since this information can not be acquired through the optical head because of its AC-coupling feature.

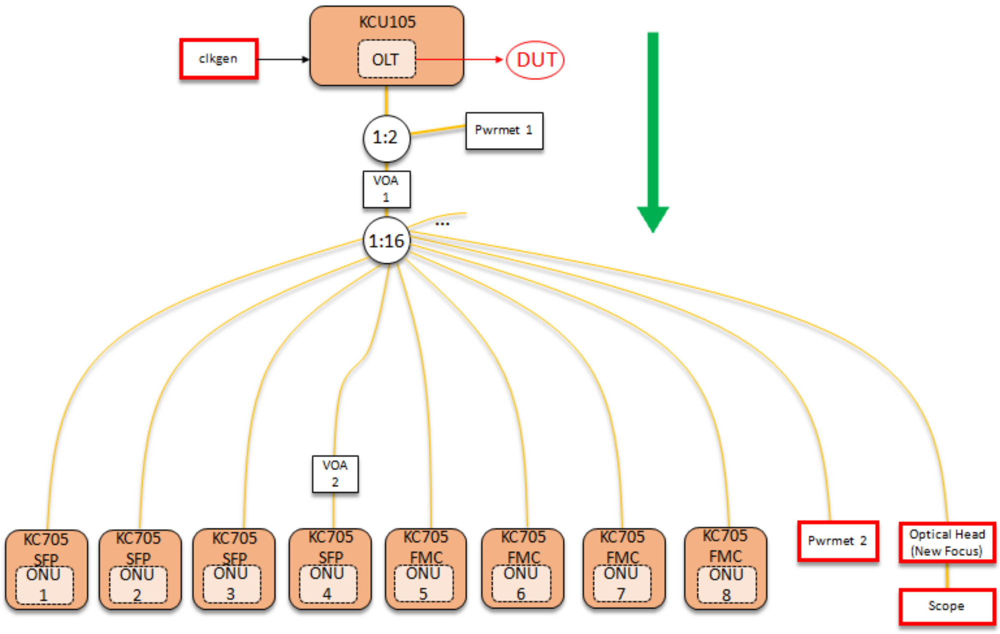

Figure 3.2: OLT Tx - Instruments used for the characterization

On the other hand, the instruments used for the measure of the receiver related parameters are indicated in figure 3.3. The two voltage optical attenuators are employed to evaluate the sensitivity in two different tests, one with dynamic range and the other without it. In particular, the attenuation imposed by Voa1 varies between 0 dB and 21 dB with 0.5 dB steps. In each attenuation point the BER is calculated and the power received by the OLT is recorded thanks to the power meter 1. The voltage optical attenuator 2, which applies continuously a fixed attenuation of 9 dB, is used only in the dynamic range test to lessen the burst amplitude of the ONU 4.

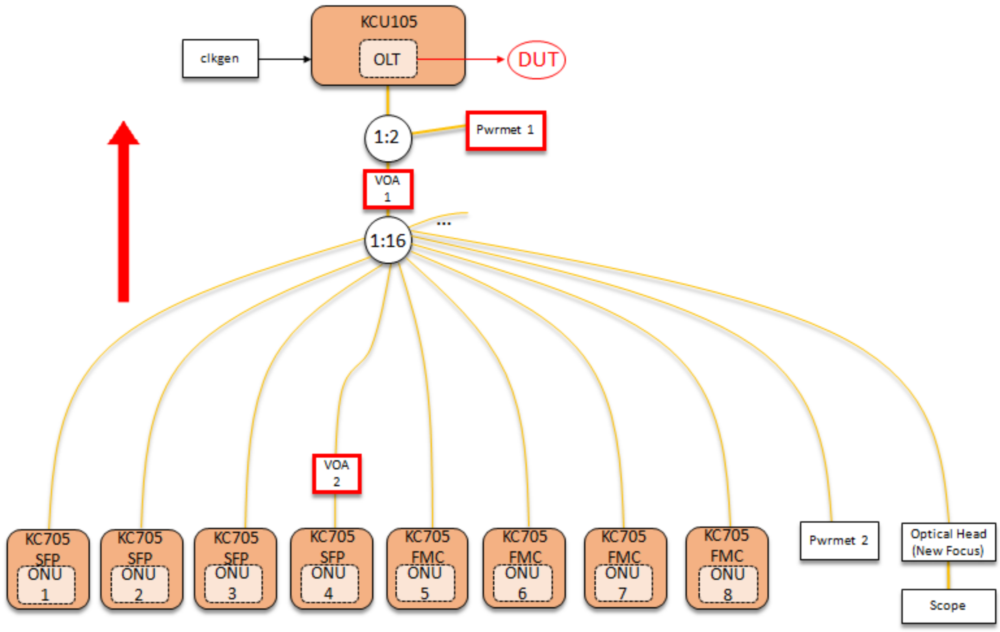

Figure 3.3: OLT Rx - Instruments used for the characterization

Observing our setup, one could argue there are various factors that, if not taken into account, can lead to a bad evaluation of the parameters of interest. As an example, since we are measuring the power transmitted by the OLT after the series of two optical splitters and a variable optical attenuator, we should consider the insertion loss of these components to have a correct estimate of the OLT Tx power. In this regard, the system calibration is the process that ensures to understand if all the components and the system configuration are working properly and will not cause any measurement distortion in the subsequent phases. The setup calibration is executed to meet these main requirements:

- Need to know the optical head conversion gain to understand how the signals are handled and modified by this component;
- Need to evaluate the network uniformity to measure properly the power

received by each ONU;

- Need to estimate the power loss of the system and, therefore, to understand if some components are not appropriate for our application since they introduce a loss too high;
- Need to determine if the optical attenuator has a good linearity or not.

To meet adequately these requests, the system calibration is divided into four phases that are described below individually.

1. Optical head calibration

   The optical head calibration process is divided into two phases. In the first one the setup is the same shown previously in figure 3.1, but a Keysight high power optical head is used in place of the New Focus one as reference. Then, in the second part of the calibration, the setup is modified and the New Focus optical head is substituted to the Keysight one. An important difference between these two instruments is that the first one is DC coupled, while the second one, how it has already been said, is AC coupled. Therefore, the latter includes a capacitor in the circuit that filters out very low frequencies removing the DC offset and normalizing the signal mean to zero. Basing on some measurements and on mathematical manipulations, is possible to determine the conversion gain of the New Focus optical head. More specifically, the measurements performed in the first and the second phase of the calibration are reported respectively in the tables 3.3 and 3.4. The one and the zero level, the eye amplitude and the mean voltage in the first phase are obtained from the optical eye diagram built using a value of 123 mV on the oscilloscope to compensate the offset of the Keysight optical head. With the name $PWR_{BRANCH\,SCOPE}$ is indicated the power measured in the branch occupied by the scope. About the parameters of the second phase, in this case the eye amplitude is derived from the optical eye diagram without using any offset value due to the AC coupling of the optical head. Finally, the parameter $PWR_{BRANCH\,PWRMETER}$ represents the power measured in the branch with the power meter, which is not necessarily equal to that measured in the branch with the scope because of the possible unbalance between them.

Parameter	Value	Unit
V_{AVG}	25.5460	mV
V_{AMP}	45.5819	mV
V_{TOP}	50.51840	mV
V_{BASE}	4.9365	mV
$PWR_{BRANCH\,SCOPE}$	-12.2500	dBm

Table 3.3: First phase measurements

Parameter	Value	Unit
V_{AMP}	105.3726	mV
$PWR_{BRANCH\,PWRMETER}$	-13.0800	dBm
$PWR_{BRANCH\,SCOPE}$	-13.1020	dBm

Table 3.4: Second phase measurements

The mathematical manipulations used to obtain the conversion gain are now described in detail. Focusing on the first phase of the calibration, is possible to evaluate the OMA_{IN} by combining the following equations:

$$C_{REF} = \frac{V_{AVG}}{PWR_{BRANCH\,SCOPE}} \tag{3.2}$$

$$V_{AMP} = C_{REF} \cdot OMA_{IN} \tag{3.3}$$

Hence:

$$OMA_{IN} = \frac{V_{AMP} \cdot PWR_{BRANCH\,SCOPE}}{V_{AVG}} \tag{3.4}$$

where all the data adopted were those indicated in tha table 3.3.

Applying to the New Focus optical head the inverse formula obtainable from the equation 3.3, we can calculate its conversion gain:

$$C_{NEW\,FOCUS} = \frac{V_{AMP}}{OMA_{IN}} \tag{3.5}$$

In this case the V_{AMP} was the value reported in the table 3.4. By doing so, we estimated a conversion gain of 1207.1 V/W.

2. Network uniformity

   Thanks to this phase of the calibration procedure we can understand to what extent the 1:16 optical splitter is unbalanced. The evaluation is done in the upstream direction connecting to the power meter each ONU one at time. In this way we evaluate the amount of power received by the various slave modules. The optical transceivers used in this stage are the same that were used for all the OLTs test. Their serial number is reported in the tabel 3.5.

Device	Manufacturer	Part Number	Serial Number
Olt	GO!FOTON	SOGX6292-PSGB	65811174800008
Onu 1	GO!FOTON	SOGX2629-PSGA	A6961174700023
Onu 2	GO!FOTON	SOGX2629-PSGA	A6961174700022
Onu 3	GO!FOTON	SOGX2629-PSGA	A6961174700005
Onu 4	GO!FOTON	SOGX2629-PSGA	A6961174700004
Onu 5	GO!FOTON	SOGX2629-PSGA	A6961174700013
Onu 6	GO!FOTON	SOGX2629-PSGA	A6961174700015
Onu 7	GO!FOTON	SOGX2629-PSGA	A6961174700006
Onu 8	GO!FOTON	SOGX2629-PSGA	A6961174700031

Table 3.5: Transceivers used for the network uniformity evaluation

The final results obtained are displayed in the table 3.6. Looking at these data, the ONU 4 shows clearly a lower power compared with the other modules because it is connected to the optical attenuator VOA2. Moreover, basing on this analysis, the position of some ONUs was changed with respect to the starting one in order to obtain a more uniform network in terms of power.

Parameter	Value	Unit
ONU 1 Rx Pwr	−14.60	dBm
ONU 2 Rx Pwr	−13.87	dBm
ONU 3 Rx Pwr	−14.10	dBm
ONU 4 Rx Pwr	−16.21	dBm
ONU 5 Rx Pwr	−14.41	dBm
ONU 6 Rx Pwr	−14.52	dBm
ONU 7 Rx Pwr	−14.22	dBm
ONU 8 Rx Pwr	−14.38	dBm

Table 3.6: Measurements of the ONUs received power

3. Total Loss

The total loss measurement is intended to estimate the power dissipated due to the components and the fibres that are used between the OLT and the ONU modules. This measurement is divided into two phases. In the first one the OLT is directly connected to the power meter to evaluate the transmitted power, while in the second one the setup is identical to that shown in the figure 3.1. In this case we measure the net power received downstream of the splitter through the power meter labelled as *Pwrmet2*. The same fibre used in the first phase to connect the OLT to the power meter is also used to connect one of the 1:16 splitter outputs to the power meter in the second phase. In this way it is possible to assume that the attenuation related to the fibre is identical in both steps of the measurement.

Calling respectively P_{direct} and P_{met} the power measured in the first and in the second phase, the total loss can be determined by subtracting these quantities. The final results are presented in table 3.7.

Parameter	Value	Unit
P_{direct}	+4.400	dBm
P_{met}	−13.895	dBm
P_{loss}	18.295	dB

Table 3.7: Total loss measurements

4. Attenuation

   During this step of the calibration process the power sent by the OLT in the downstream direction and the power transmitted by the ONUs in the upstream direction are evaluated as a function of the attenuation. The latter assumes values ranging from 0 dB to 21 dB with 0.5 dB steps. The crucial point of this analysis is to evaluate the linearity of the attenuator. Without reporting the measurement data, it was indeed verified that the power variation measured in each step was consistent with the alteration of the working conditions imposed by the attenuator.

3.2.2 Test results

How I have already said in the first section of this chapter, a total number of 80 OLTs has been tested. Among them, 78 modules were compliant, while 3 modules did not pass the test, even if two of them were very close to the specification and, therefore, were not sent back to the manufacturer. Moreover, one module between the compliant ones shown a weird behaviour that ensured us to improve our system since, thanks to the collaboration with the manufacturer, we found out how to solve the problem via software. About the two non-compliant modules, they were both out of specification in terms of sensitivity at $BER = 10^{-4}$. One of the two was non-compliant only in the test without dynamic range but, in this case, the non-compliance was negligible. The other did not respect the specification in both tests and the non-compliance was significant. Below I provide an accurate description about the failures detected for the three modules and the problem observed for the compliant OLT.

- Module n. 65861181500035

  This module was part of the second batch received and was characterized by the more relevant non-compliance. In the figure 3.4 is shown the diagram BER vs OMA with dynamic range for the ONU 4. It can be clearly noticed how the module is approximately 1 dB out of specification, since its sensitivity is -27.4 dB against the -28.3 dB of the specification, which is indicated in the plot with the black point. Moreover, it is really useful to observe the lot diagram of the related batch in terms of receiver sensitivity at $BER = 10^{-4}$. Considering that the red line in the graph represents the specification, it is simple to notice that there are two non-compliant modules in this batch. The module under analysis is the one clearly far from the specification and represents a point out from the lot distribution. The other is the transceiver I will talk about right after.

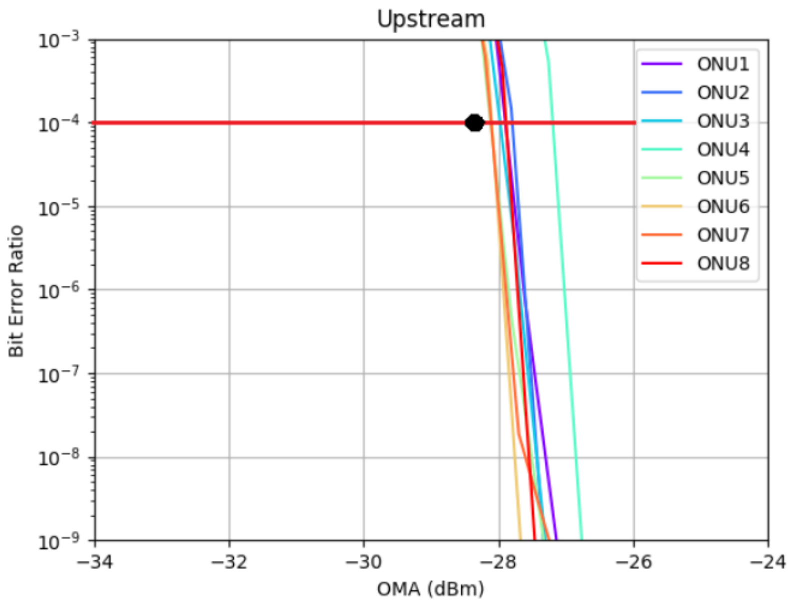

Figure 3.4: Non-compliant OLT - BER vs OMA diagram

- Module 65861181500061

  This module shows a kind of failure similar to that already presented for the previous transceiver. In fact, it is non-compliant in terms of receiver sensitivity at $BER = 10^{-4}$ in case of no dynamic range applied to the ONU 4. The discordance with the standard is really negligible since the value I obtained during the test was -28.1403 dBm, therefore only 0.2 dB out of specification. Considering the uncertainty of the measure and of the system calibration procedure, we decided to consider this module as acceptable.

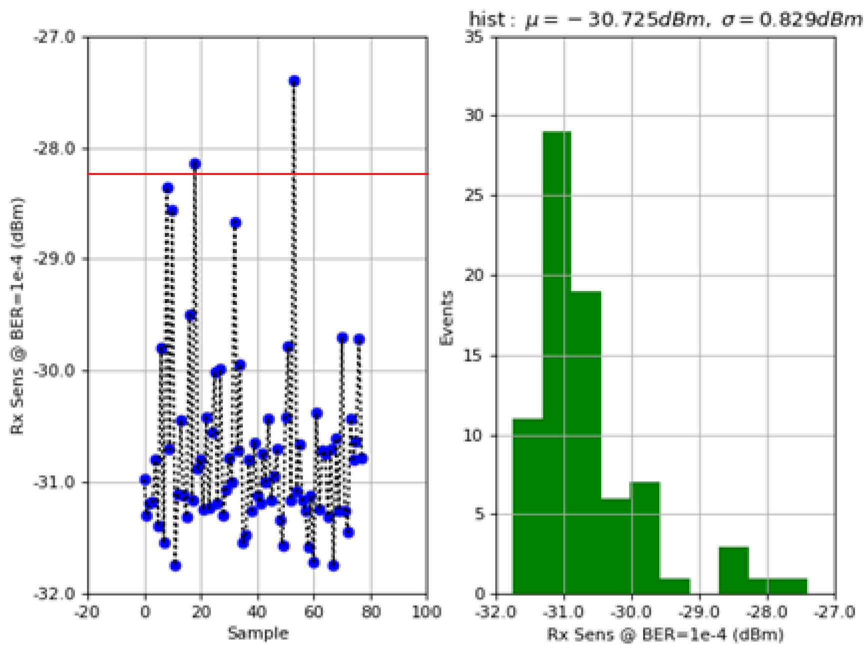

Figure 3.5: Lot diagram - Second batch

- Module n.65861181500089

  This transceiver displayed a transmitter power slightly out of specification. In particular, the value measured by the power meter was 4.3370 *dBm*. Considering the uncertainty of the measure and of the system calibration and being the transceiver non-compliant by only 0.2 *dB* (the specification about the minimum OLT Tx power is 4.5 *dBm*), we agreed on considering the module compliant.

- Module n.65861181200025

  This module shown a weird behaviour during the test. More specifically, I noticed that when the module was connected, it transmitted fine with the expected power and it was compliant with the established mask. When I reset the FPGA, the OLT transmitter stopped working and the diagnostic signal TX_{FAULT}, which reports an error in the transmission, was equal to one. Observing with the oscilloscope the TX_{RESET} signal coming from the FPGA, the waveform was characterized by around 1.55

μs 0-level followed by a 1.2 V overshoot during the reset. Thanks to the collaboration with the manufacturer, the problem was detected in this overshoot since few laser driver chips in the module were characterized by a low threshold to the large overshoot. This explanation was confirmed by the fact that disabling the OLT and enabling it only after the FPGA reset everything was working fine. In conclusion, thanks to this module, we had the opportunity to improve the system since, starting from this event, the FPGA reset software was modified implementing inside it the transmitter disable command.

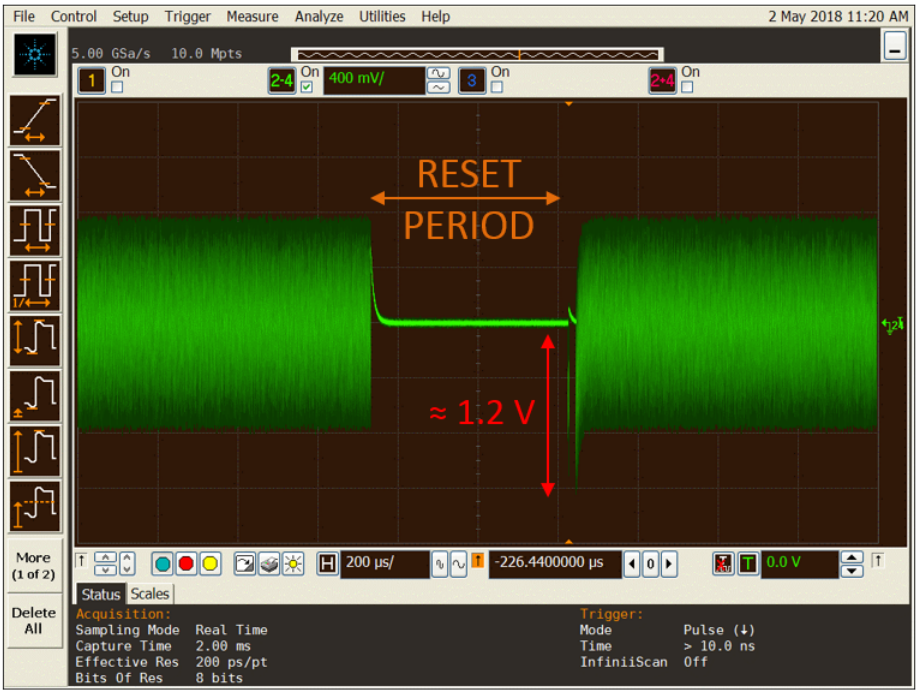

Figure 3.6: FPGA TX_{RESET} signal

3.3 ONUs test

To present the ONUs test I will proceed with the same guideline used for the OLT one. I will start talking about the setup adopted, but, to avoid being repetitive, I will not describe the calibration of the system since it is quite similar to that already described for the OLT test. On the other hand, I will explain in detail the reasons that led to a setup modification during the quality assurance process. Finally, I will present the results of the test giving some examples of the main types of failures detected.

3.3.1 Setup

The setup used to test the first three batches of ONU modules is represented in the figure 3.7. The main difference with the one used for the OLT modules is the cascade of two 1:2 splitters after the OLT. This is due to the need to connect both a power meter and a scope to monitor either the optical eye or the received power in the upstream direction. In fact, the optical head we used was AC-coupled and, therefore, a separate power meter had to be used to measure the received power in that direction. How it is indicated in the previous image, in each run we tested 4 different ONU modules, which are the ONU 1, the ONU 2, the ONU 5 and the ONU 8.

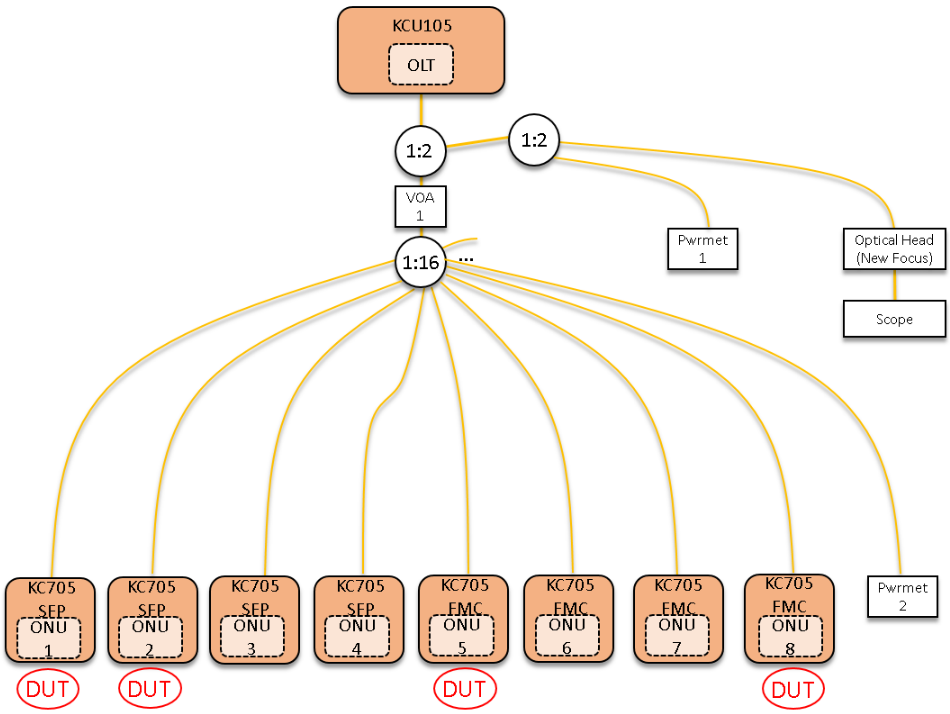

Figure 3.7: ONUs test setup

The remaining ONU transceivers were fixed, exactly as the OLT module, for all the runs. In this way, we were able to execute also a reference analysis on the fixed modules to check the robustness of the system. Another important difference from the OLT setup is the absence of the voltage optical attenuator that was connected to the ONU 4. In fact, since the measurement of the receiver sensitivity with dynamic range is meaningful only for the OLT, that instrument was not any more necessary for this test.
A direct consequence of the introduction of the second 1:2 splitter in the setup are the noisy and attenuated optical eyes we obtained from the ONU modules. An example is shown in figure 3.8. Because of the attenuation caused from the additional splitter and the subsequent reduced SNR of the transmitted optical signal, in the first three batches we observed few non-compliant modules in the eye mask test. In fact, sometimes there were some points under the mask in its boundary. Because of this we decided to change the setup for the last two batches to solve the problems correlated to the splitter.

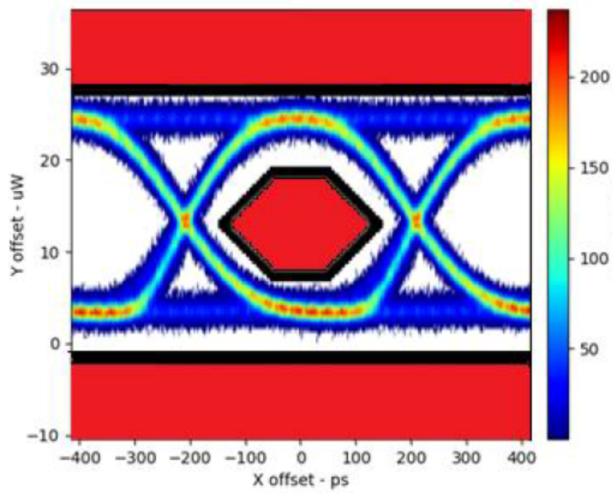

Figure 3.8: Eye diagram and mask margin with the initial ONUs test setup

The figure 3.9 shows the main change in the setup. The additive 1:2 splitter was removed and a DC-coupled reference receiver was introduced. This latter (Keysight 8163B) was equipped with an internal circuitry to measure the power, and, as a consequence, there was not anymore the need of having a separate optical head and a power meter.

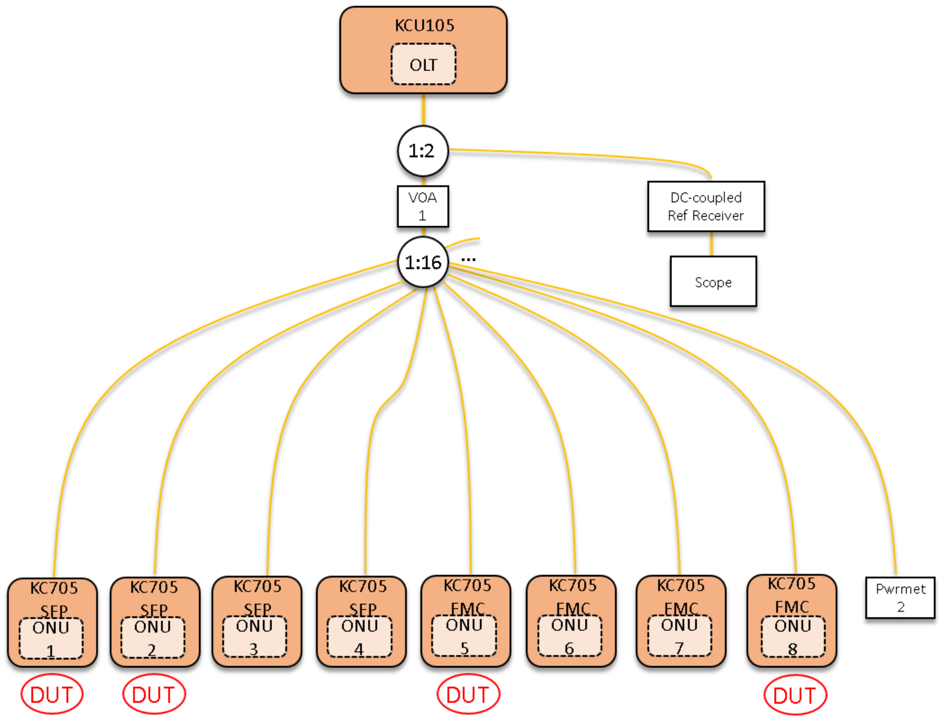

Figure 3.9: Evolution of the test setup used for the ONU modules

The main advantages obtained by changing the setup are shown in figure 3.10, where the eye diagram and the mask margin analysis are depicted for the same module analysed with the previous setup in the figure 3.8.

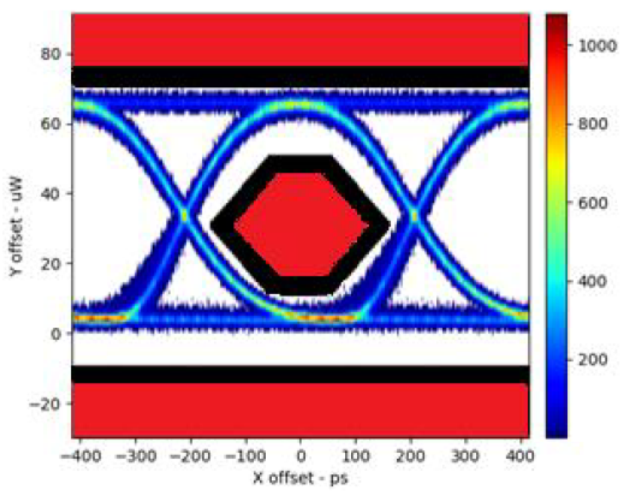

Figure 3.10: Improvements in the eye diagram and in the mask margin after the setup modification

As expected the shape of the eye is clearly unchanged, but the signal is obviously less attenuated, and then characterized by a higher signal to noise ratio. Moreover, a clear improvement in the mask margin value can be deducted, as well as in many other eye related quantities like the RMS jitter value, the rise and the fall time and so on. The batches diagrams depicted in figures 3.11 and 3.12, which ensure to observe how the main parameters vary among the five batches, provide clear evidence of what has just been said. To avoid repetitions only two examples referred to the continuous mode are shown, but similar outcomes were obtained also in burst mode.

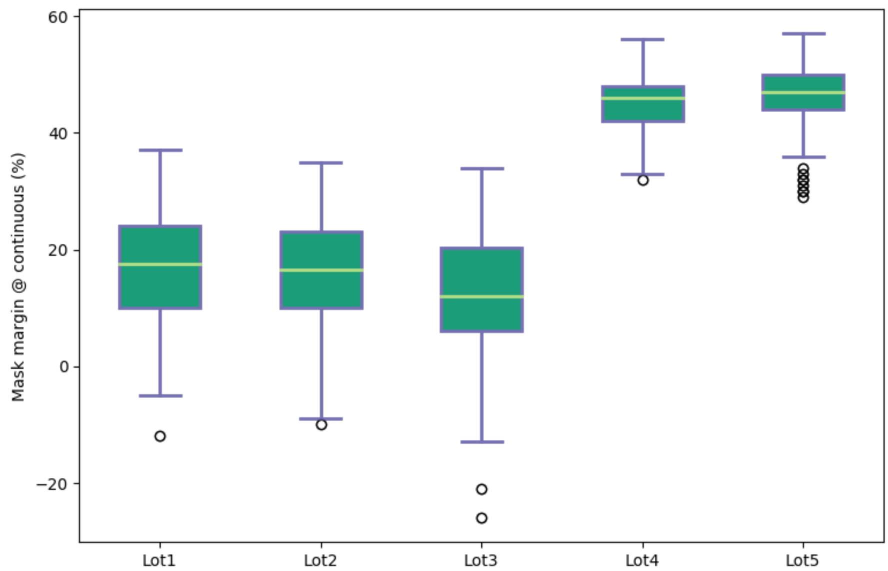

Figure 3.11: Batches diagram - Mask margin in continuous mode

To understand properly this type of diagrams, it is useful to recall the meaning of the main elements represented. The yellow line inside the box is the median value, i.e. the common measure of the center of the data, while the green box is the interquartile range (IQR) and it indicates the middle 50% of the data. Finally, the whiskers, which extend from either side of the box, represent the ranges for the bottom 25% and the top 25% of the data values. Moreover, the points outside the wiskers are called outliers and they represent samples numerically distant from the rest of the data. Looking at the figure 3.11, it can be observed how the mask margin in the last two lots is increased

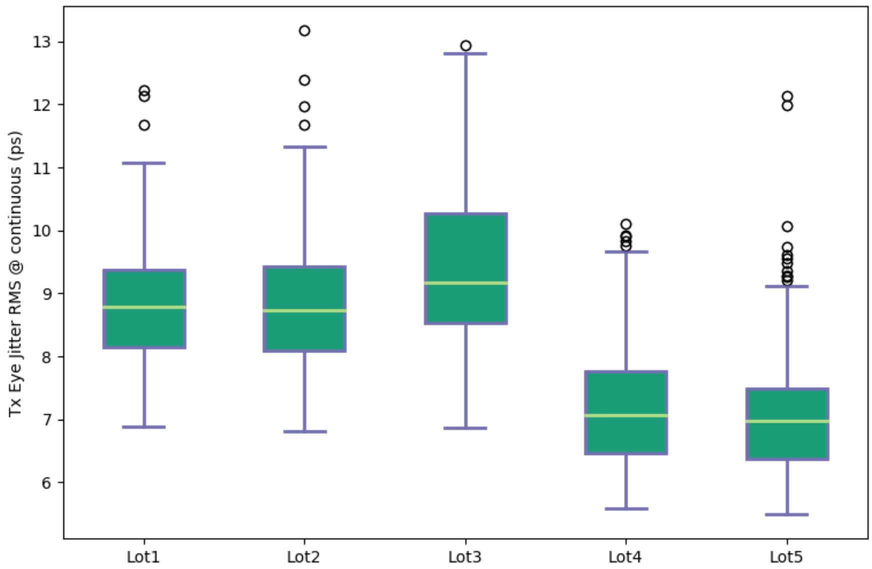

Figure 3.12: Batches diagram - RMS Jitter value in continuous mode

since his median value grew of about 20% with respect to that of the previous batches. In addition, these two boxes are also shorter in terms of whiskers and IQR compared with that of the first three lots. This means the population has a smaller standard deviation from the median value in the fourth and in the fifth batches. Also the box-plot related to the RMS jitter value provides a clear evidence of the RMS jitter reduction and, therefore, of the general improvements obtained thanks to the modification of the setup.

Returning to the description of the test setup, it is not difficult to understand what is function of each instrument and when they are used. The DC-coupled reference receiver and the scope are employed in the upstream direction to measure the power transmitted by the ONU module under test and to build the optical eye diagram in burst and in continuous mode. The remaining instruments are used in the downstream direction. In particular, the power meter 2 measures the power transmitted by the OLT, that is the power received by the ONU modules, while the voltage optical attenuator is used during the evaluation of the receiver sensitivity to apply an attenuation between 10 and 21 dB with 0.5 dB steps.

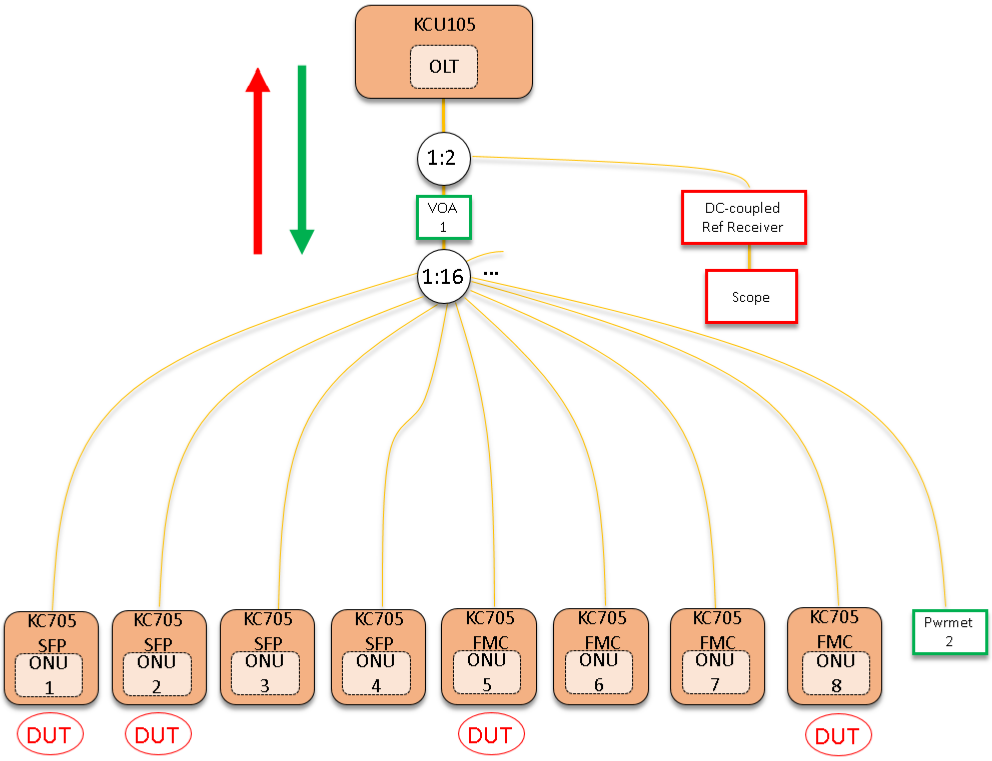

Figure 3.13: Instruments used in the downstream and in the upstream direction during the ONUs test

3.3.2 Test results

Between the 1145 ONU modules tested during the QA campaign, only three of them were non compliant. More specifically, two modules were non-compliant in terms of receiver sensitivity at $BER = 10^{-11}$, and one module was non-compliant in the eye mask test in burst mode. Moreover, it is important to specify that among the compliant modules there was one ONU that was totally not working. We sent the module to the manufacturer who fixed and shipped it back. Following an accurate description about the problems and the failure detected for these transceivers.

- Module n.A69611816000284

  This module was part of the third batch and it resulted non-compliant in terms of receiver sensitivity at $BER = 10^{-11}$ both in case of FEC application and in case of FEC absence. In the figure 3.14 is represented the sensitivity diagram with FEC, where the module in question is the number two. Recalling that in this condition the specification is -25.0 dBm, the module is non-compliant for 1 dB.

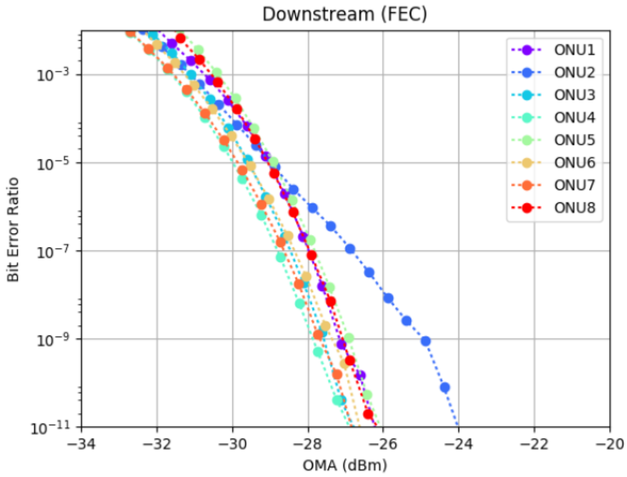

Figure 3.14: ONU n.284 - Sensitivity diagram in case of FEC application

When the FEC is not applied, the module is non-compliant for around 1.3 dB since the specification is -22.0 dBm.

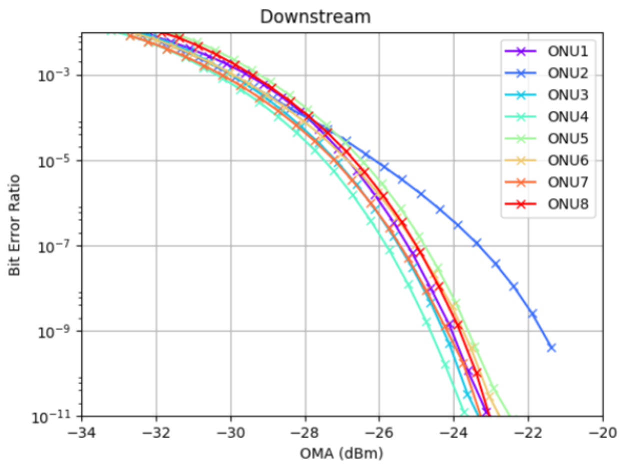

Figure 3.15: ONU n.284 - Sensitivity diagram in case of FEC absence

Finally, it is interesting to notice that in both cases the module behaves in the same way as the others until a bit error ratio of 10^{-6}, then it starts degrading exhibiting an unexpected trend.

- Module n.A6961181600575

  Also this module is non-compliant both in case of FEC application and in case of FEC absence. The behaviour is very similar to that of the previously analysed module, since until $BER = 10^{-5}$ it works properly like the other transceivers, then his performance starts degrading. From the figures 3.16 and 3.17, where the ONU under discussion is the number eight, it is clear that the module is slightly non-compliant in case of FEC application, i.e. about 0.2 dB, while is non-compliant for 0.7 dB when FEC is not adopted.

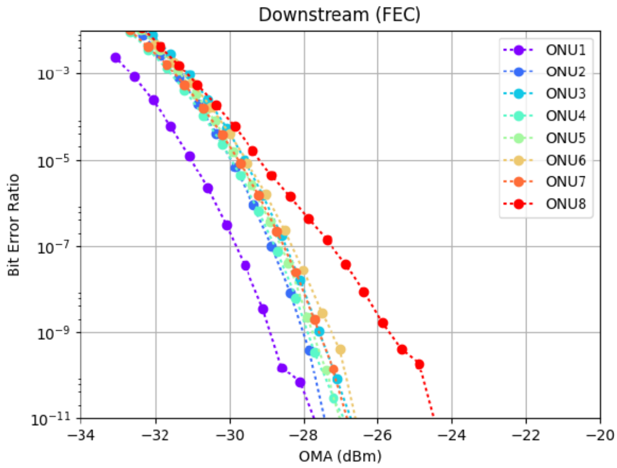

Figure 3.16: ONU n.575 - Sensitivity diagram in case of FEC application

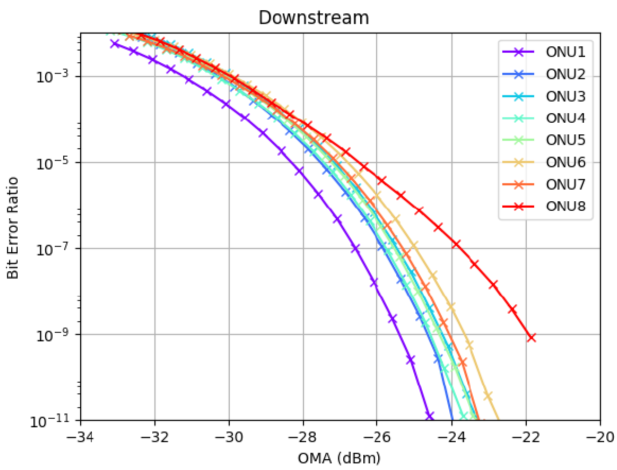

Figure 3.17: ONU n.575 - Sensitivity diagram in case of FEC absence

- Module n.A6961180900265

  This module was between the ONUs of the first batch that were retested with the improved setup, since they were initially non-compliant in the eye mask test due to the attenuation caused by the additional splitter in the first setup. This was the only transceiver that was non-compliant when tested with both the setups. In particular, it shown a distorted eye either in continuous mode or in burst mode. In the latter case, it was non-compliant with a mask margin equal to -6.0 %, and from our test we found out that there were six hits with the mask. Furthermore, this module represented a point out from the distribution in the first batch because its average transmitter power was significant higher compared with that of the other modules (6.0 dBm).

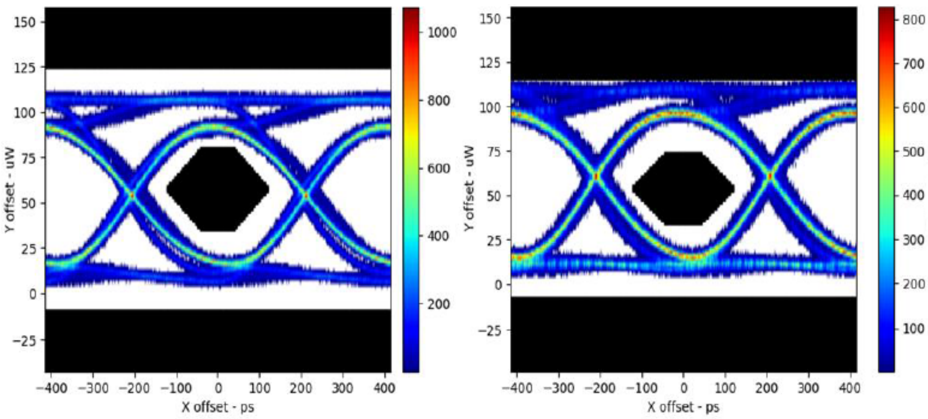

Figure 3.18: ONU n.265 - Eye diagram in continuous and burst mode

- Module nA6961180900092

  During the test of this module, which was part of the second batch, I noticed that it was not able to transmit in continuous mode and the transmitted power read via II2 was -40 dBm. Even disabling and enabling the ONU nothing changed. Because of this, we sent it back to the manufacturer who confirmed the module was broken. More specifically, the problem was that the Tx flexible printed circuit in the transceiver was dirty and shifting slightly, and this caused a short circuit between the $LD+$ and the $LD-$ pins leading to no Tx power for the module.

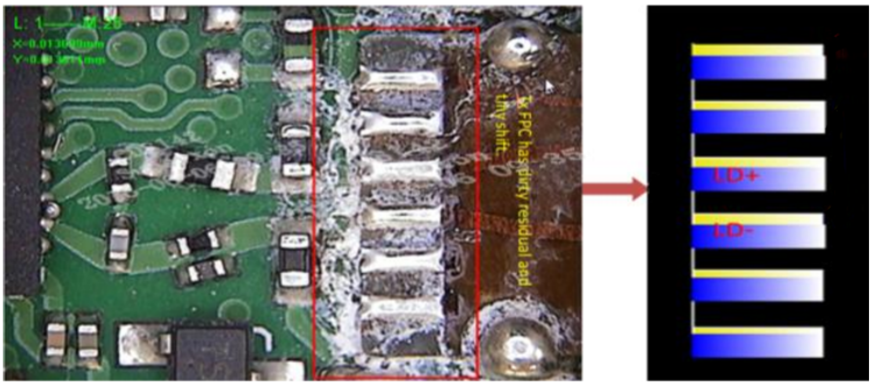

Figure 3.19: Internal short circuit in the non-working ONU module

The manufacturer fixed the module and sent it back inside the fifth batch. With a new test we verified that, after the adjustment, the ONU was totally compliant with our specifications.

3.4 Temperature test

The temperature tests were performed both on some samples of ONU and OLT modules to understand how the transceivers performances were affected by temperature variations. Our attention was mainly focused on the ONU modules because some pre-series samples were characterized by APC failures. In fact, it was observed that the bias current was constant and the transmitter power was reducing about 3 dB by increasing the temperature from 20 to 60°C. The manufacturer performed some modifications on the ONU transceivers to ensure the APC to work properly. Therefore, the main purpose of the temperature tests on the ONUs was to verify that the APC malfunction was effectively solved. As a control, it was decided to perform the same type of test also for the OLT modules to have a complete quality assurance process on both types of transceivers.

3.4.1 ONUs test

Like stated previously, the first temperature tests on some pre-series ONU modules shown an improper APC behaviour since the transmitter power and

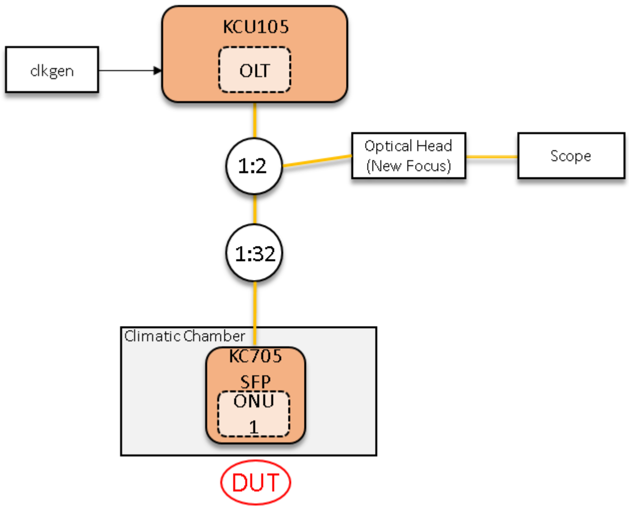

Figure 3.20: Setup used for the first ONU temperature tests

the bias current were not able to adapt to temperature changes. The test, which was executed by other members of the section before my arrival, consisted in observing the ONU bursts with the oscilloscope to capture any possible distortion and in the analysis of the transmitter power and the bias current values registered through the internal I2C diagnostic monitoring interface. The setup used is represented in figure 3.20. Three steps of temperature were performed for the climatic chamber, i.e. 35, 45 and 60°C. The measured bias current remained constant over the whole range of temperatures and the transmitter power decreased, likely due to the laser threshold increasing with temperature.

Device	Manufacturer	Part Number	Serial Number
Clkgen	Stanford	CG635	002954
Scope	Agilent	DSA91204A	MY48240177
Optical head	New Focus	1544-A	5468
Onu	GO!FOTON	SOGX2629-PSGA	65711164500004

Table 3.8: Devices used for the first temperature test

Therefore, in this test the laser of the module seemed to be directly biased by a constant source without any kind of feedback compensation. The test results are reported in the table 3.9, where can be clearly observed how the module was 1 dB out of specification in terms of transmitted power at 60°C.

Temperature chamber	Temperature module (I2C monitor)	Tx bias (I2C monitor)	Tx power (I2C monitor)
35°C	34.6°C	21.5 mA	3.3 dBm
45°C	45.3°C	21.5 mA	2.8 dBm
60°C	62.7°C	21.5 mA	1.0 dBm

Table 3.9: Data registered by the I2C monitoring interface during the first ONU temperature test

The manufacturer performed some modifications to the APC circuitry and sent us two samples to let us verify directly that the malfunction was solved. Also this verification test was performed before my arrival at CERN. The last difference in the setup with respect to that shown in figure 3.20 is the presence of two modules in the climatic chamber, because both the modified transceivers were analysed simultaneously. The test results were encouraging because the measured bias current increased and the transmitted power reduced slightly for one module, but the variation was much smaller than that measured in the previous test, and was approximately constant for the other. The transmitted power was within the data sheet limits at all the temperatures tested and for both the modified modules. Therefore, our conclusion was that the APC modification performed by the manufacturer was working properly.

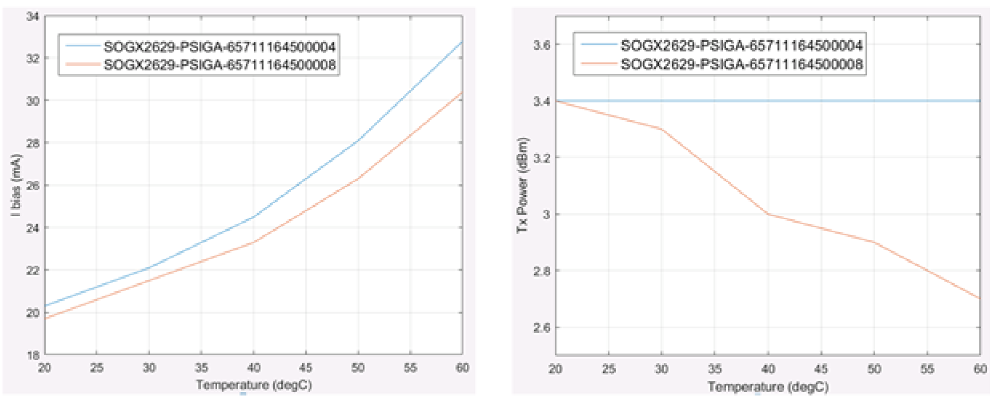

Figure 3.21: Results of the temperature test on the modified ONU modules

Returning to the quality assurance process, it was impossible to test all the modules in temperature due to the high number of transceivers received.

Accordingly, our strategy was that of testing only a small subset of ONUs among that received. In this regard, a total number of 22 modules, almost equally distributed between the pre-series and the first three batches, was tested in the climatic chamber. Both the test structure and the setup used were very different compared with those previously described. The first diversity was that four steps of temperature were performed for the climatic chamber, i.e. 15, 40, 50 and 60°C. Moreover, the test was divided in two phases: in the first one we moved from 15 to 60°C and we checked the values of the Tx bias, Tx power and temperature through the I2C diagnostic monitoring interface in each point aforementioned, while in the second phase we moved in the same temperature points but in the opposite order executing the classical QA test in each step. The setup was similar to that used for the QA process with the only difference that two ONU slaves were inside the climatic chamber and represented the devices under test.

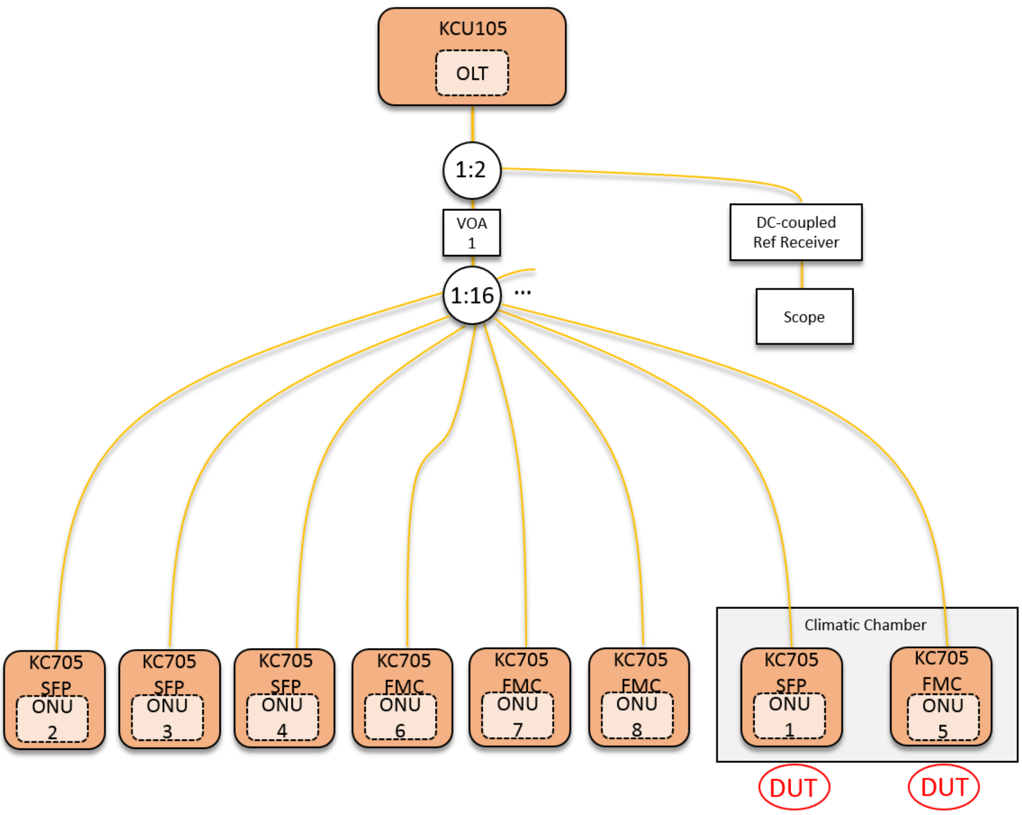

Figure 3.22: QA ONUs temperature test - Setup

About the results, all the modules shown a Tx Bias increase and a Tx power decrease during the step-up temperature cycle. In the figures 3.23, 3.24, 3.25 and 3.26 the behaviour of the aforementioned parameters acquired through the I2C monitoring interface is represented.

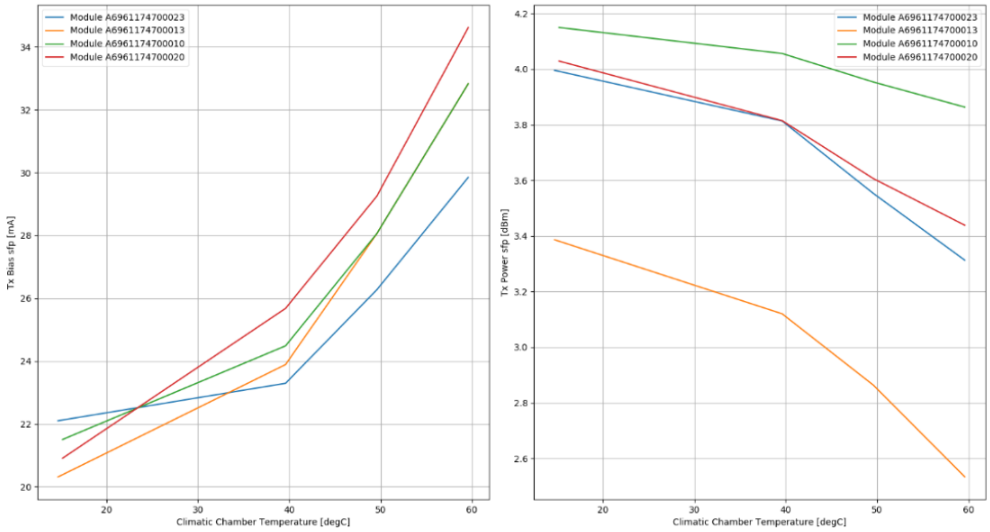

Figure 3.23: Results of the temperature test for the ONU modules analysed from the pre-series

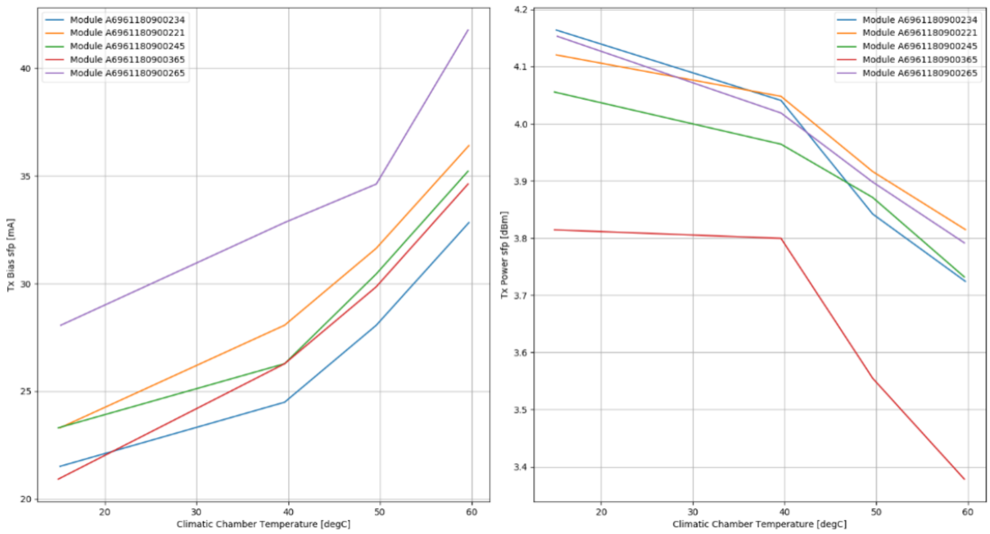

Figure 3.24: Results of the temperature test for the ONU modules analysed from the first batch

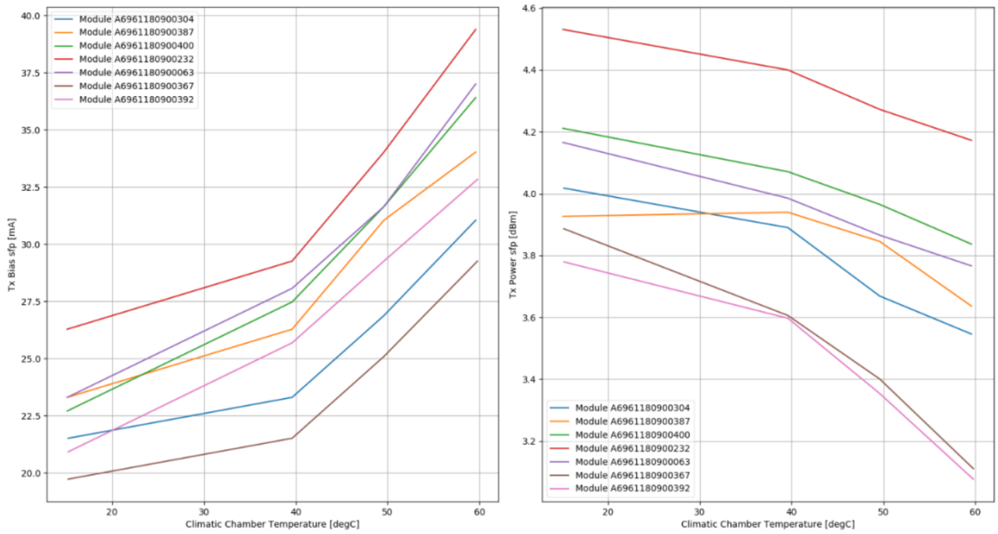

Figure 3.25: Results of the temperature test for the ONU modules analysed from the second batch

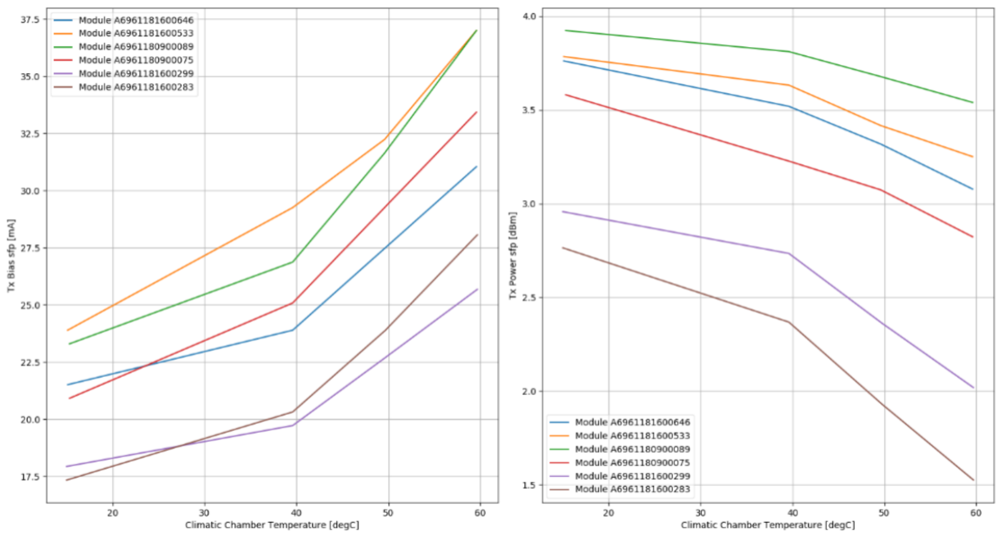

Figure 3.26: Results of the temperature test for the ONU modules analysed from the third batch

From these diagrams it looks clear that, in general, there was respectively a sharper increase and decrease of the Tx bias and the Tx power starting from 40°C. Moreover, it is possible to deduce that all the modules were compliant in terms of Tx power, except one ONU of the third batch (serial number $A6961181600283$) which had a Tx power (1.6 dBm) lower than the minimum one provided by the specification at the temperature of 60°C. However, the following graphs, which represent the Tx power measured by the multimeter during the QA test in the temperature step-down transient, show how the SFP values were not accurate (± 3 dBm) and how the module previously mentioned was actually compliant (Tx power $= 2.5$ dBm). Furthermore, these measures prove that the power was not always decreasing like the IIC graphs depicted, but it was approximately constant with the temperature variation for some modules. This behaviour confirms what was already observed in the verification test on the modified ONU modules.

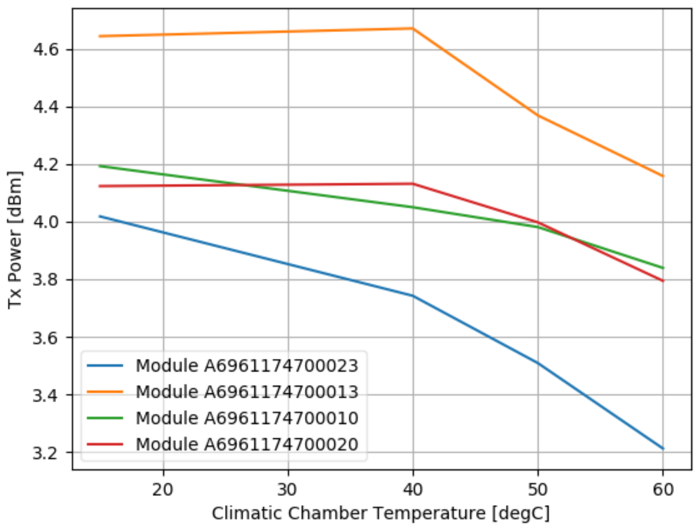

Figure 3.27: QA temperature tests - Power meter measurements for the modules analysed from the pre-series

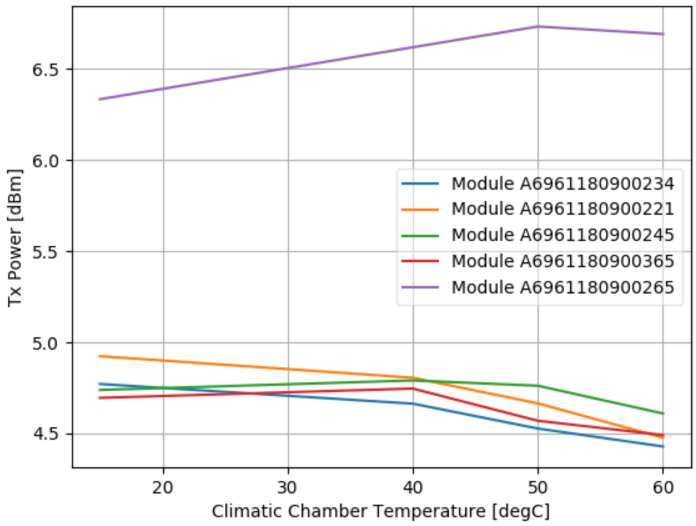

Figure 3.28: ONUs QA temperature test - Power meter measurements for the modules analysed from the first batch

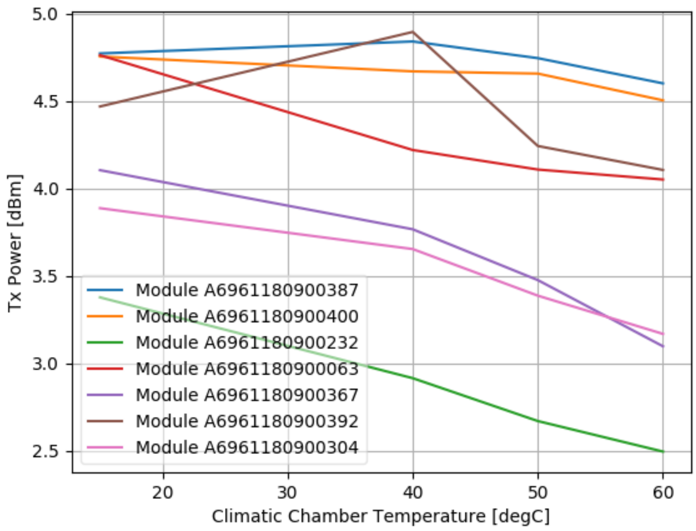

Figure 3.29: ONUs QA temperature test - Power meter measurements for the modules analysed from the second batch

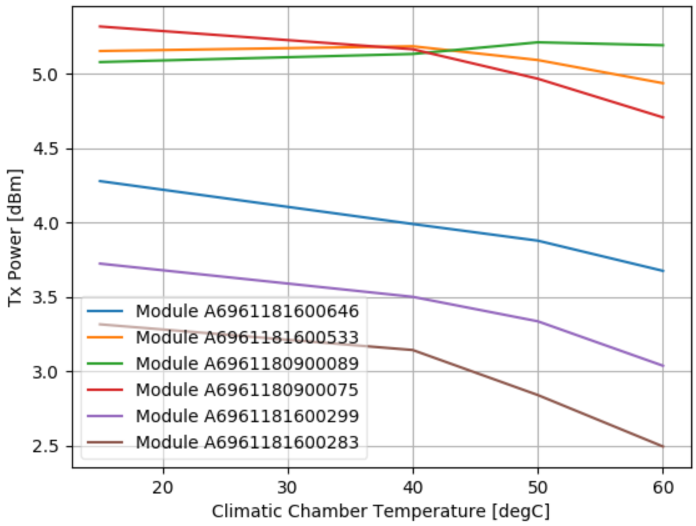

Figure 3.30: ONUs QA temperature test - Power meter measurements for the modules analysed from the third batch

Regarding the step-down transient analysis, all the modules passed the QA test in each temperature point analysed. To avoid being repetitive the data and the graphs acquired are not reported.
In conclusion, the temperature tests on the ONU modules confirmed the strength of the modifications made by the manufacturer. In fact, all the modules analysed were characterized by a correct functioning of the APC and, therefore, proved the ability to adapt to the temperature variations within the range defined in our specifications.

3.4.2 OLT test

The test structure used to study the temperature behaviour of the OLT modules is the same adopted for the ONU transceivers. In fact, also in this case four temperature points were analysed in the climatic chamber, i.e. 15, 40, 50, and 60°C. Again, during the temperature step-up transient we controlled the values of the Tx bias and the Tx power thanks to the I2C monitoring interface, while during the step-down transient we performed the classical QA test in each point. The setup used for the test is shown in figure 3.31.

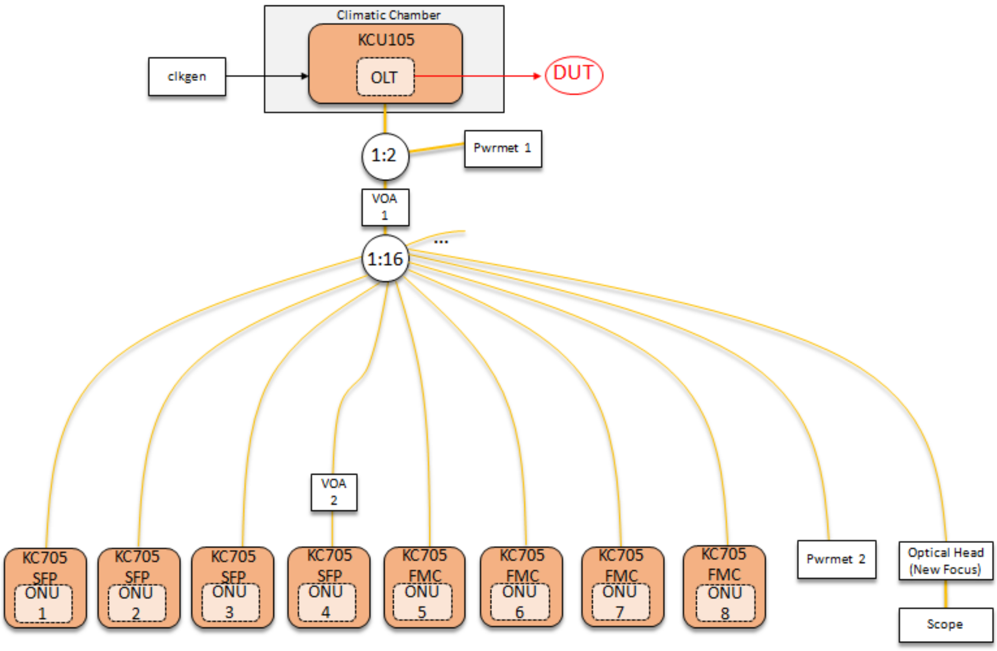

Figure 3.31: QA OLT temperature test - Setup

A total number of eight modules was tested. They were extracted randomly from the pre-series, the first and the second batch. Specifically, one was from the first batch, three from the second batch and four from the pre-series. Observing the data acquired through the I2C diagnostic monitoring interface, all the modules shown a Tx power approximately constant for the whole range of temperatures analysed, while the Tx bias current was or constant or slightly decreased. In the step-down transient tests, the Tx power measured by the power meter presented a different behaviour compared with that estimated by the I2C monitoring interface. In fact, the power frequently decreased moving from the first temperature point to the last one. In more detail, from the figure 3.32 can be deducted that the difference in power between 15 and 60°C is within the range of 1 dB and 1.3 dB for the modules of the first and the second batch and for the module 65811174800021 of the pre-series. Instead, there is a different behaviour for the other modules of the pre-series since there was no variation for the module 65811174800008, a decrease of 0.5 dB for the module 65811174800026, and finally there was a power increase of 0.5 dB for the module 65811174800016.

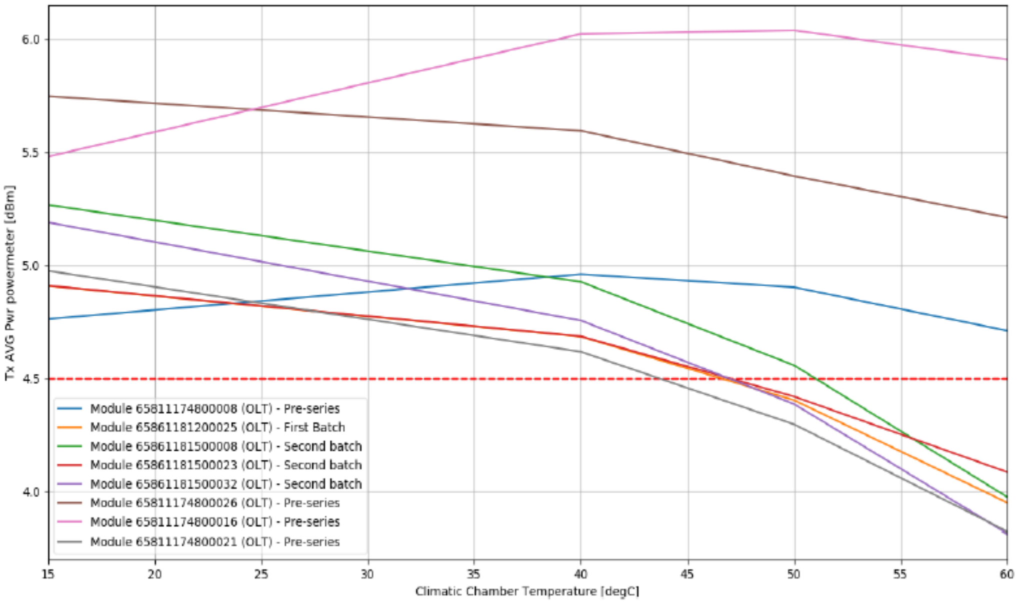

Figure 3.32: QA OLT temperature test - Tx Power measured by the power-meter

In the aforementioned figure, the temperature on the horizontal axis is the one of the climatic chamber, but we observed from the I2C monitoring interface that the corresponding temperature of the module was usually 10°C higher. The decrease in power was a problem for the majority of the modules. Starting from 50°C, they were non-compliant with our specification, indicated with the dashed red line, with the last exception of the following module:

- Module 65861181500008 from the second batch, non-compliant only at 60°C;
- Modules 65811174800026, 65811174800016 and 65811174800008 from the pre-series, always compliant because of the smaller power reduction.

The different behaviour of the power obtained through the power meter and the I2C diagnostic interface can be justified with the uncertainty of $\pm 3\ dB$ that characterize the latter. Moreover, beyond the transmitter power problems, it is worth mentioning that all the modules were compliant in terms of receiver sensitivity and optical eye in each temperature point analysed.

After a discussion with the manufacturer, we concluded that our data were different from the ones acquired by *Go!Foton* in its component test due to diverse methods used to calibrate the power meter. In fact, for the same module, there was a good agreement in the power variation measured between temperature points, but the absolute power at the first temperature analysed was considerably different. For this reason, we agreed on considering the temperature behaviour of the OLT modules as satisfying since, beyond the divergence in the value at the starting point of our measurement, the degradation of the power transmitted by the transceivers was not compromising.

Conclusion

The quality assurance campaign led to interesting results. Among the received 80 OLT modules, two transceivers were non-compliant in terms of receiver sensitivity at $BER = 10^{-4}$ and one OLT displayed a transmitted power lower than the minimum one provided by the TTC-PON specifications. Taking into account the uncertainty of the measure and of the system calibration procedure, only one between these three modules was clearly out-of-specifications and, therefore, will be replaced by the manufacturer. Furthermore, between the compliant modules there was an OLT that shown a weird behaviour. More in detail, few laser driver chips in the transceiver were characterized by a low threshold and, due to this problem, there was a failure in the transmission after the FPGA reset command. This event gave us the opportunity to improve the system since the FPGA reset software was modified to avoid this malfunction. About the ONU modules, between the 1145 tested transceivers, two were non-compliant in terms of receiver sensitivity at $BER = 10^{-11}$, and one module shown a distorted optical eye diagram with a failure in the eye mask test in burst mode. All these three transceivers are currently under discussion with the manufacturer. Moreover, among the compliant modules there was an ONU that was initially not working. After some analysis performed by the manufacturer, we found out that it was not able to transmit because the flexible printed circuit in the transceiver was dirty and shifting slightly. This caused a short circuit that resulted in the previously mentioned malfunction. The manufacturer fixed this transceiver which, by that point, passed our quality assurance test. Finally, the results of the temperature tests, which were carried out only on some samples of ONU and OLT modules, proved that the transceivers performances were not significantly degraded by temperature variations between 20 and 60°C, and that some modifications performed by the manufacturer on the APC circuitry of the ONU modules were working properly. In the coming period some reliability tests will be implemented on ONU and OLT devices at high temperature trying to determine the mean-time-to-failure and understand if there is any potential weakness not found in the modules so far.

Bibliography

[1] J.Varela, ed., *Timing and Synchronization in the LHC Experiments*, September 2000.

[2] P. Gällnö, ed., *Modules development for the TTC system*, September 1999.

[3] E. Mendes, S.Baron, C. Soos, L.Saint-Germain, and F. Vasey, eds., *Demonstrating TTC-PON robustness and flexibility*, September 2017.

[4] M. B. Marin, S. Baron, S. Feger, P. Leitao, E. Lupu, C. Soos, P. Vichoudis, and K. Wylliea, eds., *The GBT-FPGA Core: Features and Challenges*, September 2014.

[5] E. Mendes, S.Baron, D. Kolotouros, C. Soos, and F. Vasey, "The 10g ttc-pon: challenges, solutions and performance," *Journal of Instrumentation*, vol. 12, February 2017.

[6] D. Kolotouros, S. Baron, C. Soos, and F. Vasey, eds., *A TTC upgrade proposal using bidirectional 10G-PON FTTH technology*, September 2014.

[7] S. Papadopoulos, "Transceivers for passive optical networks." Presentation for ACEOLE meeting, April 2009.

[8] A. Company, "Understanding eye pattern measurement," March 2010.

[9] H. Fu and R. Maydern, "Signal integrity simulation and on-chip evaluation for low-cost fpga transceivers," December 2017.

[10] B. Taylor, ed., *TTC distribution for LHC detectors*, IEEE, Nov 1997.

[11] P. M. J. Christiansen, A. Marchioro and T. Toifl, *TTCrx Reference Manual.* CERN- EP/MIC, Geneva, Switzerland, 3.9 ed., October 2004.

[12] I. Papakonstantinou, C. Soos, S. Papadopoulos, S. Détraz, C. Sigaud, P. Stejskal, S. Storey, J. Troska, F. Vasey, and I. Darwazeh, "A fully bidirectional optical network with latency monitoring capability for the distribution of timing-trigger and control signals in high-energy physics experiments," *IEEE TRANSACTIONS ON NUCLEAR SCIENCE*, vol. 58, pp. 1628–1640, August 2011.

[13] F. Vasey, C.Soos, J.Troska, S.Kwan, A.Prosser, A.Xiang, J.Ye, T.Huffman, and T.Weidberg, *The Versatile Link Application Note.* CERN, Geneve, Switzerland, 2.6 ed., 11 2015.

[14] X. Zhang, *VLSI Architectures for Modern Error-Correcting Codes.* CRC Press, 1 ed., 7 2015.